Energy Research and Development Division
FINAL PROJECT REPORT

WASTE HEAT RECOVERY FROM CORROSIVE INDUSTRIAL EXHAUST GASES

Prepared for: California Energy Commission
Prepared by: Gas Technology Institute

AUGUST 2013
CEC-500-2014-098

PREPARED BY:

Primary Authors:
Dr. Rachid Slimane
Dr. John Wagner
Mr. John Pratapas
Mr. Harry Kurek
Mr. Shriram Reguraman (North Carolina State University)
Dr. Alexei V. Saveliev (North Carolina State University)

Gas Technology Institute
1700 S Mount Prospect Rd
Des Plaines, IL 60018
Phone: 847-768-0580 | Fax: 847-768-0984

Contract Number: 500-08-037

Prepared for:

California Energy Commission

Leah Mohney
Contract Manager

Virginia Lew
Office Manager
Energy Efficiency Research Office

Laurie ten Hope
Deputy Director
ENERGY RESEARCH AND DEVELOPMENT DIVISION

Robert P. Oglesby
Executive Director

DISCLAIMER

This report was prepared as the result of work sponsored by the California Energy Commission. It does not necessarily represent the views of the Energy Commission, its employees or the State of California. The Energy Commission, the State of California, its employees, contractors and subcontractors make no warranty, express or implied, and assume no legal liability for the information in this report; nor does any party represent that the uses of this information will not infringe upon privately owned rights. This report has not been approved or disapproved by the California Energy Commission nor has the California Energy Commission passed upon the accuracy or adequacy of the information in this report.

PREFACE

The California Energy Commission's Energy Research and Development Division supports public interest energy research and development that will help improve the quality of life in California by bringing environmentally safe, affordable, and reliable energy services and products to the marketplace.

The Energy Research and Development Division strives to conduct the most promising public interest energy research by partnering with research, development, and demonstration (RD&D) entities, including individuals, businesses, utilities, and public or private research institutions.

Energy Research and Development Division funding efforts are focused on the following RD&D program areas:

- Buildings End-Use Energy Efficiency
- Energy Innovations Small Grants
- Energy-Related Environmental Research
- Energy Systems Integration
- Environmentally Preferred Advanced Generation
- Industrial/Agricultural/Water End-Use Energy Efficiency
- Renewable Energy Technologies
- Transportation

Waste Heat Recovery from Corrosive Industrial Exhaust Gases is the final report for the Waste Heat Recovery from Corrosive Industrial Exhaust Gases project (contract number 500-08-037) conducted by Gas Technology Institute. The information from this project contributes to the Energy Research and Development Division's Industrial/Agricultural/Water End-Use Energy Efficiency Program.

When the source of a table, figure or photo is not otherwise credited, it is the work of the author of the report.

For more information about the Energy Research and Development Division, please visit the Energy Commission's website at www.energy.ca.gov/research/ or contact the Energy Commission at 916-327-1551.

ABSTRACT

Many industrial processes operate at low efficiencies because there are no commercial means available to economically recover heat from hot-process furnace exhaust gases containing corrosive elements such as chlorine and fluorine. The Gas Technology Institute has developed a Gas Guard Recuperator technology that takes a practical, innovative approach to heat recovery that uses a pair of reactors to clean the exhaust. In one reactor, hot exhaust gas passes through a regenerative bed that absorbs heat from this gas, and then passes through a guard bed that removes chlorinated and fluorinated contaminants, which stay permanently in the guard bed. In a second reactor, cold combustion air flows in the opposite direction. The combustion air passes through the guard bed and then through the regenerative bed and picks up heat before continuing to the furnace burner. The reactors alternate functions using a pair of four-way switching valves that cause combustion air to flow alternately through the one reactor, then the other, depending on the position of the valve.

Testing showed that preheating combustion air in this manner recovers 63 percent of the energy in the hot exhaust stream. Testing also showed that the concentration of corrosive hydrogen chloride in the exhaust gas was reduced by 96 percent.

Gas Guard Recuperator technology improves the energy efficiency of natural gas-fired industrial systems and reduces emissions. This technology captures the most corrosive components in exhaust gases from process furnace exhaust streams that normally could not be used for preheating of combustion air and stimulates innovation in developing low oxides of nitrogen burner technology using highly preheated air. The technology is projected to result in a 15 to 30 percent energy savings with a corresponding reduction in greenhouse gas emissions. By lowering energy costs, this technology is expected to improve the competitiveness of industries in California.

Keywords: Waste heat recovery, recuperator, regenerator, corrosive gas, industrial furnace, melter, aluminum, hydrogen chloride, HCl, hydrogen fluoride, HF, sorbent, gas guard

Please use the following citation for this report:

Wagner, John, Rachid Slimane, John Pratapas, Harry Kurek (Gas Technology Institute), Shriram Reguraman, Alexei V. Saveliev (North Carolina State University). 2013. ***Waste Heat Recovery from Corrosive Industrial Exhaust Gases.*** California Energy Commission. CEC-500-2014-098.

TABLE OF CONTENTS

PREFACE ..... **i**

ABSTRACT ..... **ii**

TABLE OF CONTENTS ..... **iii**

LIST OF FIGURES ..... **iv**

LIST OF TABLES ..... **vii**

EXECUTIVE SUMMARY **1**

Introduction 1

Project Purpose 1

Project Objective 1

Project Conclusions 2

CHAPTER 1: Waste Heat Recovery from Corrosive Industrial Exhaust Gases **3**

CHAPTER 2: Technical Tasks **5**

2.1 Task 1: Adminstration 5

2.2 Task 2: Guard Bed Design and Lab Testing 5

2.2.1 Objective 5

2.2.2 Approach and Schedule 5

2.2.3 Results and Discussion 11

2.3 Task 3: Fabrication and Field Testing 38

2.3.1 Objective 38

2.3.2 Approach and Schedule 38

2.3.3 Results and Discussion 38

2.4 Task 4: Technology Transfer Plan 87

REFERENCES **91**

GLOSSARY **93**

LIST OF FIGURES

Figure 1: Task 3 Schedule 6

Figure 2: High-Temperature Sorbent/Catalyst Test Facility in GTI's Hot Gas Cleanup Laboratory 8

Figure 3: Photo of the Proposed Sorbent/Catalyst Test Facility 8

Figure 4: Quartz Reactor/High-pressure Vessel Arrangement 9

Figure 5: Fourier Transform Infrared Unit Available to this Project 9

Figure 6: Micro-gas Chromatograph (μGC) for Online Measurement of Major Gas Components from Dry Samples 10

Figure 7: Setup for Continuous HCl Sampling from Reactor Offgas and Analysis via Ion Chromatography Instrument (Dionex DX-320/IC 20) 10

Figure 8: HCl Batch Sampling System for Offline Analysis 11

Figure 9: HCl Concentration in Flue Gas after Equilibration with Various Potential Sorbent Candidates at very High Temperatures 15

Figure 10: Equilibrium HCl Concentration for the Na_2O/NaCl System in the 1,400-2,100ºF Temperature Range 16

Figure 11: HCl and HF Removal by Nahcolite or Trona 17

Figure 12: Schematic of the High-Temperature Sorbent Test Facility 19

Figure 13: Photo of the GTI High-Temperature Sorbent Test Facility 20

Figure 14: HCl/Halide removal sorbents: Actisorb Cl2, Previously Named G-92C (left), and HTG-1 (right). 23

Figure 15: HCl Removal Performance of the G-92C Material at 1,400°F 30

Figure 16: HCl Removal Performance of the G-92C (Actisorb Cl2) Material at 1,200, 1,400, and 1,600°F 31

Figure 17: Process Flow Diagram for a GGR Process Field Demo Configuration 32

Figure 18: Chloride Removal Performance with the G-92C Material at 1,400°F and 1,200°F with 2 Different Levels of HCl in the Feed Gas 33

Figure 19: Reproducibility of Test Results 34

Figure 20: Preliminary Design of a Candidate Slipstream GGR Unit Showing Arrangement of Sorbent Material and Bed Inert Material and Supports 37

Figure 21: GGR Concept 39

Figure 22: Diagram of Model with Ceramic Porous and Sorbent Porous Media 40

Figure 23: Temperature distribution at 300 seconds (s), forward cycle. 41

Figure 24: Temperature distribution at 1,800 s, forward cycle. 41

Figure 25: Velocity Distribution at 1,800 s, forward cycle. 41

Figure 26: Pressure drop at 1,800 s, forward cycle. 41

Figure 27: Temperature distribution at 300 s, reverse cycle. 42

Figure 28: Temperature distribution at 1,800 s, reverse cycle. 42

Figure 29: Velocity distribution at 1,800 s, reverse cycle. 42

Figure 30: Pressure drop at 1,800 s, reverse cycle. 42

Figure 31: Temperature Variation across the Axial Position over Three Different Cycles 43

Figure 32: Solid Diffusion through the Product Layer 44

Figure 33: Concentration Profile at the End of 20th Cycle Across the Bed for 50 Ppm Inlet Concentration. 45

Figure 34: Thickness Variation of the Product Layer on the Sorbent Material during 20th Cycle 45

Figure 35: Concentration Profile at the End of 50th Cycle across the Bed for 50 ppm Inlet Concentration 46

Figure 36: Thickness Variation of the Product Layer on the Sorbent Material during 50th Cycle.46

Figure 37: Product Layer Thickness Increase on the Sorbent Surface 46

Figure 38: Concentration Profile at the End of 50th Cycle across the Bed for 900 ppm Inlet Concentration. 47

Figure 39: Thickness Variation of the Product Layer on the Sorbent Material during 50th Cycle.47

Figure 40: Location of Parameter Study 48

Figure 41: Temperature Curves at Interface for Varying Inlet Temperature 48

Figure 42: Velocity Curves at Interface for Varying Inlet Temperature 49

Figure 43: Temperature Curves at Interface for Varying Inlet Velocity 50

Figure 44: Velocity Curves at Interface for Varying Inlet Velocity 50

Figure 45: Concentration Curves across the Sorbent Media for Varying Inlet Concentration 51

Figure 46: Pressure Drop for Various Particle Sizes under Consideration 51

Figure 47: Velocity Curves at the Interface for Temperature Dependent Viscosity Value 52

Figure 48: Velocity Contour Curves 52
Figure 49: Temperature Contour Curves 53
Figure 50: Velocity Profile at the Interface for Temperature Independent Viscosity Value 53
Figure 51: Preliminary Dimensions of the Recuperator 55
Figure 52: Location of Study Where Temperature is Monitored 57
Figure 53: Axial Temperature Profiles for Different Cycles 59
Figure 54: 2-D Temperature Distribution at the End of the Forward Run during the 26th Cycle 60
Figure 55: 2-D Temperature Distribution at the End of the Backward Run during the 26th Cycle 60
Figure 56: Concept Design of a GGR Demonstration Unit 61
Figure 57: Concept Operation of a GGR Demonstration Unit 62
Figure 58: General Arrangement View of a Gas Guard Recuperator 64
Figure 59: Elevation Views of a Gas Guard Recuperator 65
Figure 60: Valve Arrangements 66
Figure 61: 4-Way Switching Valve Design 67
Figure 62: Proposed General Layout View of the GGR Laboratory Test Setup 68
Figure 63: Proposed Front Elevation View of the GGR Laboratory Test Setup 68
Figure 64: Proposed Side Elevation View of the GGR Laboratory Test Setup 68
Figure 65: GGR Reactor Sections with Refractory Insulation 70
Figure 66: Bed Support Plate with Screens and Gasket 70
Figure 67: GGR Reactors Assembled with Interconnecting Piping 71
Figure 68: 4-Way Switching Valve with Actuator 71
Figure 69: HCl Injector Subsystem for Flue Gas 72
Figure 70: General Layout View of the External Piping 73
Figure 71: Front Elevation View of the External Piping 74
Figure 72: Side Elevation View of the External Piping 75
Figure 73: Piping to/from GGR Reactors 76
Figure 74: HCl Injector on the Side of Insulated Pipe 76
Figure 75: Insulated Piping to GGR Reactor 77

Figure 76: Cold Air Line from Blower 77
Figure 77: Burner Connections 78
Figure 78: Data Acquisition System 78
Figure 79: Thermocouple Wiring 78
Figure 80: Thermocouple Wells 78
Figure 81: Beads in Left GGR Reactor 79
Figure 82: Beads in Right GGR Reactor 79
Figure 83: Thermocouples in Left GGR Reactor 79
Figure 84: Thermocouples in Right GGR Reactor 79
Figure 85: Thermocouples Wired to Left GGR Reactor 80
Figure 86: Thermocouples Wired to Right GGR Reactor 80
Figure 87: Combustion Air Blower and Power Box 81
Figure 88: Pressure Gauges and Sampling Ports with Switching Solenoid in Background 81
Figure 89: HCl Piping Train and Manometer for Cold Air Orifice 82
Figure 90: Heat Shielding 82
Figure 91: Heated Sampling Line on Right GGR Reactor Outlet and Heated Filter Box 84
Figure 92: Partially Obscured Load in Furnace 84
Figure 93: Inlet and Outlet Temperatures at the Right GGR Reactor Showing Cycling 86
Figure 94: Heat Recovery Results 86
Figure 95: Acid Gas Removal Results 86

LIST OF TABLES

Table 1: Simulated Flue Gas Composition 14
Table 2: Equilibrium HCl Concentration for the Na_2O/NaCl System 16
Table 3: Examples of Chloride Removal Materials and their Sources 21
Table 4: Criteria and Rationale for the Test Matrix 24
Table 5: Test Matrix Initially Defined for the Laboratory Testing Task 25
Table 6: Chemical and Physical Properties of Selected Candidate HCl Removal Materials 28

Table 7: Results Summary of Testing with Alumina as a Bed Material 29

Table 8: Preliminary Sizing Estimates for the Slipstream Gas Guard Recuperator (GGR) Unit .. 36

Table 9: Design Parameters for the Regenerator 54

Table 10: Preliminary Design Specifications of the Regenerator 56

Table 11: Temperatures at the Sorbent/Inert Interface 58

Table 12: Pressure Drops and Exit Temperatures of Air Leaving the Regenerator 58

Table 13: GTI Technology Transfer Plan Fundamentals 89

EXECUTIVE SUMMARY

Introduction

Many industrial processes operate at low efficiencies because there are no commercial methods available to economically recover heat from hot exhaust gases containing halogenated compounds - corrosive elements such as chlorine and fluorine. Aluminum melting furnaces, in particular, are excellent candidates for such a technology. Incinerators also produce acidic exhaust gases, and heat recovery in these systems can be complicated by their corrosive effects.

The Gas Technology Institute has developed a Gas Guard Recuperator technology that takes a practical, innovative approach to recovering industrial waste heat using a pair of reactors. In one reactor, hot exhaust gas passes through a regenerative bed that absorbs heat from exhaust gas. Cooled exhaust gas then passes through a guard bed of sodium minerals that scour chlorinated and fluorinated contaminants from the gas and absorb some additional heat. In a second reactor, cold combustion air flows in the opposite direction. The combustion air picks up some heat, however, no halogenated compounds from the guard bed. The warmed combustion air then passes through the regenerative bed and gathers more heat. The reactors alternate functions after the first reactor has reached a limiting temperature and the second reactor has somewhat cooled off. A pair of four-way switching valves performs the task of alternating flows through the reactors. Each reactor has a layer of inert ceramic material (heat transfer substance) topped by a layer of sorbent material for hydrogen chloride removal. The sorbent and ceramic beds are supported by a perforated plate and three layers of screens. The reactors are lined on the inside with hard refractory (material that maintains its strength at high temperatures) backed by insulating boards. The top and bottom lids of each reactor are removable to fill and inspect the bed.

The only furnace change required is to operate burners on preheated air instead of ambient air. The flows of exhaust gas and combustion air remain continuous. Heat is recaptured, significantly increasing the energy efficiency of the furnace, without incurring an excessive capital cost for major system modifications. However, the sacrificial sodium minerals in the guard bed must be replaced after several months of operation.

Project Purpose

This project developed an industrial Gas Guard Recuperator technology recovering waste heat that is capable of 15- to 30-percent energy savings for targeted market applications.

Project Objective

A heat recovery system, the Gas Guard Recuperator, was designed, built and tested to confirm that performance targets can be achieved on this technology.

Field Demonstration

A Gas Guard Recuperator demonstration unit was designed, fabricated, and installed on a test furnace at the Gas Technology Institute facility.

Testing showed that combustion air was preheated from 124°F to 810°F using 1,006°F exhaust from the furnace and represented 63 percent of the energy in the exhaust. Testing also showed that the concentration of hydrogen chloride in the exhaust gas was reduced from 46.2 ppm to 1.9 ppm. The average removal was 96 percent.

Project Conclusions

Conventional recuperators, which can be damaged when used to recover heat from corrosive flue gas, provide 450°F to 750°F pretreated combustion air using 1,300°F to 1,600°F exhaust. For a furnace with 1,800°F of corrosive exhaust gas, the ability to preheat the combustion air to 800°F usint the Gas Guard Recuperator technology is expected to:

- Increase furnace thermal efficiency from 35 to 45 percent
- Increase fuel savings to 23 percent

Using the technology for a furnace with 1,800°F exhaust and being able to preheat the combustion airt to to 1,000°F rather thatn 800°F is expected to

- Increase furnace thermal efficiency from 35 to 49 percent.
- Increase fuel savings to 28 percent.

Gas Guard Recuperator technology improves the energy efficiency of natural gas fired industrial systems and lowers emissions by capturing most corrosive elements in exhaust gases. The technology is projected to result in a 15- to 30-percent energy savings with a corresponding reduction in greenhouse gas emissions. By lowering energy costs, the Gas Guard Recuperator is expected to improve the competitiveness of industries in California that install and use it.

CHAPTER 1:
Waste Heat Recovery from Corrosive Industrial Exhaust Gases

Many high-temperature industrial processes operate at low efficiencies. There are currently no commercial methods available to recover heat economically from hot exhaust gases containing highly corrosive halogenated elements such as chlorine and fluorine. Aluminum remelt furnaces, in particular, are excellent candidates for such a technology, as they typically operate at 30% efficiency with 60% of the input energy lost to the exhaust gas without recovery. Incinerators also produce acidic exhaust gases, and heat recovery in these systems can be complicated by their corrosive effects. The Gas Technology Institute (GTI) developed a Gas Guard Recuperator (GGR) technology that takes a practical, innovative approach to heat recovery. The GGR uses a pair of reactors, each containing an inert ceramic thermal bed and an absorbent guard bed. In one reactor, hot exhaust gas passes through a ceramic bed that absorbs heat from exhaust gas. Cooled exhaust gas then passes through a guard bed of sodium minerals that scour chlorinated and fluorinated contaminants from the gas and absorb additional heat. In a second reactor, cold combustion air flows in the opposite direction. The combustion air picks up some heat, but no halogenated compounds from the guard bed. The warmed combustion air then passes through the regenerative bed and gathers more heat. The reactors alternate functions after the first reactor has reached a limiting temperature and the second reactor has cooled off. A pair of four-way switching valves performs the task of alternating flows through the reactors.

This technology only requires furnances to operate burners on preheated air instead of ambient air. The flows of exhaust gas and combustion air remain continuous. Heat is recaptured, significantly increasing the energy efficiency of the furnace without incurring an excessive capital cost for system modifications. The sodium minerals in the guard bed, however, must be replaced after several months of operation.

While the guard bed section is entirely new, the remainder of the GGR system is built with readily available components. This keeps costs low and minimizes technical risk. The guard bed is practical because sodium minerals have been shown in thermodynamic simulations to simultaneously reduce chlorine and fluorine content to less than 1 ppm at high temperatures.

The project team was:

- GTI – technical leadership, GGR design and construction, laboratory and demonstration units testing
- Thorock Metals – originally committed the demonstration site, but was unfortunately not able to participate in the project due to unforeseen circumstances

- Thermal Transfer Co. – industrial partner, GGR demonstration unit engineering, potential commercialization partner
- CDS Consulting – disabled veteran business enterprise (DVBE), support of GTI's technology transfer effort

CHAPTER 2:
Technical Tasks

The project included four tasks: administrative, design and laboratory testing; fabrication and field testing; and finally technology transfer activities.

2.1 Task 1: Adminstration

This task consisted of a kickoff meeting, various Critical Project Review (CPR) meetings during the project, and a final meeting, held on March 7, 2013, at the conclusion of the project. This task also included preparing and distributing monthly progress reports and the final report.

2.2 Task 2: Guard Bed Design and Lab Testing

2.2.1 Objective

Task 2 was developed the necessary information to design a suitable gas/solid guard bed contactor to optimize contaminant (hydrogen chloride [HCl] and hydrogen fluoride (HF) removal efficiency as well as sorbent utilization. Suitable materials were selected to achieve removal of contaminants from aluminum remelt furnace exhaust to meet the targets set for the GGR Process. Experimental approaches and analytical techniques were developed to demonstrate technical feasibility of the concept and generate reaction conversion performance data.

2.2.2 Approach and Schedule

Work was divided into six focus areas: comprehensive literature search, thermodynamic and kinetic simulations, laboratory facility and materials preparation, test plan development and laboratory testing, development of GGR unit design guidelines for field demonstration in Task 3, and reporting. Work in Task 3 started on August 1, 2009 and was completed within one year. Task 3 activities progressed according to the approximate schedule presented in Figure 1.

Figure 1: Task 3 Schedule

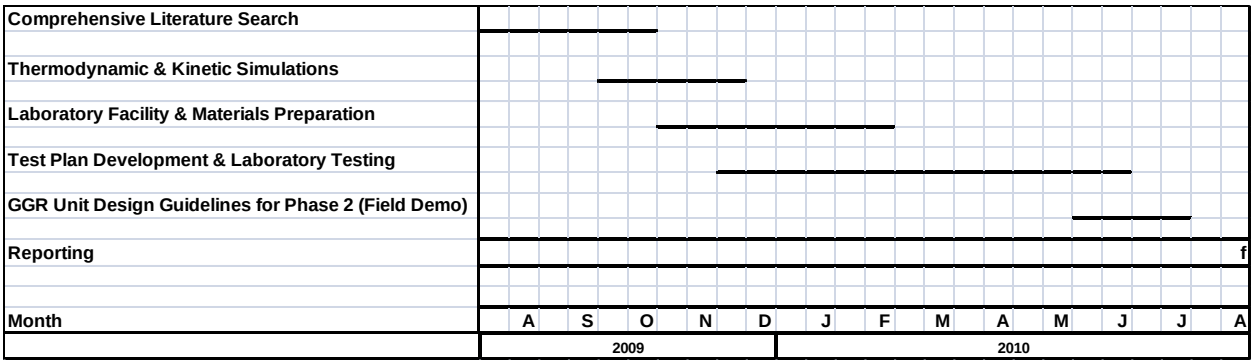

Source: Gas Technology Institute

2.2.2.1 Comprehensive Literature Search

A comprehensive literature search was conducted during the first three months to:

a. Identify candidate sorbent materials for HCl and HF removal under conditions representative of the aluminum remelt furnace exhaust:

   - Temperature: 1,400 to 1,800°F
   - Low HCl and HF inlet levels (up to 25 parts-per-million by volume [ppmv] HCl and 10 ppmv HF)
   - Low pressure

b. Assess practicality of candidate materials (e.g. nahcolite, trona, etc.) for commercial application, such as availability, stability in the flue gas environment, cost, and any disposal requirements

c. Identify potentially suitable gas-solid contactor designs for field demonstration of the GGR process concept in Task 3

2.2.2.2 Thermodynamic and Kinetic Simulations

This part of the work was performed during the initial few months of the project and focused essentially on thermodynamic analyses and simulations to estimate the expected gas cleaning efficiency of selected materials. The HSC software package (Roine, A. 2010) was used.

2.2.2.3 Preparation of Laboratory Facility and Materials Procurement

GTI's Hot Gas Cleanup Laboratory houses several small-scale reactor facilities for conducting basic research studies that involve contacting of solids and gases. One of these facilities, similar to the one shown in

Figure 2 through Figure 4, was modified to meet the needs of the project: proper screening testing of candidate HCl and HF removal materials, assessment of contaminant removal efficiency and effective capacity (pre-breakthrough conversion of the material's active component) of promising candidates under a wide range of process conditions (i.e., parametric testing), and long-term testing of selected sorbent materials for field demonstration in Task 3. Facility modifications affected configuration of the reactor containing the sorbent bed and sampling and analysis section of feed and product gases. Whenever possible, online instruments (such as Fourier Transform Infrared [FTIR], micro-gas chromatographs, ion chromatograph, (Figure 5, Figure 6, and Figure 7, respectively) were used, but batch sampling (Figure 8) and offline analysis (at GTI's Environmental and Chemical Research Services [ECRS] Laboratory) was also used to complement the online analyses and provide independent confirmation analyses.

Sufficient quantities of selected candidate sorbents would be procured. Any necessary chemical and physical properties of selected materials were determined. Portions of the procured materials would be processed for testing either as fine granules suitable for injection, or as bigger particles, depending on the selected configuration for the laboratory gas-solid contactor. Shakedown testing of the modified test facility was performed to confirm validity of testing and gas sampling procedures, calibration equipment, and sensitivity of gas analysis instruments.

2.2.2.4 Test Plan Development and Laboratory Testing

The literature search and materials procurement activities were expected to identify up to five candidate sorbent materials for HCl removal, and up to three candidate materials for HF removal. Some of the materials identified were tested to determine if they would be for both contaminants, which was highly desirable. A detailed Test Plan was developed for the entire project task to:

a. Performed screening testing of all procured materials under baseline operating conditions (overall simulated flue gas composition, HCl and HF inlet levels, temperature, etc.)

b. Performed additional testing on promising materials to evaluate effects of key gas cleaning process parameters (such as temperature, space velocity [SV] or contact time, sorbent-to-contaminant ratio, etc.)

c. Combined HCl and HF removal

d. Performed long-term testing of top-performing HCl and HF removal sorbents to determine their ultimate or effective contaminant removal capacity (i.e., grams of HCl or HF removed per 100 grams of sorbent)

    - Confirmed breakthrough test results by Chlorine (Cl) and Fluorine (F) analyses using spent sorbent samples
    - Characterized selected spent sorbent samples to assess any requirements for disposal

Figure 2: High-Temperature Sorbent/Catalyst Test Facility in GTI's Hot Gas Cleanup Laboratory

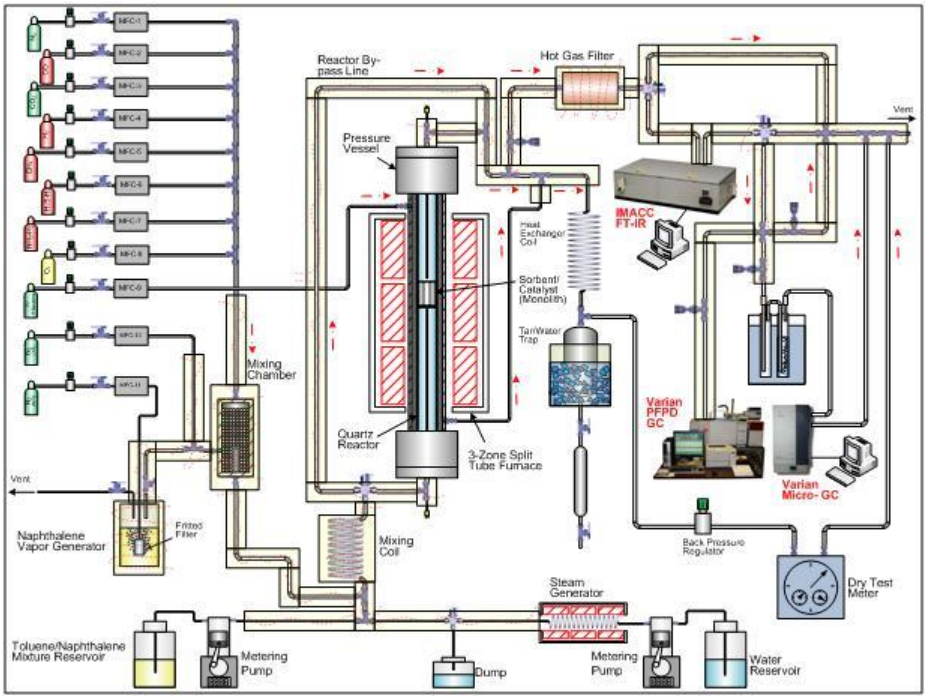

Quartz reactor placed within a pressure-containing vessel and heated externally by a three-zone high-temperature furnace.
Source: Gas Technology Institute

Figure 3: Photo of the Proposed Sorbent/Catalyst Test Facility

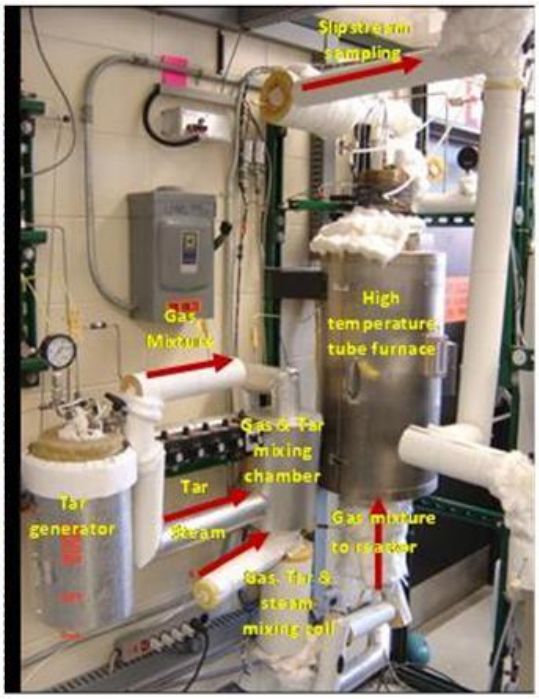

Photo Credit: Gas Technology Institute

Figure 4: Quartz Reactor/High-pressure Vessel Arrangement

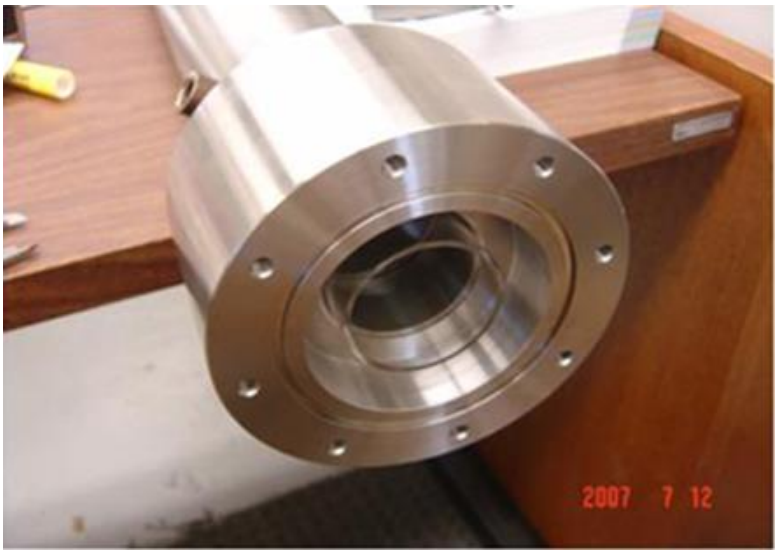

Use of quartz minimizes/eliminates loss of contaminants to reactor walls

Photo Credit: Gas Technology Institute

Figure 5: Fourier Transform Infrared Unit Available to this Project

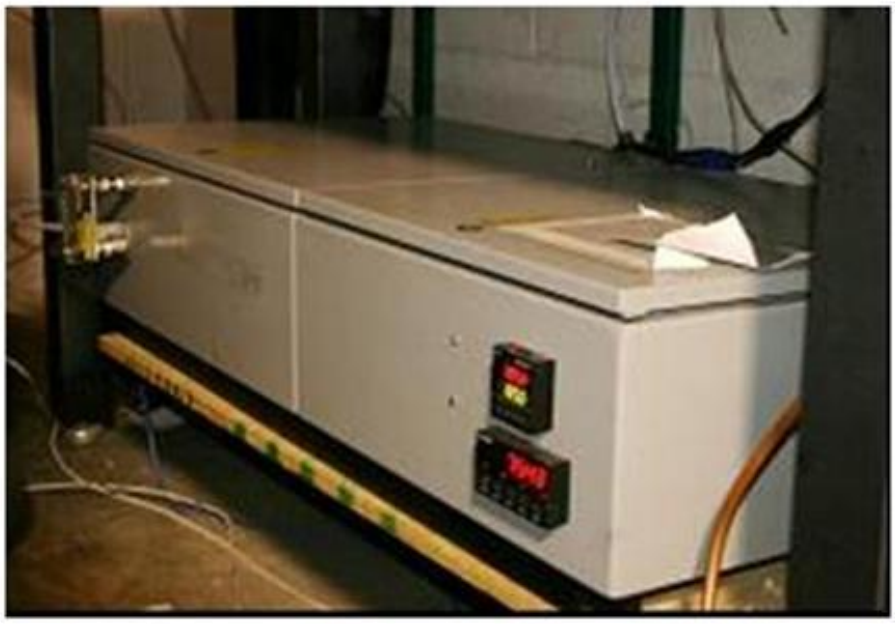

The FTIR provides the capability to measure water vapor (H_2O) in hot wet syngas.

Photo Credit: Gas Technology Institute

Figure 6: Micro-gas Chromatograph (µGC) for Online Measurement of Major Gas Components from Dry Samples

Photo Credit: Gas Technology Institute

Figure 7: Setup for Continuous HCl Sampling from Reactor Offgas and Analysis via Ion Chromatography Instrument (Dionex DX-320/IC 20)

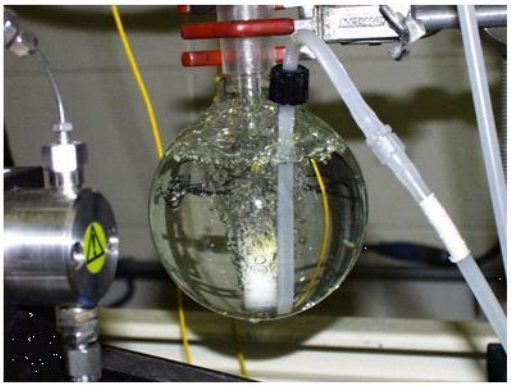

Photo Credit: Gas Technology Institute

Figure 8: HCl Batch Sampling System for Offline Analysis

Photo Credit: Gas Technology Institute

2.2.2.5 GGR Unit Design Guidelines (Field Demo)

Based on laboratory test results and analyses, guidelines and projections were developed for the design of a field demonstration GGR unit to be built and tested in Task 3 of the project.

2.2.2.6 Reporting

Progress in Task 2 was communicated periodically through:

a. Weekly review meetings including the project manager, principal investigator, and test engineers

b. Monthly progress reports prepared and submitted to the California Energy Commission (Energy Commission) Commission Agreement Manager (CAM)

c. A Phase 1 Task 2 Final Report on GGR development, experimental results, and Task 3 design considerations

   - Develop a full report of calculations, analyses, test results, and projections for the demonstration unit to be built and tested in Task 3

d. Participation of the Project Manager in Energy Commission CPR Meetings

2.2.3 Results and Discussion

2.2.3.1 Comprehensive Literature Search

A comprehensive review of relevant information in the literature was conducted, using GTI's extensive Library services. The primary focus of the review was to:

- Identify highly efficient hydrogen chloride (HCl) and/or hydrogen fluoride (HF) materials from high-temperature (1,400 to 1,800°F) flue gas
- Identify potentially suitable ways for gas/solid contacting at such high temperature (one of the challenges in the project is to develop a contactor device for integration into a slipstream from an aluminum remelt furnace exhaust for field demonstration of the GGR cleanup process).

Other items of interest/key words included:

- HCl and HF sampling and measurement methods (applicable to laboratory and field environments)
- Cleanup of hot corrosive industrial exhaust gases containing corrosive elements such as chlorine and fluorine
- Aluminum remelt furnace exhaust gas contaminants
- Classification of spent absorbents in regards to disposal
- Sodium- and potassium carbonate-containing minerals for chloride removal (two candidates that are expected to be effective both technically and economically)
- Exhaust heat recovery from aluminum remelt furnaces
- Acid gas control in combustion systems

The comprehensive search utilized four sets of keywords:

1. secondary + aluminum + emissions
2. "hot gas" + cleaning + HCl + HF
3. "acid gas" + cleanup + hot + gas + flue + HCl + HF
4. "potassium-carbonate-containing minerals"

Reviewed information resources included the Chemical Abstracts 1997- 2007 database, scientific and technical databases available on Dialog, including Metals Abstracts, Analytical Abstracts, Science Citation Index, Aluminum Industry Abstracts, Engineering Index, Corrosion Abstracts, Metalbase, and any other databases that produced relevant hits as well as GTI internal databases (journal tables of contents, research reports, etc.). The literature search generated 52 articles and conference papers. From those, 43 documents were selected as relevant, and consequently were retrieved or purchased. Google/Google Scholar searches were also conducted, but they yielded no relevant papers.

The compiled information revealed that a number of solid compounds were claimed to have high removal efficiency of HCl and HF in the mid- to high-temperature range. They were calcium-based [Garea. 2003, pp. 227-236; Hsu, J. 2007; Hisashi, K. 2001 pp. 624-628; Jatta, P. 2005 pp. 1664-1673; Jatta, P. 2005 pp. 1674-1684], sodium-based [Cook, C. 1992; Brockhoff, R. 2000], potassium-based [Brockhoff, R. 2000], and magnesium-based [Hsu, J. 2007; Binlin, D. 2007 pp. 1019-1023] compounds. However, the sodium-bearing compounds were singled out as the

most efficient and economical for capturing both HCl and HF. Cook et al. invented a process for removing HCl and HF from coal-derived fuel gas at elevated temperatures by contacting the gas with sodium based sorbents such as nahcolite, sodium bicarbonate or sodium carbonate in a powder form [Cook, C. 1992]. They reported that 98 percent of HCl removal was achieved at 650°C (1,202°F). Brockhoff et al. also described another process for removing HCl and HF from industrial furnace exhaust gases [Brockhoff, R. 2000]. They favored sodium-based and potassium-based materials. More importantly, this patent also showed how the spent sorbent materials could be recycled back to the aluminum remelting furnace to act as blanketing agents as a way to utilize them and reduce solid waste generation. This approach also can reduce generation of other contaminants such as dioxin and furan. This offers an additional pollution reduction benefit.

The information developed from the literature review effort helped to focus selection of candidate materials, and to define the scope and approach of the ensuing thermodynamic analyses and laboratory testing. Clearly, sodium-bearing, naturally-occurring minerals nahcolite ($NaHCO_3$) and trona ($Na_2CO_3 \cdot NaHCO_3 \cdot 2H_2O$) emerged as preferred materials for capturing both HCl and HF in the project.

2.2.3.2 Thermodynamic Simulations of Sorbent-based HCl and HF Removal

This part of the project focused on conducting thermodynamic analyses and simulations to estimate the expected gas cleaning (HCl and HF removal) efficiency of candidate materials that were being identified as the comprehensive literature review was finalized. The commercially available "HSC Chemistry®" software package [Roine, A. 2010] was selected as one of the best tools for this study. HSC is designed for various kinds of chemical reactions and equilibria calculations, and therefore has a wide range of application possibilities in scientific education, research, and industry. The name of the program is based on the feature that all calculation options automatically utilize the same extensive thermo-chemical database which contains enthalpy (h), entropy (s), and heat capacity (c).

The initial, principal criterion used for sorbent selection was based on thermodynamic equilibrium calculations to limit the choice of the active sorbent materials to those that could reduce the HCl concentration in the flue gas (assumed to range from 5 to 50 ppmv) to an acceptable level (to be determined based on other considerations) in the temperature range from 1,400 to 2,100ºF and ambient pressure. The composition of the expected flue gas used is presented in Table 1. It was intended to provide a representative, but simplified, gas test environment relative to a commercial flue gas. The inlet HCl concentration was assumed to be in the range 5-50 ppmv, and no other contaminants (such as sulfur dioxide [SO_2] or oxides of nitrogen [NO_x]) were considered. In addition, the sorbent candidate being sought could be used in an external high-temperature reactor configuration (placed between the furnace and the recuperator equipment) either as a once-through sorbent or as a regenerable sorbent, depending on characteristics, cost, and other factors.

Table 1: Simulated Flue Gas Composition

Gas Component	Vol. percent
Carbon Dioxide (CO_2)	15
Water Vapor (H_2O)	9
Oxygen (O_2)	2
Hydrogen Chloride (HCl)	5 – 50 ppmv
Nitrogen (N_2)	balance

Source: Gas Technology Institute

As mentioned earlier, the commercially-available "HSC Chemistry®" software package [Roine, A. 2010] was used and two thermodynamic simulation approaches were applied. In the first approach, the simplified, simulated flue gas composition was equilibrated in the presence of candidate solids over the range of temperatures of interest (1,400 to 2,100°F), in increments of 100°F. The solids selected included compounds of calcium (Ca), iron (Fe), potassium (K), magnesium (Mg), manganese (Mn), molybdenum (Mo), and sodium (Na). For each sorbent candidate system, all potentially stable solid phases were considered during the equilibration process with flue gas. For example, for the Na system, the solids considered included sodium oxide (Na_2O), sodium superoxide (NaO_2), nahcolite ($NaHCO_3$), trona ($Na_2CO_3 \cdot NaHCO_3 \cdot 2H_2O$), sodium carbonate ($Na_2CO_3$), sodium chloride (NaCl), sodium chlorite ($NaClO_2$), sodium chlorate ($NaClO_3$), and sodium perchlorate ($NaClO_4$). The results obtained with the selected materials (and for an inlet HCl concentration of 50 ppmv) are summarized in

As clearly shown, only Na is capable of reducing the HCl concentration to a very low level throughout the temperature range considered.

In addition to providing the expected HCl concentration in the cleaned product flue gas, this first approach predicted the stable form of the sorbent's active component in equilibrium with the flue gas and the stable form of the solid product to which chloride (Cl) was tied up. For example, for the Sodium (Na) system, Na_2O was expected to be the stable form of the active sorbent material and NaCl that of the product. Therefore, the governing reaction for HCl removal from this flue gas could be written as:

$$Na_2O + 2HCl = 2NaCl + H_2O \qquad (1)$$

Figure 9: HCl Concentration in Flue Gas after Equilibration with Various Potential Sorbent Candidates at very High Temperatures

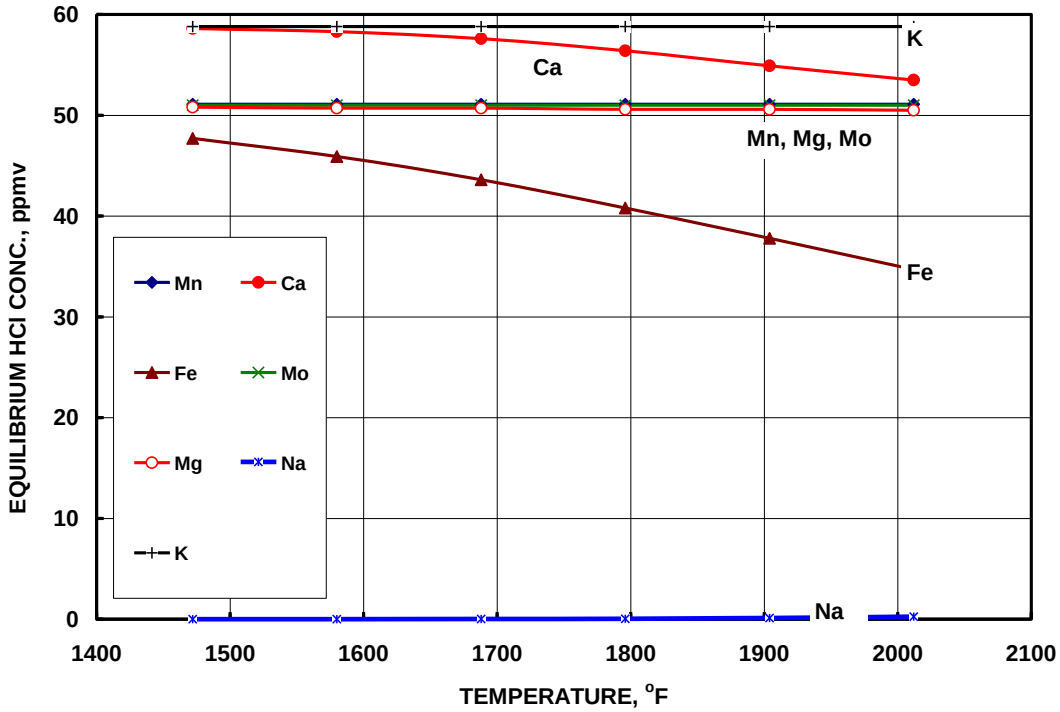

Source: Gas Technology Institute

This information was used as the starting point for the second approach. Here, the HSC process simulation software was used to calculate the equilibrium constant for the HCl removal reaction (1) and the results were used to calculate the equilibrium HCl concentration (see Table 2). As shown in Figure 10, the equilibrium HCl concentration in the product (cleaned) flue gas was well below 0.5 ppmv throughout the entire temperature range of interest. Therefore, it appeared feasible to achieve very high HCl removal levels (91 percent to 99 percent) using sodium-containing materials (such as nahcolite or trona, which are abundantly available and cheap). Even if the HCl concentration in the inlet flue gas was as low as 5 ppmv, thermodynamics predicted ~91 percent HCl removal could be achieved at 2,100ºF (the HCl equilibrium concentration was 0.433 ppmv).

Table 2: Equilibrium HCl Concentration for the Na_2O/NaCl System

Na2O + 2HCl(g) = 2NaCl + H2O(g)					
Temp., C		Log (K)	Log (pHCl)	pHCl	ppmv HCl
800	1472	16.548	-8.80	1.5963E-09	0.002
850	1562	15.676	-8.36	4.3563E-09	0.004
900	1652	14.882	-7.96	1.0867E-08	0.011
950	1742	14.154	-7.60	2.5126E-08	0.025
1000	1832	13.473	-7.26	5.5033E-08	0.055
1050	1922	12.838	-6.94	1.1432E-07	0.114
1100	2012	12.249	-6.65	2.2523E-07	0.225
1150	2102	11.681	-6.36	4.3313E-07	0.433

Source: Gas Technology Institute

Figure 10: Equilibrium HCl Concentration for the Na_2O/NaCl System in the 1,400-2,100ºF Temperature Range

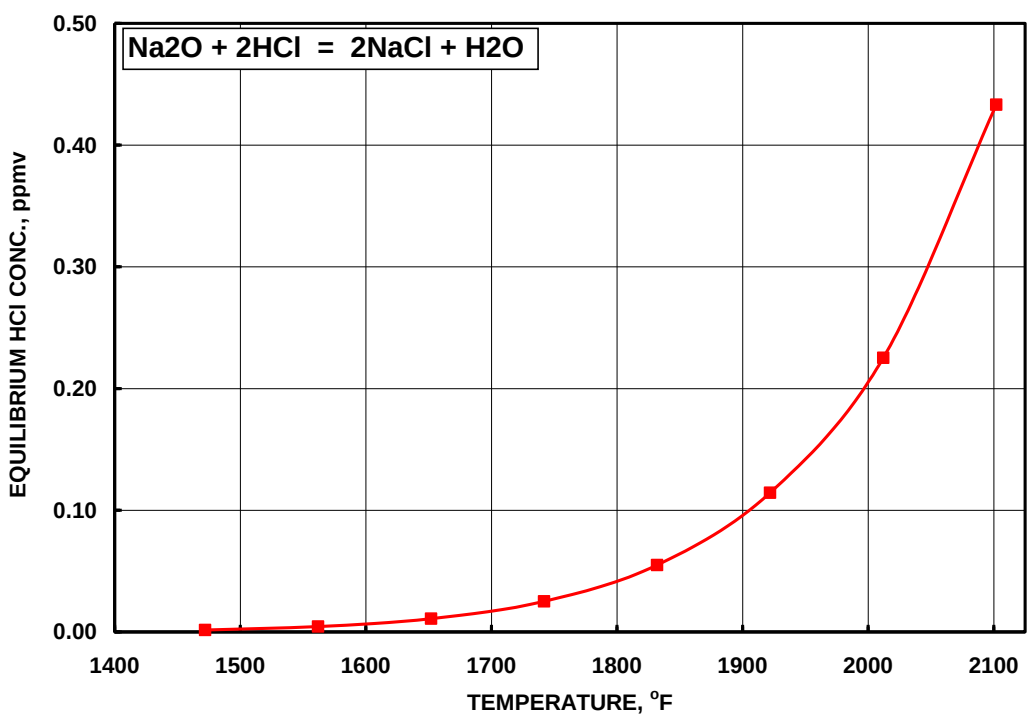

Source: Gas Technology Institute

A similar approach was applied to address HF removal to acceptable levels. A quick screening of selected candidates also identified Na-based materials as potentially suitable for HF control. Figure 11 shows that at flue gas temperatures up to about 1,800ºF, sub-ppm HF levels could be

expected in the cleaned flue gas upon equilibration with Na_2O ($Na_2O + 2HF = 2NaF + H_2O$). This is desirable since one single material could be injected to control both HCl and HF simultaneously. It remains to be seen if any synergy exists so that HCl removal would bring about more efficient removal of HF in the temperature range 1,800 to 2,100ºF. Alternatively, efforts should be directed at conducting a more thorough assessment to identify an alternative, more efficient material to remove HF to the desired level in this temperature range.

Figure 11: HCl and HF Removal by Nahcolite or Trona

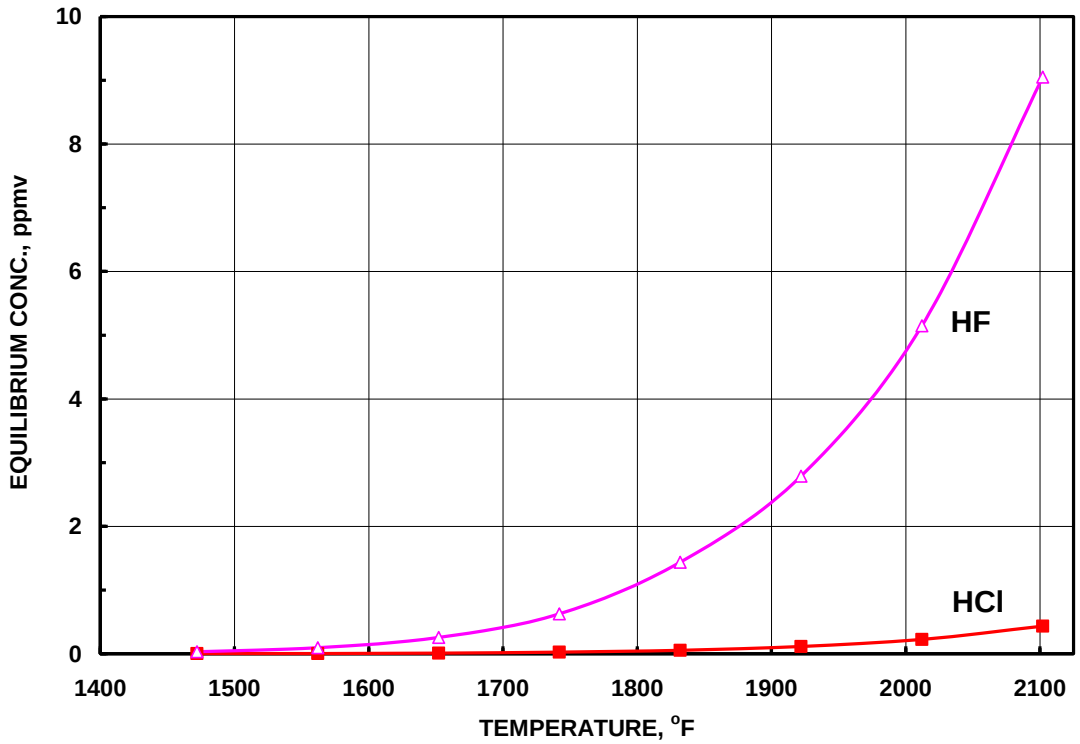

Source: Gas Technology Institute

These HSC-based simulations provided encouraging indications (based solely on thermodynamics) that the sorbent-based approach might work for removing HCl and HF from the aluminum remelt furnace exhaust gases to very low levels at temperatures up to 2,100ºF. Neutralizing both HCl and HF simultaneously (to alleviate or eliminate their corrosive effects on a metallic reformer module and metallic recuperator) appeared to be feasible by injecting one single material. However, other issues must be considered, notably extensive experimental testing, to further assess the practicality of this approach. Finely divided sorbent material might cause a higher pressure drop than desirable. Coarse material, which would address the pressure drop issue, might have very little active surface area for reaction relative to finer material) and its activity might thus be depleted rapidly, resulting in high cleanup system maintenance costs. Given the very high temperatures involved, there was every reason to expect that a good balance could be struck between the sorbent particle size and utilization of the active component (e.g. Na). The project team expected that even if relatively coarse particles

(~1 mm [0.0394 inch] particle diameter), high Na utilization might result despite the low contaminant concentrations in the feed gas. Obviously, this would be desirable to minimize the quantity of this once-through sorbent.

Clearly, in addition to the experimental work conducted in this project, future efforts should be devoted to determining a suitable gas/solid contactor that could be used for this application. The project team would utilize its experience in other related gas cleaning projects to select a suitable contactor (low pressure drop and sufficient residence time) to optimize sorbent utilization and contaminant (HCl and HF) removal efficiency.

2.2.3.3 Preparation of Laboratory Facility and Materials Procurement

GTI's Hot Gas Cleanup Laboratory housed the small-scale reactor facility that was selected in this basic research study for performing tests which involved contacting of solids and gases. A schematic diagram of the modified high-temperature sorbent test facility is shown Figure 12 below.

Figure 12: Schematic of the High-Temperature Sorbent Test Facility

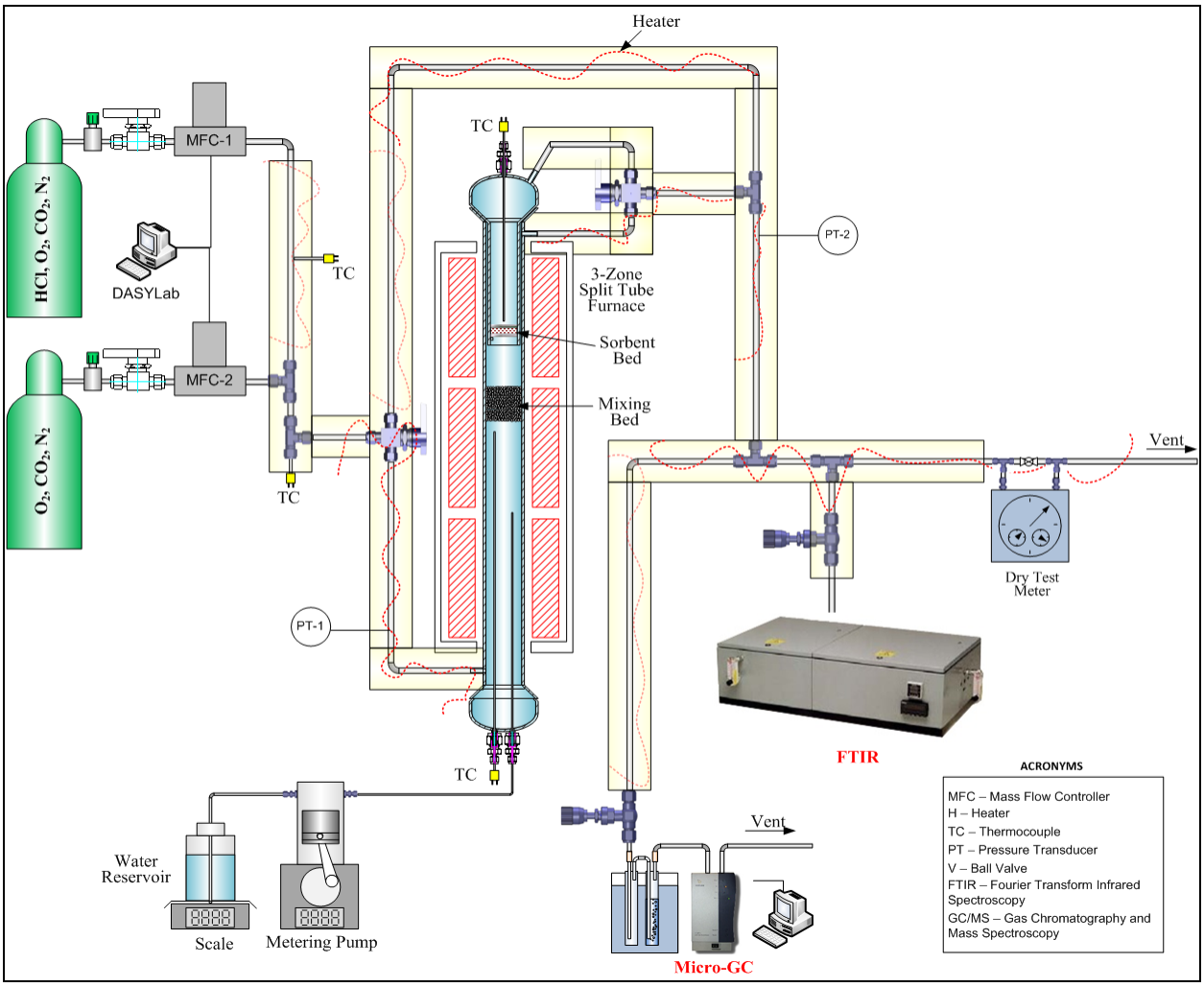

Source: Gas Technology Institute

A photo of the actual facility is shown in Figure 13. Flue gas compositions produced during aluminum remelting were simulated by combining two streams of certified gas mixtures containing: 0.15 percent HCl, 2.2 percent O_2, 16.5 percent CO_2, 81.25 percent N_2 and 2.2 percent O_2, 16.5 percent CO_2, 81.25 percent N_2. The necessary moisture content was added in steam form as shown in Figure 12. The HCl concentration was selected to be higher than concentrations of HCl typical for aluminum remelting furnace exhaust flue gases. This was done to reduce the time needed to observe the sorbent saturation and loss of its HCl removal capacity. A Fourier Transform Infrared Spectrometer (FTIR) was used to monitor the levels of residual HCl (and HF, if used) during testing. A Varian CP-4900 Micro-Gas Chromatograph was utilized to monitor the concentrations of CO_2, O_2, and N_2.

Figure 13: Photo of the GTI High-Temperature Sorbent Test Facility

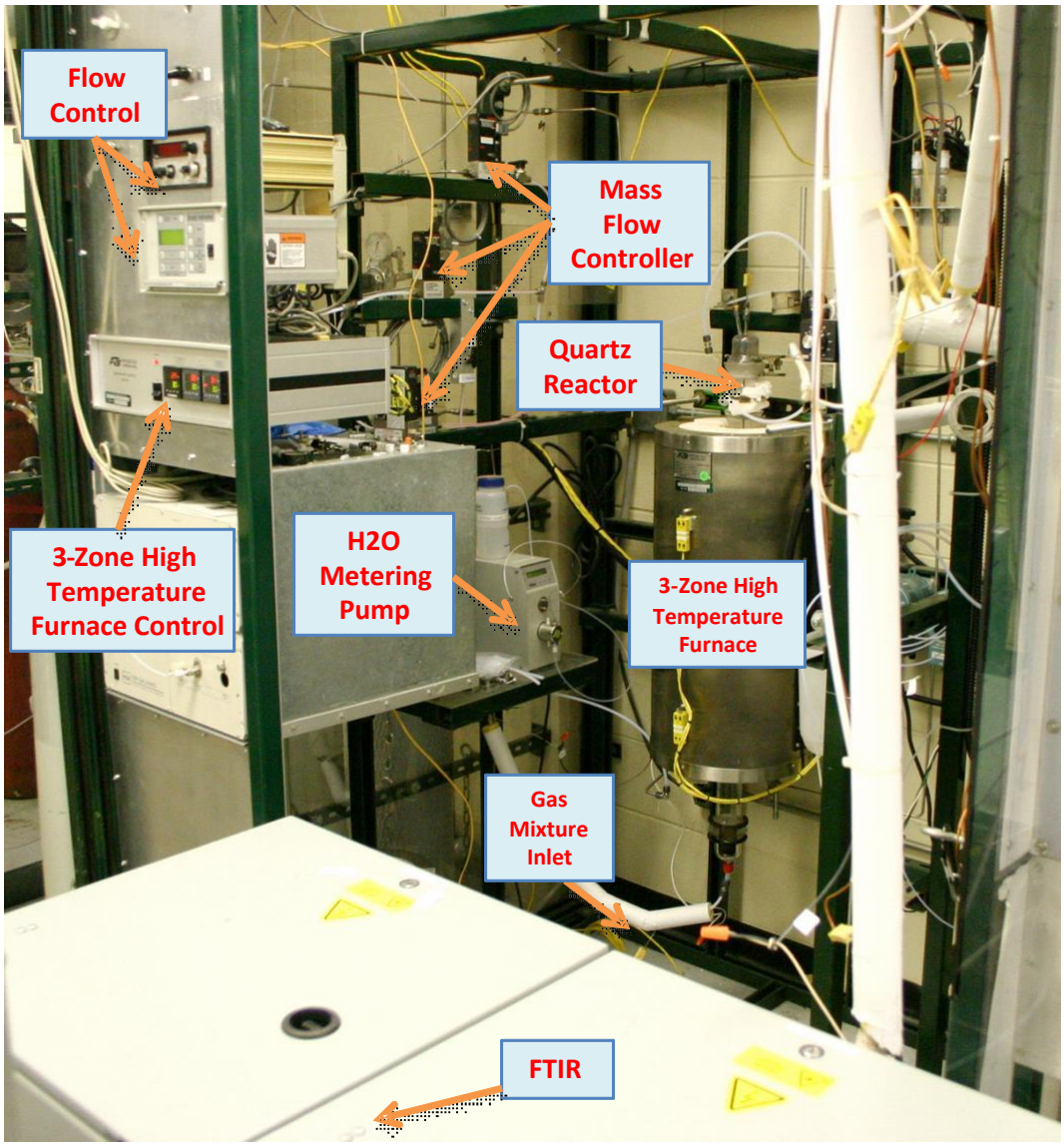

Photo Credit: Gas Technology Institute

The commercial catalyst/sorbent manufacturers identified initially as potential sources for the selected sorbent materials are shown in Table 3.

Table 3: Examples of Chloride Removal Materials and their Sources

Material	Source
Nahcolite ($NaHCO_3$)	White River Nahcolite Minerals LLC, Rifle, Colorado
Trona ($Na_2CO_3 \bullet NaHCO_3 \bullet 2H_2O$)	FMC, Green River, Wyoming
Synthetic Dawsonite	Chattem Chemicals, Chattanooga, Tennessee
Katalco 59-3	Synetix (USA), Oakbrook Terrace, Illinois
G-92C	United Catalysts, Inc. (now Süd-Chemie), Louisville, Kentucky
Na-bearing minerals	Solvay Minerals, Green River, Wyoming

Source: Gas Technology Institute

GTI used its prior experience with halide removal to identify sorbent materials to screen in the laboratory tests. Known vendors were contacted to obtain sample material from the most likely sorbents in their product line. The sorbents that could be used at Thorock Metals will be either pellets or powder. The pellet materials are typically fixed in a container that the gas flows through, like in a car's catalytic converter. The powder materials are typically injected into the gas, and then removed by filters downstream. The decision about which material to select for the field demonstration involved trade-offs between cost, material handling, and performance. The laboratory tests helped quantify the differences in performance to inform the material selection decision.

The materials selected for screening are listed below:

1. <u>Sodium Bicarbonate</u> (Nahcolite), from vendor Solvay Chemicals
    a. Nahcolite is a naturally occurring mineral
    b. Operating range: 275-800°F (possibly can sinter at higher temperatures)
    c. Filling density: 68-75 lb/ft^3 (powder)
    d. Composition: $NaHCO_3$ > 99 percent by weight
    e. Anticipated fluidization velocity: 0.05 actual liters/minute (0.013 gallons/minute); expected to fluidize at laboratory flow rates
2. <u>Trona (Solvay T-50 or T-200)</u>, from vendor Solvay Chemicals
    a. Trona is a naturally occurring mineral
    b. Operating range: 300-1,800°F

c. Filling density: 69 lb/ft^3 (powder)

d. Composition: $Na_3H(CO_3)_2 \cdot 2H_2O$ 90-93.5 percent; H_2O, insoluble, 6.4-10 percent; NaCl 0.1-0.3 percent

e. Anticipated fluidization velocity: 4 actual liters/minute (1.06 gallons/minute); expected to fluidize at laboratory feed rates

3. <u>HTG-1</u>, from vendor Haldor-Topsøe

   a. HTG-1 is an engineered catalyst

   b. Operating range: ambient – 750°F

   c. Filling density: 42. lb/ft^3 (extruded rings)

   d. Maximum capacity: 31.5 lb Cl/ft$_3$ of sorbent (18 lb Cl / 100 lb material)

   e. Composition: potassium chloride (KCO_3), Aluminum oxide (Al_2O_3)

   f. Anticipated pressure drop over a fixed bed: 0.2 psi (low flow) to 1.7 psi (high flow)

4. <u>Actisorb Cl2</u>, from vendor Süd Chemie

   a. Actisorb Cl2 (formerly G-92C) is an engineered catalyst

   b. Operating range: above 650°F

   c. Filling density: 45±5 lb/ft^3 (pellets)

   d. Composition: Na_2O 7 percent; Al_2O_3, balance

   e. Anticipated pressure drop over a fixed bed: 0.1 psi (low flow) to 1 psi (high flow)

The operating temperature of the gas guard recuperator is expected to be around 1,600°F, meaning the Trona and the Actisorb Cl2 will probably perform best.
Figure 14 is a photograph of the two received catalysts.

Figure 14: HCl/Halide removal sorbents: Actisorb Cl2, Previously Named G-92C (left), and HTG-1 (right).

Photo Credit: Gas Technology Institute

2.2.3.4 Test Matrix Development

Selection of candidate materials and testing approaches and priorities were determined based on the following criteria:

a. Contaminant removal efficiency

b. Operation at highest possible temperature

c. Effective contaminant removal capacity

d. Feasibility of removing both contaminants (HCl and HF) with one material

These criteria and their rationale were explained further in Table 4. Based on these considerations and the prior limited test results in an earlier in-house study at GTI [Slimane, R. 2008], the Test Matrix shown in Table 5 was carefully defined to guide laboratory testing in the project. Because of the challenging nature of working with HCl and HF (tendency to stick to flow control equipment, transport lines, gas preheat sections, etc.) and the difficulties associated with sampling and analysis of these two species at sub-ppmv levels, the Test Matrix emphasized developing definite answers to key GGR Process performance questions rather than maximizing the number of tests that might have mixed results.

Table 4: Criteria and Rationale for the Test Matrix

Criterion	Rationale
1. HCl removal **efficiency**	Although it was not exactly known at this point in the GGR Process development effort what residual HCl concentration the recuperator could handle long-term (would be determined in future field testing of integrated GGR/thermo-chemical recuperator process), the goal in this project was to remove at least 90 percent of the HCl in the feed gas. Given that HCl in the furnace exhaust gas might be as low as 10 ppmv, project team's first screening criterion was to achieve sub-ppmv levels in the cleaned gas. Based on thermodynamics and prior limited testing at GTI [Slimane, R. 2008], this was achievable with Na-containing materials.
2. Functionality at the **highest possible temperature** within the 1,400 to 1,800°F, while still achieving targeted removal efficiency	Minimize or eliminate the need to cool the exhaust gas
3. Effective chloride removal **capacity** (grams of Cl removed/100 g of sorbent material) at breakthrough (defined arbitrarily in this project at 1 ppmv in the test reactor off-gas)	Optimize material utilization in this once-through application to prolong sorbent use and minimize required change-outs, and reduce sorbent-related costs (procurement and disposal).
4. **Bi-functionality**, i.e. capability to remove HF in addition to HCl with the same sorbent material	Provide a "one-box" solution for both contaminants to improve GGR Process economics.

Source: Gas Technology Institute

Table 5 presents details on the Test Matrix, which comprised approximately 10 comprehensive laboratory tests. Most of the materials selected for these tests were very specific, and had previously been used in prior GTI projects (typically in coal and/or biomass gasification and gas cleaning applications) [Slimane, R. 2001]. Some of the materials, such as nahcolite and trona, might be acquired from different vendors.

Table 6 shows already available analyses for selected materials; their properties add credence to both their selection for testing in this project as well as to the testing priorities that were proposed. Not all process parameters could be investigated in this limited-scope task. For example, whenever possible, particle sizes for test materials were limited to 180-300 μm (0.18 – 0.30 in) to ensure good gas/solid contact and avoid gas channeling, and to evaluate all materials in an identical reactor configuration. Finally, it was emphasized from the onset that certain underlying assumptions might or might not pan out, and therefore, the Test Matrix was to be regarded as a "live" document that would be continually modified as needed based on test results. A good example was the decision to proceed initially with using an HCl concentration of about 1500 ppmv (up to 150 times the HCl concentration in the actual aluminum remelt furnace exhaust) in the inlet gas to accelerate the laboratory testing.

Table 5: Test Matrix Initially Defined for the Laboratory Testing Task

Test No.	Material and Test Details	Rationale
1	**Actisorb Cl2 (G-92C)**: evaluate at 1,400ºF, 1,600ºF, and 1,800ºF for 4 hours at each temperature	Establish HCl removal efficiency and highest possible operating temperature. The Actisorb Cl2 material was selected for this purpose due to prior encouraging results.
2	**Katalco 59-3**: evaluate at 1,400ºF, 1,600ºF, and 1,800ºF for 4 hours at each temperature	Evaluate as a potentially cheaper and with higher effective chloride capacity than Actisorb Cl2.
3	**Actisorb Cl2 (G-92C)**: evaluate at highest possible temperature for as long as needed to achieve breakthrough	Determine effective chloride removal capacity
4	**Katalco 59-3**: If Test No. 2 results were favorable, evaluate at highest possible temperature for as long as needed to achieve breakthrough	Determine if higher Na content for this material translate into higher effective chloride removal capacity, i.e., a more economical alternative to Actisorb Cl2

Test No.	Material and Test Details	Rationale
5	**Actisorb Cl2 or Katalco 59-3** (depending on test results): evaluate combined HCl and HF removal in a long-duration test (to breakthrough) under conditions identical to those of Tests 3 or 4. [Note: feasibility remained to be determined based on safety considerations related to handling of HF in a laboratory facility]	Evaluate bi-functionality and any adverse effects on HCl removal performance; establish reproducibility of HCl removal test results
6	**Synthetic Dawsonite**: evaluate at highest possible temperature for HCl removal efficiency, and if results were favorable, continue testing to breakthrough.	This material should be cheaper than Actisorb Cl2 and Katalco 59-3. Similar to these two materials, it did contain Na that was also supported by alumina. Its higher Na content could be an advantage.
7	**Nahcolite**: If material sustained the above test conditions (to be determined based on additional thermodynamic analysis), evaluate at highest possible temperature for HCl removal efficiency, and if results were favorable, continue testing to breakthrough.	Material abundantly available as a cheap mineral. [Note: at the highest possible temperature, the manufactured materials might not have significant advantage over minerals, because of sintering]
8	**Trona**: If material sustained the above test conditions, evaluate at highest possible temperature for HCl removal efficiency, and if results were favorable, continue testing to breakthrough.	Material abundantly available as a cheap mineral. [Note: at the highest possible temperature, the manufactured materials might not have significant advantage over minerals, because of sintering]
9	**Best performing material**: evaluate effect of space velocity based on anticipated operating conditions in the actual application	Develop guidelines for gas-solid contactor design for field-testing in Task 3.

Test No.	Material and Test Details	Rationale
10	**Best performing material**: effect of HCl concentration in feed gas on chloride removal efficiency and effective sorbent capacity	More realistic assessment of best performing material by using a significantly lower HCl concentration than used in tests 1 through 9.

Source: Gas Technology Institute

Table 6: Chemical and Physical Properties of Selected Candidate HCl Removal Materials

Nahcolite:	$NaHCO_3$
Trona:	$Na_2CO_3 \bullet NaHCO_3 \bullet 2H_2O$
Synthetic Dawsonite:	$NaAl(OH)_2CO_3$

		Trona	Nahcolite	Synthetic Dawsonite	Katalco 59-3	Actisorb Cl2 (G-92C)*
Aluminum	Al			17.6	37.3	39.6
Carbon	C	10.68	14.07	7.51		
Hydrogen	H	1.84	1.38	2.52		
Sodium	Na	35.6	26.9	13.5	9.98	6.41
Moisture	H_2O	**	**	**	2.00	---
Theoretical Cl Capacity (g Cl/100 g material)		54.9	41.5	20.8	15.4	9.9
BET N_2 Surface Area (m^2/g)		8.65	9.69	---	66.5	165

* A heterogeneous catalyst for sulfur and chloride removal; support material is Al_2O_3.

** Moisture analysis could not be performed on these materials because of carbonate decomposition during drying step.

Source: Gas Technology Institute [Slimane, R. 2001]

2.2.3.5 Laboratory Testing and Results

Testing with Inert Alumina

Testing with inert alumina (in granular form, 1 to 2 mm [0.392 – 0.787 in] in diameter) was conducted initially to confirm laboratory facility readiness for HCl removal testing with the selected sorbent materials. Test conditions and measured results were summarized in Table 7. This test comprised several testing periods or segments. During each period feed gas or reactor

off-gas was first conditioned and then a slipstream was directed first through the FTIR instrument for measurement of HCl, H_2O, and CO_2; FTIR exit gas was then cooled to remove moisture and the dry sample directed to the micro-gas chromatograph for measuring CO_2, O_2, and N_2. FTIR and micro-gas chromatograph results were then combined to fully characterize the feed and/or reactor off-gas. In Table 7, the measured results were compared to the test target gas composition during each period. In Test Period 1, the feed gas was directed through the reactor by-pass to verify the feed gas composition. In Periods 2, 3, and 4 the feed gas was directed through the alumina bed material at 1,400ºF, 1,600ºF, and 1,800ºF, respectively. In Period 5, the feed gas was again directed through the reactor by-pass. As shown in Table 7, throughout this 3-hour "composite" test, the measured feed gas and reactor off-gas compositions were very close to the target simulated flue gas composition, indicating there were no issues with HCl retention (adsorption) in the gas feed-section equipment, by-pass line, reactor parts, and off-gas conditioning and transport lines to the measuring instruments. These results confirmed system readiness for HCl removal testing.

Table 7: Results Summary of Testing with Alumina as a Bed Material

Test Period	1	2	3	4	5
Feed Gas to:	By-pass	Reactor	Reactor	Reactor	By-pass
Bed material	Alumina	Alumina	Alumina	Alumina	Alumina
Temperature, ^{o}F	1400	1400	1600	1800	1800
Pressure, psia	14.7	14.7	14.7	14.7	14.7
Space Velocity, h^{-1}	2500	2500	2500	2500	2500
Feed Gas Flowrate, cc/min	4220	4220	4220	4220	4220
Test Date, M/DD/YYYY	4/23/2010	4/23/2010	4/23/2010	4/23/2010	4/23/2010
Selected SS Period, hh:mm	11:12 - 11:26	11:28 - 12:00	12:16 - 12:45	13:01 - 13:35	13:37 - 13:53
Target Gas Composition					
CO2, %	15.3	15.3	15.3	15.3	15.3
O2, %	2.0	2.0	2.0	2.0	2.0
H2O, %	7.5	7.5	7.5	7.5	7.5
N2, %	75.1	75.1	75.1	75.1	75.1
HCl, ppmv	1437.0	1437.0	1437.0	1437.0	1437.0
FTIR					
CO2, %	15.1	15.2	15.3	15.3	15.0
H2O, %	7.5	7.4	7.2	7.8	7.9
HCl, ppmv	1458.0	1448.0	1390.0	1344.0	1461.0
Micro-GC (dry basis)					
CO2, %	15.9	15.9	15.9	16.0	15.9
O2, %	2.1	2.1	2.1	2.1	2.1
N2, %	79.2	79.2	79.3	79.3	79.3
Micro-GC (wet basis)					
H2O, %	7.5	7.4	7.2	7.8	7.9
CO2, %	14.7	14.7	14.7	14.8	14.7
O2, %	2.0	2.0	2.0	2.0	2.0
N2, %	73.2	73.2	73.3	73.3	73.3

Source: Gas Technology Institute

Testing with the G-92C Material

The second test evaluated a granular form (300 to 500 micron [0.30 to 0.50 inch]) of the G-92C (aka, Actisorb Cl2) material (produced by staged crushing and sieving of the 2.4 mm by 4.0 mm (0.095 inch by 0.16 inch) extrudates obtained from Süd-Chemie) at 1,400ºF and other conditions

similar to the alumina test. Approximately 52 grams (1.15 lb) of sorbent material was used. Test results were summarized in Figure 15 as measured HCl concentration in the cleaned gas versus sorbent chloride loading (as a more practical unit than test time since it provided for a quick evaluation of the sorbent effective loading at breakthrough). Under the test conditions used, pre-breakthrough time was about 180 minutes, which corresponded to approximately 2.9 g Cl/100 g material loading. During this period, the HCl levels in the cleaned gas were measured at 7 ppmv in average, corresponding to removal efficiencies of 99.5 percent. The sharp breakthrough curve (Figure 15) was an indication of the high reactivity of this material. The somewhat modest conversion of the Na_2O HCl removal component in the G-92C material was likely related to a combination of factors, including its relatively low Na content (6.4 percent), the high HCl inlet gas concentration (about 30 times higher than actual), high space velocity, etc. However, overall this test result was sufficiently encouraging to warrant a follow up test at 1,600ºF to evaluate both the HCl removal efficiency at this higher temperature as well as the sorbent's effective chloride capacity (i.e., Cl loading at breakthrough).

Figure 15: HCl Removal Performance of the G-92C Material at 1,400°F

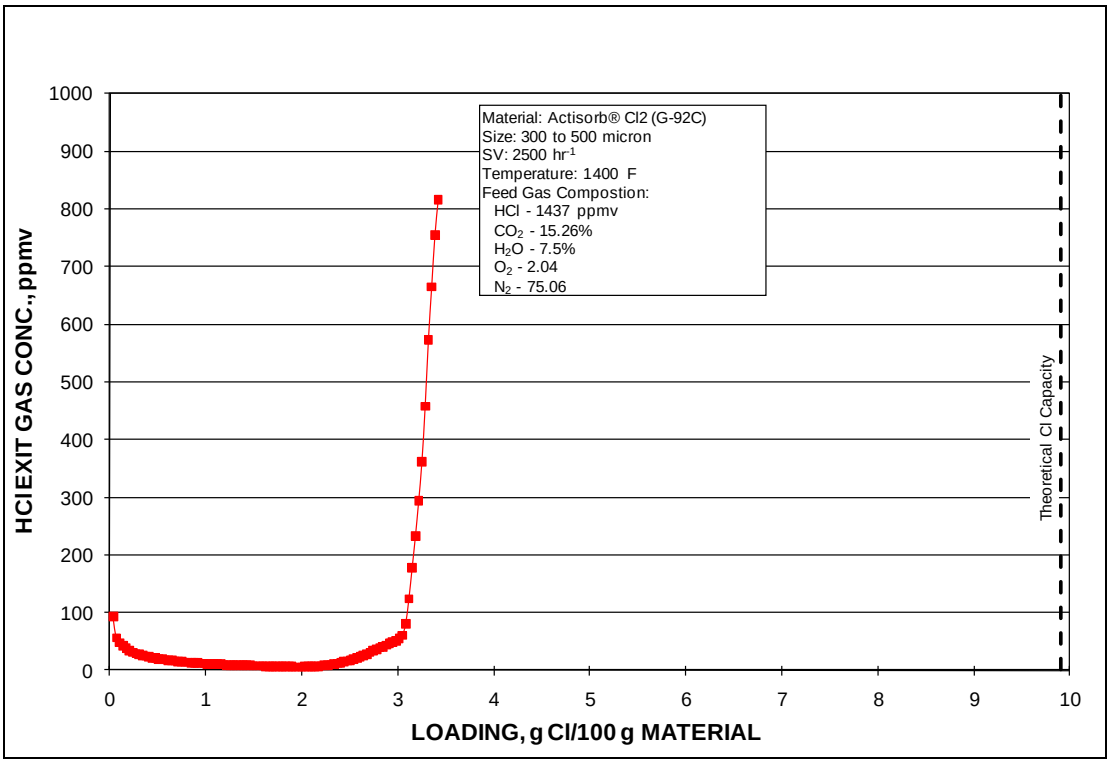

Source: Gas Technology Institute

Based on the 1,400°F test results, the follow up HCl removal test at 1,600°F was conducted to evaluate both the HCl removal efficiency at this higher temperature as well as the sorbent's effective chloride capacity (i.e., Cl loading at breakthrough). Similar to previous tests, the G-92C material used was in granular form (300 to 500 microns [0.30 to 0.50 inch]) and the inlet HCl concentration was maintained at approximately 1,500 ppmv. Moreover, based on the results from tests at 1,400°F and 1,600°F, another test was also conducted at 1,200°F to evaluate any

improvements in HCl removal efficiency and effective chloride capacity at this lower temperature. Such improvements could potentially lead to substantial reductions in sorbent requirements, and therefore improve overall GGR process economics. The results obtained in all three tests were shown in Figure 16. At 1,600°F, both the HCl removal efficiency and chloride loading capacity at breakthrough appeared to be severely reduced, indicating that the G-92C material usefulness for this application might not be realized at temperatures higher than 1,400°F. Significant improvement in HCl removal efficiency (essentially quantitative removal) was measured during testing at 1,200°F, but as shown in Figure 16, only a very modest improvement in effective chloride capacity was obtained. The material achieved approximately 3.25 g Cl/100 g at breakthrough, which corresponded to approximately 33 percent utilization. Based on these results, it was considered quite possible to achieve > 40 percent sorbent utilization (as estimated in the preliminary GGR vessel design guidelines, to be discussed later in this report) in these laboratory tests by reducing the inlet HCl concentration ($[HCl]_0$) in the simulated furnace exhaust gas mixture (for example, from 1,500 ppmv to 250 ppmv). It should be noted that the laboratory tests were conducted at a space velocity that was very similar to that used in the preliminary design estimates. [Note: space velocity is a measure of residence time and represents the number of volume changes through the sorbent bed per unit time, with gas volume converted to standard temperature of 70°F and standard pressure of 14.696 psia].

Figure 16: HCl Removal Performance of the G-92C (Actisorb Cl2) Material at 1,200, 1,400, and 1,600°F

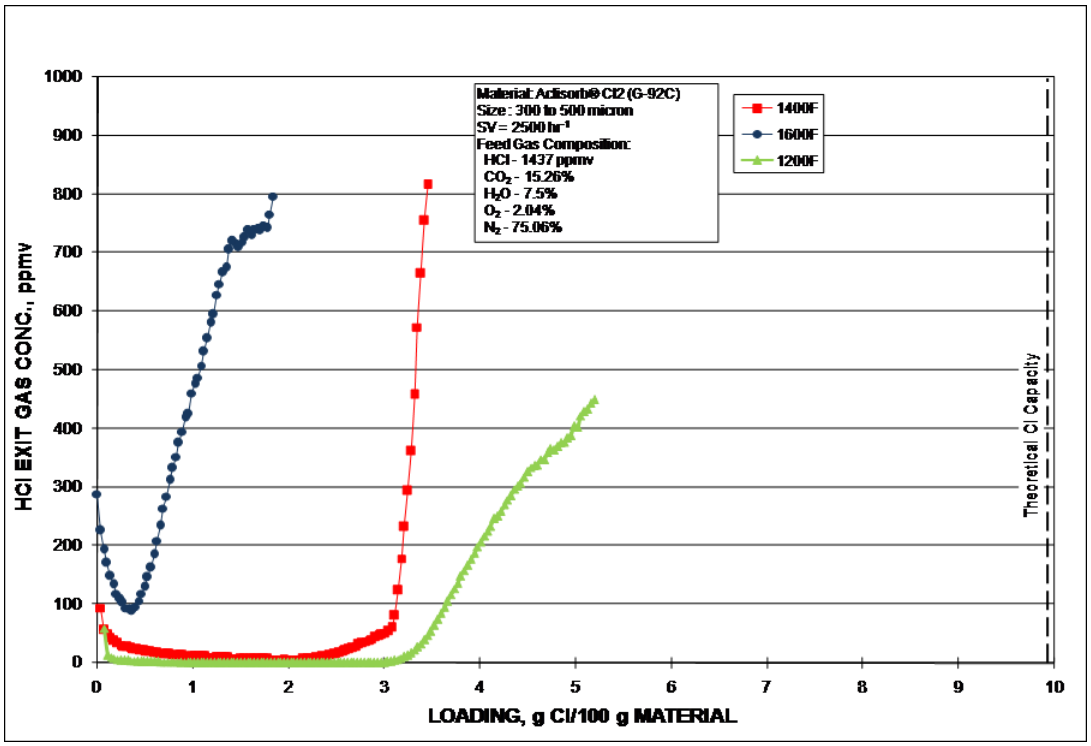

Source: Gas Technology Institute

Based on test results subsequent testing focus shifted to: (a) evaluating the G-92C material HCl removal performance with lower inlet HCl content in the simulated exhaust furnace flue gas (i.e., approximately 250 ppmv instead of 1,500 ppmv), in order to promote sorbent utilization and evaluate performance under conditions closer to those that would be experienced in the field; (b) use test results as a basis for deciding whether or not to evaluate the G-92C material at lower temperature (1,200°F); and (c) prepare alternative chloride removal materials for testing, as planned.

The granulated G-92C material (300 to 500 microns [0.30 to 0.50 inch]) was evaluated again at 1,400°F, but with a feed gas containing only about 250 ppmv HCl. The certified (2.21 percent O_2, 16.49 percent CO_2, 81.14 percent N_2, 1,559 ppmv HCl) flue gas mixture was first diluted with air (63 vol percent gas mixture/37 vol percent air, consistent with the anticipated field demo conditions shown in Figure 17) and then diluted further with N_2. The resulting feed gas mixture consisted of approximately 1.3 vol percent H_2O, 2.6 percent O_2, 2.7 percent CO_2, 93.3 percent N_2, and 250 ppmv HCl. The space velocity was maintained at approximately 2,500 h^{-1}, consistent with prior testing as well as preliminary GGR vessel design estimates. Because results from this test did not show any improvement in performance (and additionally were inconsistent with expectation, as explained below), another fresh batch of the granulated G-92C material was prepared and also evaluated under similar conditions, but at the lower temperature of 1,200°F. Results from these two tests were provided in Figure 18, along with previous results at 1,400°F with this material with approximately 1,437 ppmv HCl in the feed gas (7.5 vol percent H_2O, 2.0 percent O_2, 15.3 percent CO_2, 75.2 percent N_2).

Figure 17: Process Flow Diagram for a GGR Process Field Demo Configuration

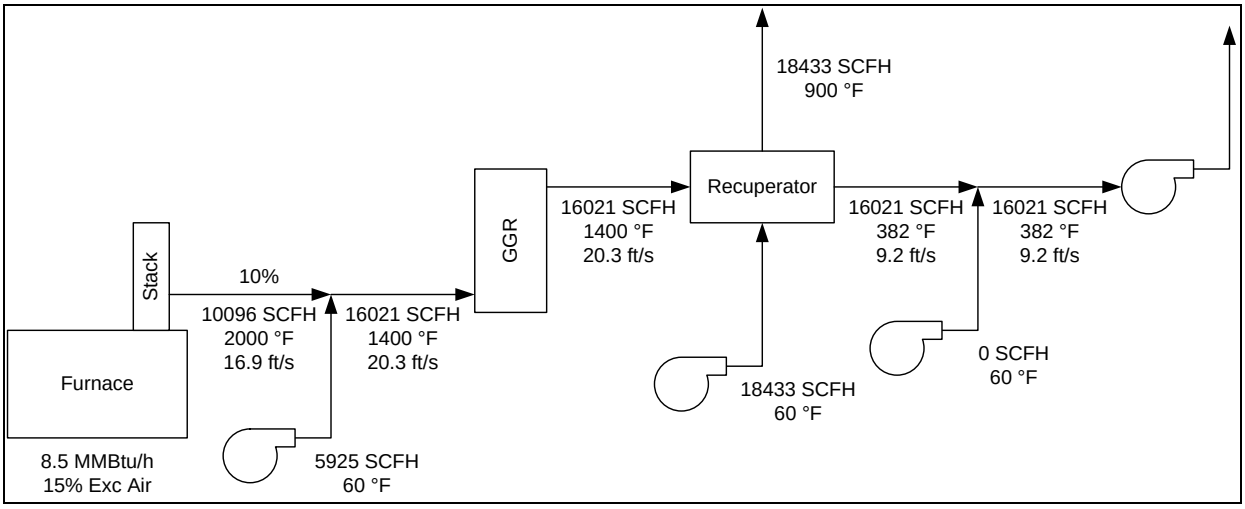

Source: Gas Technology Institute

Figure 18: Chloride Removal Performance with the G-92C Material at 1,400°F and 1,200°F with 2 Different Levels of HCl in the Feed Gas

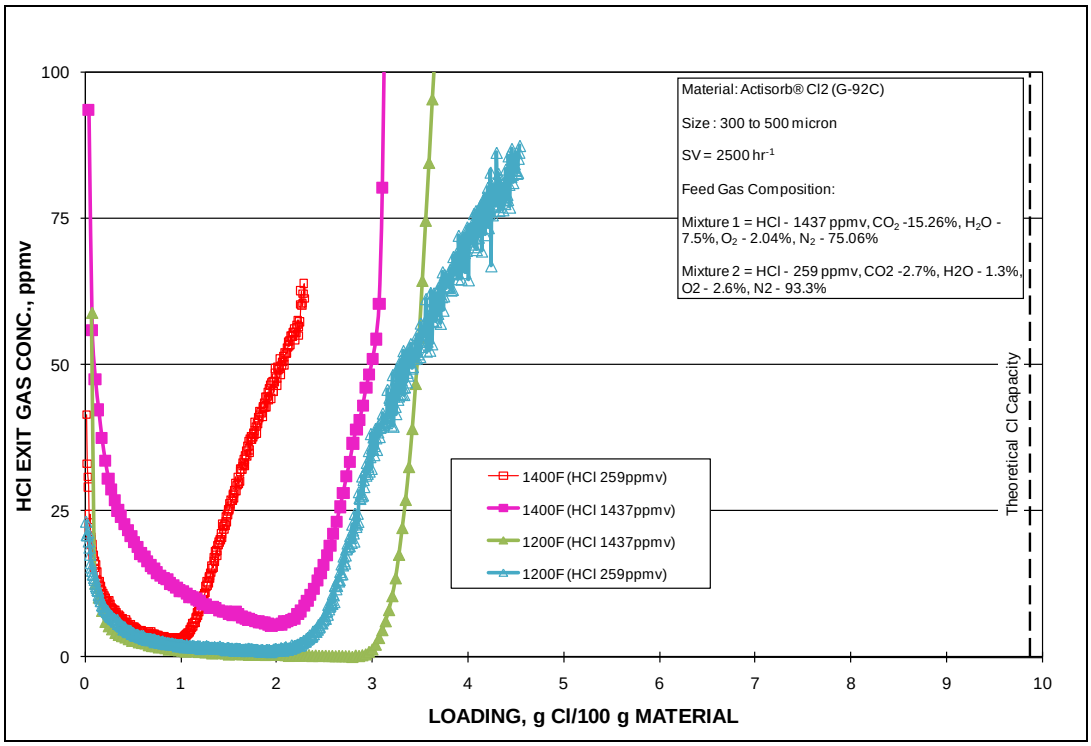

Source: Gas Technology Institute

At 1,400°F, results indicated the G-92C material achieved slightly more efficient chloride removal with lower HCl in the feed gas; essentially similar efficiencies were measured at 1,200°F, independent of the HCl level in the feed gas. However, inconsistent with expectation, in both cases (at 1,400°F and 1,200°F) the effective chloride removal capacity (i.e., at breakthrough) was significantly lower when using 250 ppmv HCl in the feed gas compared to 1,437 ppmv. These results were surprising because at a given temperature (in this case 1,400°F), one would expect a sorbent material to achieve higher (or at least similar) chloride loading when using lower contaminant (e.g., HCl) concentration in the feed gas.

As previously described, the 1,400°F test with 1,437 ppmv HCl lasted 2 hours 36 minutes, which corresponded to an effective chloride removal capacity of about 2.6 g Cl/100 g of material. The test at the same temperature, but with 250 ppmv HCl lasted 5 hours 3 minutes, an effective chloride removal capacity of about 1 g Cl/100 g of material. Similarly, at 1,200°F the test with 1,437 ppmv HCl lasted 3 hours (3.2 g Cl/100 g of material), while the test with 259 ppmv lasted approximately 11 hours 19 minutes (2.1 g Cl/100 g of material).

Since there was no logical explanation for these results, two additional tests were conducted to develop some further understanding. First, an additional test (1,200°F, 1,437 ppmv HCl) was completed to establish reproducibility and ensure there were no technical issues with use of HCl in the feed gas. Second, another test was completed also at 1,200°F and 1,437 ppmv HCl,

but this time the sorbent bed was held under nitrogen flow at the test temperature (1,200°F) for about 9 hours before the simulated furnace exhaust gas was introduced to the reactor. The main purpose was to verify if sorbent exposure to high temperature for prolonged periods had an adverse effect on its chloride removal performance (this would have undesired consequences for the field demo unit, if the G-92C material was to be recommended as the best sorbent candidate). Results from the reproducibility test are shown in Figure 19, indicating reasonably good agreement.

Figure 19: Reproducibility of Test Results

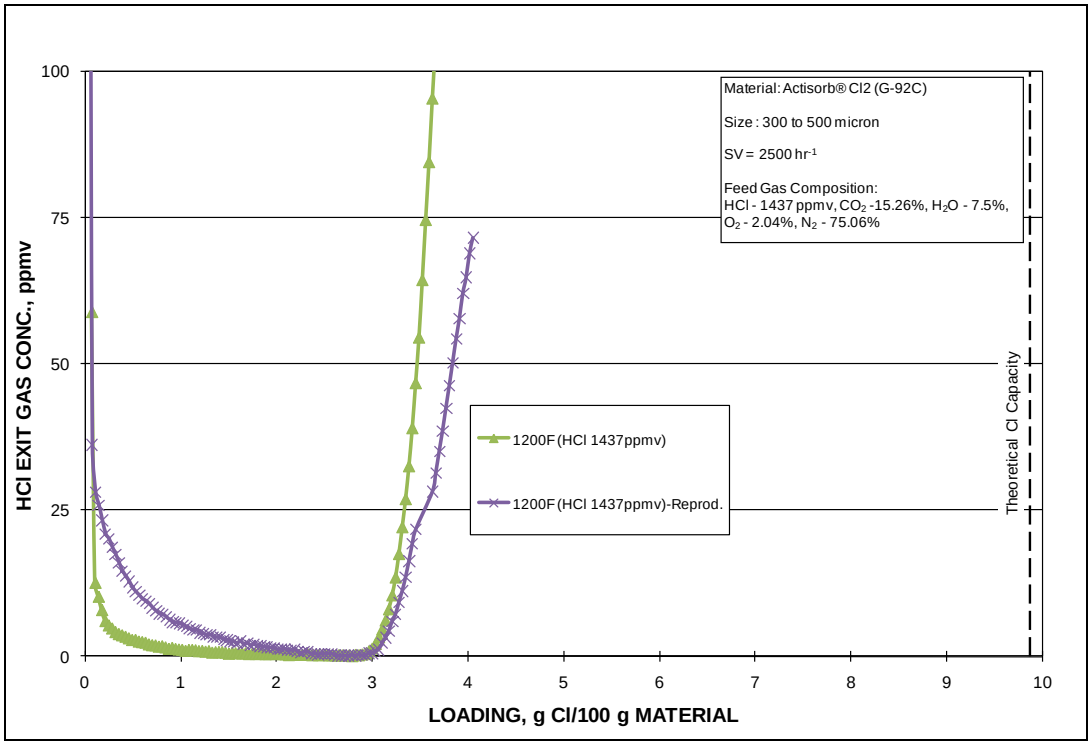

Source: Gas Technology Institute

2.2.3.6 Preliminary Design of the Slipstream GGR Unit

Preliminary sizing estimates were developed for the Slipstream GGR unit. The main purpose for this initial design was for use in discussions with potential host sites in the field demonstration work in Task 3 of this project. Table 8 summarizes the key process variables taken into consideration in this exercise and the assumptions made. The Slipstream GGR unit was designed to handle approximately 10 percent of the exhaust gas stream from a typical industrial aluminum re-melt furnace containing 50 ppmv HCl and 10 ppmv HF, and having an overall composition similar to that used in the laboratory support work (overall composition is not a key performance factor). A 90 percent HCl and HF removal efficiency was imposed, and was assumed to be realized by the Actisorb Cl2 (G-92C) commercial chloride guard material, which contained approximately 6.4 percent Na (corresponding to a theoretical chloride removal capacity of about 9.8 g Cl/100 g of material). Given the prior results obtained with this material and its favorable physical and chemical characteristics (see Table 6), the expected sorbent

utilization was estimated at 40 percent (i.e., sorbent-to-contaminant molar ratio of 2.5). Another important consideration in this initial sizing estimate was that the Slipstream GGR unit should accommodate up to five (5) continuous days of field testing before sorbent change-out would become necessary. This relatively long field-testing duration, the use of inlet HCl and HF concentrations that were likely higher than those in a real aluminum re-melt furnace, and a sorbent material with relatively low Na content, made these sizing estimates somewhat conservative, which was desirable. Yet, as shown in Table 8 the Slipstream GGR unit could potentially be relatively compact, with a diameter less than 2 feet and a height less than 5 feet.

Estimated dimensions are provided in Figure 20. It should be emphasized that the schematic shown in Figure 20 by no means represented a final design for the Slipstream GGR unit, as other considerations, most notably pressure drop, must also be taken into account. In this initial effort, it was constructed similar to a Sulfur Guard Bed vessel design (installed in GTI's pilot-scale gasification facilities, Flex-Fuel Test Facility) with some modifications to accommodate the much higher temperatures required in this application, as shown in Figure 20.

Table 8: Preliminary Sizing Estimates for the Slipstream Gas Guard Recuperator (GGR) Unit

	Initial Slipstream GGR Sizing Estimates	
Feed Gas Flowrate, SCFH	13566	Assume 10% of exhaust gas stream produced by a typical industrial re-melt furnace
Estimated Composition, mol%		
O2	2.0	
CO2	15.0	
H2O	9.0	
HCl	0.0050	Assume 50 ppmv HCl and 10 ppmv HF before dilution w/ air
HF	0.0010	
N2	73.9940	
Molecular Weight, lb/lb-mol	29.59	
Feed Gas Flowrate, lb-mol/h	37.808	
HCl Flowrate, lb-mol/day	0.045	
HF Flowrate, lb-mol/day	0.009	
HCl to be removed, lb-mol/day	0.041	Assume 90% removal requirement for both HCl and HF
HF to be removed, lb-mol/day	0.008	
Stoichiometric Na Required, lb-mol/day	0.049	Na2O + 2HCl = 2NaCl + H2O
		Na2O + 2HF = 2NaF + H2O
Estimated Sorbent Utilization, %	40	Estimate to be revised based on lab test results
Sorbent-to-Contaminant Ratio	2.5	
Daily Na Requirements, lb-mol/day	0.122	
lb Na/day	2.82	
Sorbent Na Content, %	6.41	Assume Actisorb Cl2 (G-92C) from Sud-Chemie (5 x 8 mesh)
Daily Sorbent Requirements, lb/day	43.93	
Bulk Density, lb/ft3	45	
Active GGR Bed Required Volume, ft3/day	0.976	
Required GGR Active Bed Volume, ft3	4.882	Assume 5-day continuous field testing
Total Volume of GGR Vessel, ft3	8.136	Assume active sorbent bed occupies 60% of total GGR vessel
Sorbent Bed L/D	1.6	Similar to Flex-Fuel Test Facility Sulfur Guard Bed (R-2002)
GGR Vessel Diameter (Internal), ft	1.6	
Sorbent Bed Height, ft	2.53	
Total GGR Vessel Height, ft	4.2	

L/D = length/diameter

Source: Gas Technology Institute

Figure 20: Preliminary Design of a Candidate Slipstream GGR Unit Showing Arrangement of Sorbent Material and Bed Inert Material and Supports

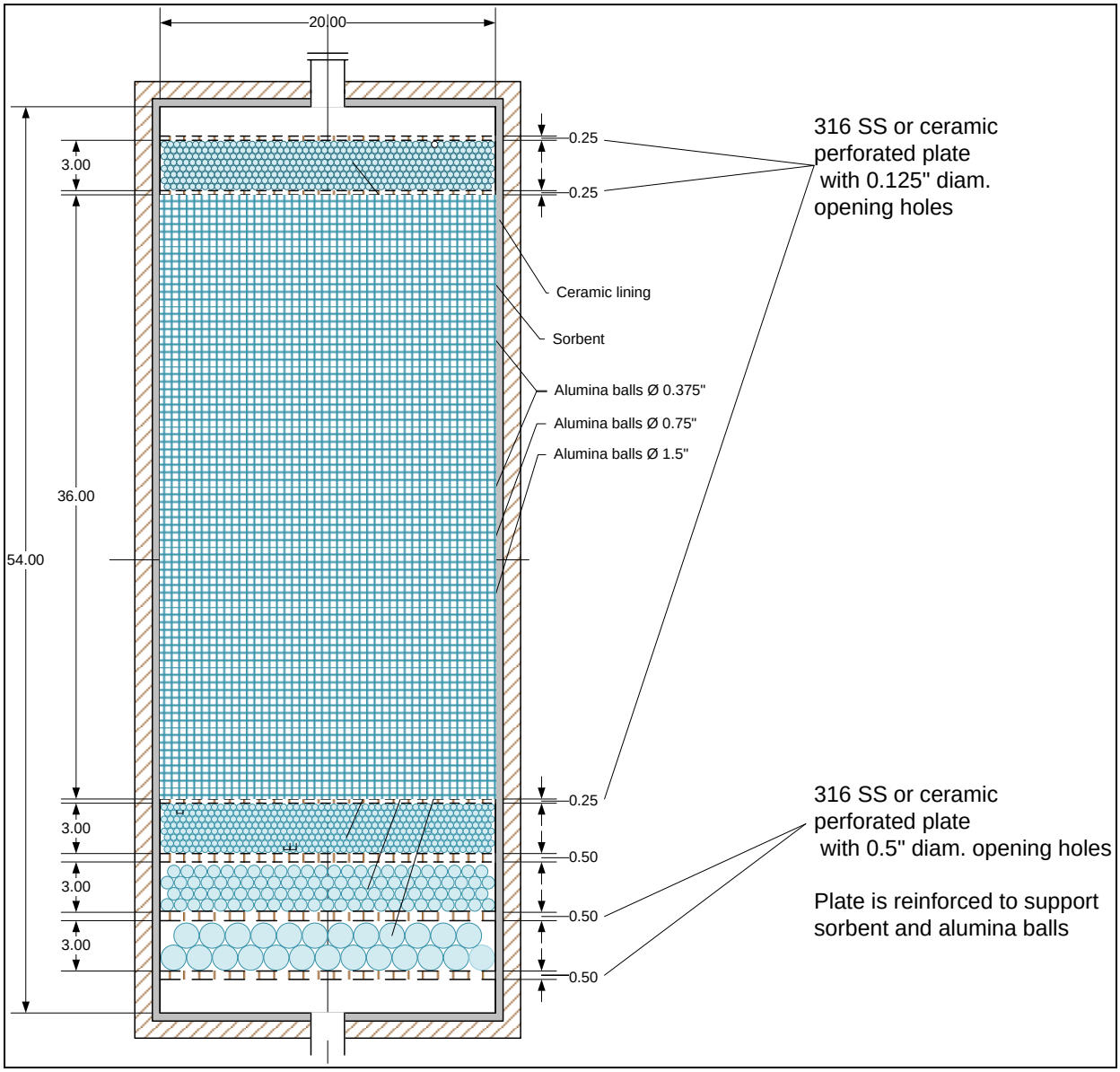

SS = stainless steel

Source: Gas Technology Institute

2.3 Task 3: Fabrication and Field Testing

2.3.1 Objective

The main goal of Task 3 was to fabricate and test a GGR demonstration unit.

2.3.2 Approach and Schedule

Work in this task was divided into three (3) focus areas: designing a GGR demonstration unit and producing fabrication drawings; constructing the GGR demonstration unit and installing it on a furnace; and testing the GGR demonstration unit and analyzing the results.

2.3.2.1 Designing the GGR Demonstration Unit

Extensive modeling was conducted by North Carolina State University (NCSU) to determine the performance of a GGR demonstration unit. This led to a simplification of the preliminary design from Task 2: Phase 1 from five layers of sorbent and ceramic to just two layers. The simplified design was developed into an engineering design by Thermal Transfer Corporation. The engineering design was further refined by GTI and fabrication drawings were produced. A high-temperature 4-way switching valve was also designed by GTI during this effort.

2.3.2.2 Fabrication of the GGR Demonstration Unit

The GGR demonstration unit was constructed, lined with insulation, filled with ceramic and sorbent, interconnected with switching valves, and attached to the exhaust of a furnace at GTI. The unit was instrumented with thermocouples, pressure gauges, and flow meters.

2.3.2.3 Testing of the GGR Demonstration Unit

The GGR demonstration unit was subjected to a cold dry (no HCl) test to set flow rates, and a hot dry test to set furnace conditions and switching frequency. An HCl analyzer was rented. A series of hot wet (with HCl) tests were then conducted.

2.3.3 Results and Discussion

2.3.3.1 Modeling of a Regenerative Gas Guard Recuperator

Introduction

Increasing energy costs require essential improvements in energy utilization efficiencies of industrial systems. In particular, the efficiencies of aluminum melters could be increased by regeneration of useful energy represented by the enthalpy contained in the high temperature exhaust stream. Traditional methods have a limited applicability for these streams due to the presence of corrosive fluoride compounds. Concurrently, the removal of fluoride compounds from high temperature streams is impractical due to the low efficiencies of the absorbents at high temperatures. GGR technology achieves simultaneous removal of toxic and corrosive fluorine compounds and regenerates the energy contained in the high temperature exhaust stream. This concept is depicted in Figure 21.

Figure 21: GGR Concept

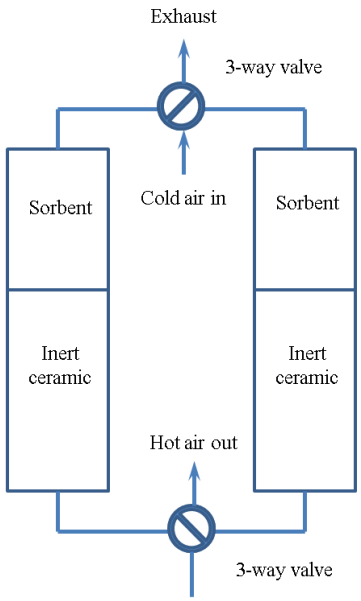

Source: Gas Technology Institute

Project Objectives

The project objective was to develop a numerical model of the regenerative gas guard recuperator. The developed model was used to determine the design specifications of the recuperator and its optimized performance characteristics.

The research efforts were focused on the following tasks:

- Development of a numerical model for heat regeneration in the GGR.
- Development of a numerical model for toxic fluorine compound removal in the GGR.
- Parametric modeling of the GGR to achieve optimal performance characteristics.
- Development of preliminary design specifications based on the numerical predictions of the model.

Results and Discussion

Development of Numerical Model of Heat Regeneration in the GGR

The model is based on the two-dimensional axisymmetric geometry shown in Figure 22. Heat transfer occurring between the solid and gas media is considered. The following assumptions are made to simplify the problem: (i) the geometry is considered to be axisymmetric, taking advantage of faster solution time and lower memory requirements; (ii) the porous media consists of solid pellets dispersed homogeneously and the porosity variation near the wall is neglected; (iii) Kaowool is used as insulation material and it is exposed to natural convection to the ambient.

Figure 22: Diagram of Model with Ceramic Porous and Sorbent Porous Media

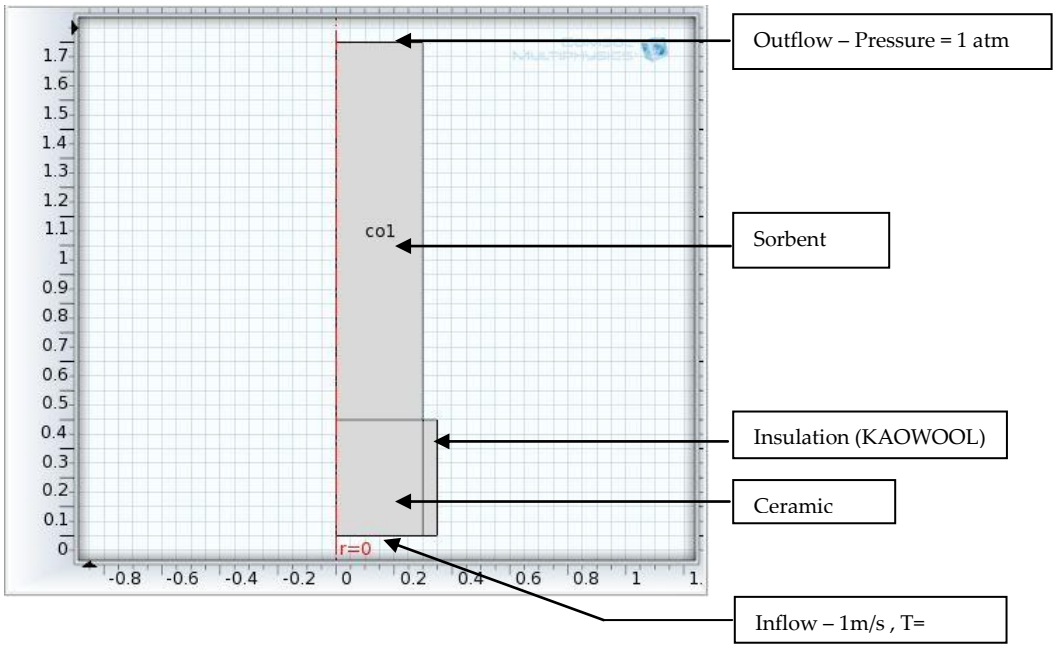

Source: North Carolina State University

An inlet velocity of 1 m/s (3.281 ft/sec) and an inlet temperature of 1,000 degrees Kelvin (K) (1,340.3 °F) are given as input conditions with initial temperature and pressure being 298 K (76.7 °F) and 1atmosphere (atm) (14.7 psia), respectively. The constraint of the analysis is to assure the inlet temperature for the sorbent material was about 650 K (710.3 °F) and the pressure drop across the both domains to be < 500 Pasqual (Pa) (0.07 psia). At the end of the forward cycle, cool air of 300 K (80.3 °F) is forced through the back of the domain for 1,800 seconds to push the temperature profile back to original state.

Forward Cycle

Figure 23 and Figure 24 show the temperature profile variation with time. From Figure 25, we can see that the temperature at the end of the forward cycle to be around 650 K (710.3 °F), continuously increasing as time proceeds. Also the fluid flow velocity in Figure 25 is 0.3 meters per second (m/s) (30.52 ft/sec) near the end of the pipe. In Figure 26 the pressure drop across the two domains is found to be around 515 Pa (0.075 psia).

Figure 23: Temperature distribution at 300 seconds (s), forward cycle.

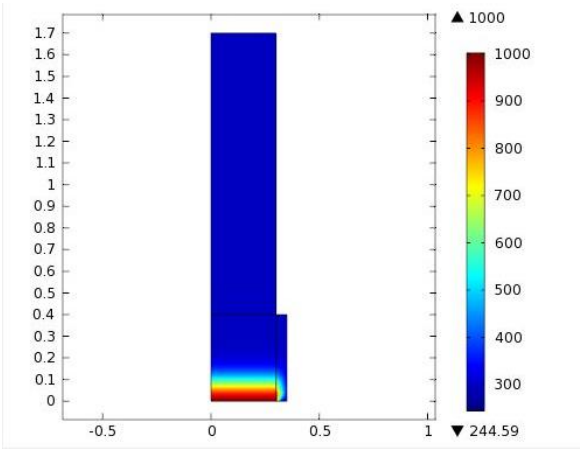

Source: North Carolina State University

Figure 24: Temperature distribution at 1,800 s, forward cycle.

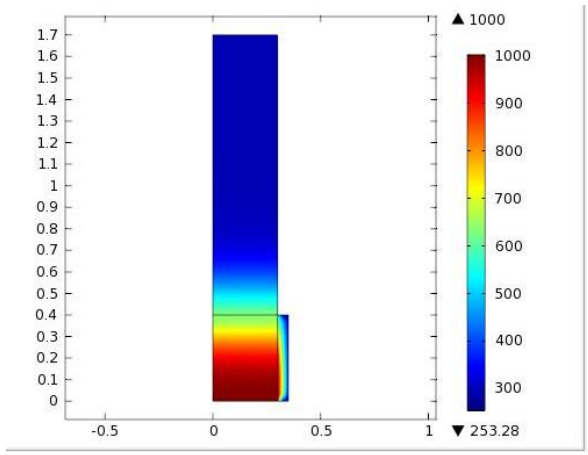

Source: North Carolina State University

Figure 25: Velocity Distribution at 1,800 s, forward cycle.

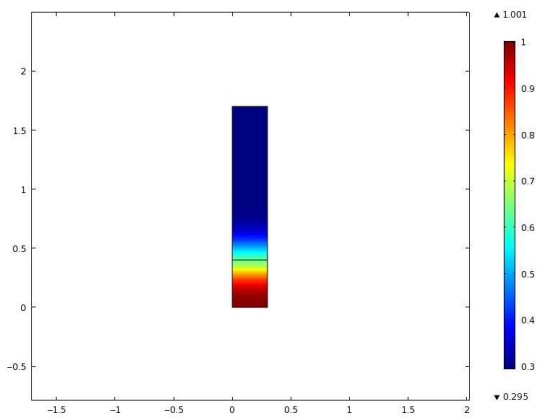

Source: North Carolina State University

Figure 26: Pressure drop at 1,800 s, forward cycle.

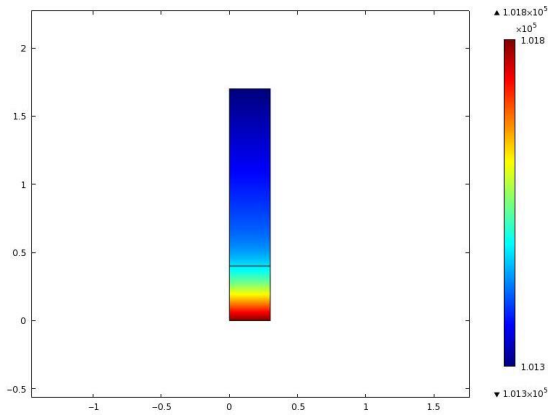

Source: North Carolina State University

Reverse Cycle

Now the boundary conditions are changed and the cold fluid is forced through the top of the pipe at around 300 K (80.33 °F), 0.75 m/s (2.46 ft/sec) and the initial condition for the analysis are taken from the last results of the above state.

As seen from Figure 27 and Figure 28 for the reverse cycle, the temperature profile is pushed backward and the temperature of the domain is close to around 300 K (80.33 °F) in Figure 28 at the end of 1,800 seconds, losses being to natural convection through the insulation boundaries.

Figure 29 shows the velocity distribution at the end of 1,800 seconds. Also the pressure drop shown in Figure 30 across the pipe is close to ~500 Pa (0.07 psia).

Figure 27: Temperature distribution at 300 s, reverse cycle.

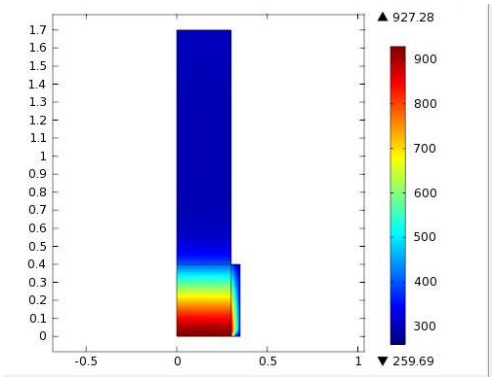

Source: North Carolina State University

Figure 28: Temperature distribution at 1,800 s, reverse cycle.

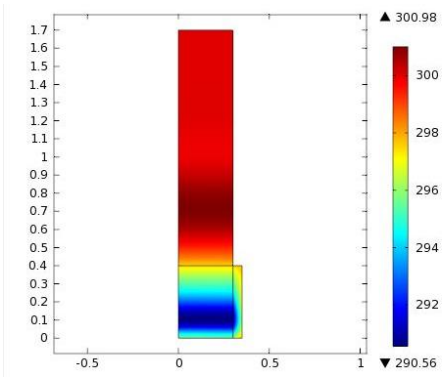

Source: North Carolina State University

Figure 29: Velocity distribution at 1,800 s, reverse cycle.

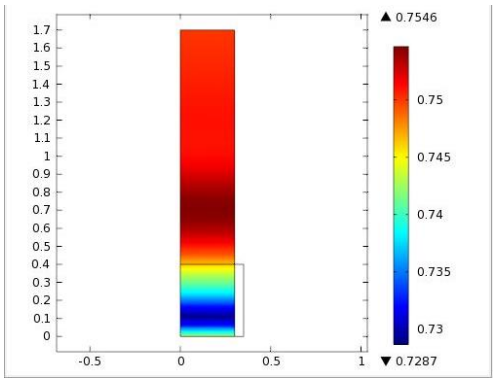

Source: North Carolina State University

Figure 30: Pressure drop at 1,800 s, reverse cycle.

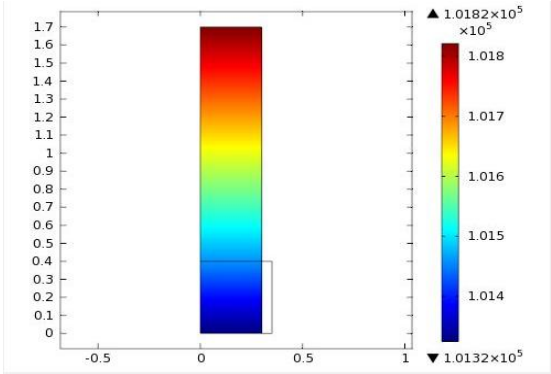

Source: North Carolina State University

The thermal insulation was introduced in the geometry. The external natural convection was added to realistically model the object. The material chosen for insulation is Kaowool, and its properties for thermal conductivity have been incorporated in the model. The cycling required has also been incorporated in the model, enabling the results to be seen at quasi steady state.

Shown below is the change in temperature near the interface between the two porous media over different cycles. This location is critical, from this point the sorbent material will begin and we would like to have the temperature around ~640 K (692.33 °F) or below for effective sorbent adsorption.

Figure 31 shows the temperature variation on the axial center line of the porous model. Over many cycles, the change in temperature is quite small, with differences of about only 130 F (over 10 cycles). As such, the system may have already achieved quasi steady state.

Figure 31: Temperature Variation across the Axial Position over Three Different Cycles

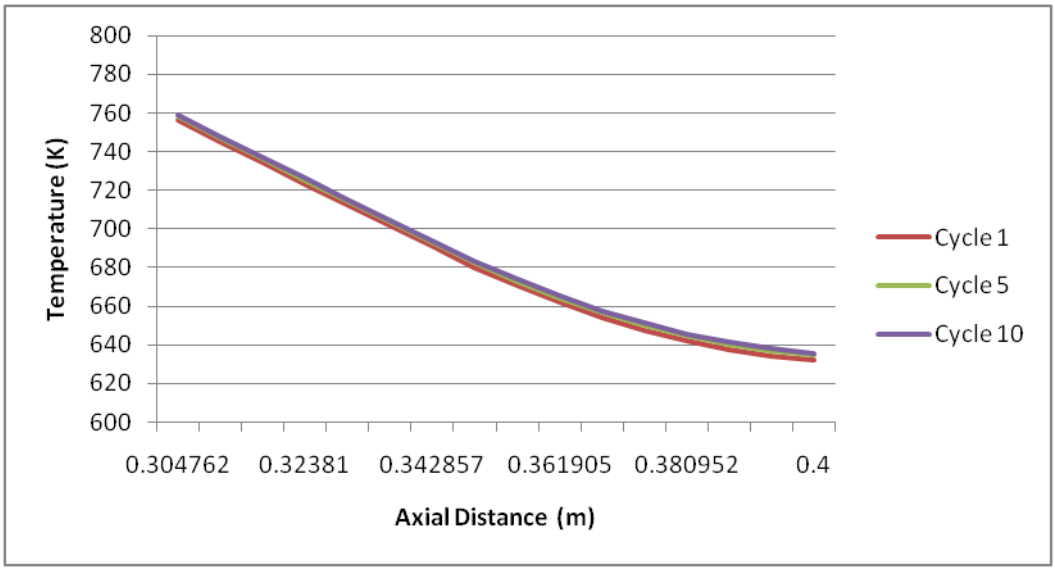

Source: North Carolina State University

Development of Numerical Model of Toxic Fluorine Compound Removal in GGR

A number of sorbents were considered for this application based on published literature. Among the sorbents they had considered includes Na_2CO_3, $NaHCO_3$, $CaCO_3$, CaO and $Ca(OH)_2$. The results indicated Sodium Carbonate was the most effective sorbent, holding Cl for the longest time beyond which breakthrough started to occur.

The sorbent material selected was Sodium Carbonate. Sodium Carbonate is an effective sorbent and has capacity to reduce chorine and fluorine from flue gas having concentration up to 5,000 ppm. Our inlet flue gas composition is only about 50 ppm of HCl or HF.

The reactor model adopted was based on the particle grain model [Wen, C.Y. 1968 pp. 34-35; Mura, G. 1994; Duo, W. 1996 pp. 2541-2546; Weinell, E.C. 1992 pp. 164-171; Verdone, N. 2006 pp. 7487-7496; Pigford, R.L. 1973 pp. 85-91]. . The first equation governs the flow in the porous media and the second equation takes into account the shrinking surface of the grain as the reaction process continues.

The general gas-solid non catalytic reaction can be written as

$$\epsilon_B \frac{\partial C_o}{\partial t} = -U_o \frac{\partial C_o}{\partial x} + D \frac{\partial^2 C_o}{\partial x^2} - r_p \tag{2}$$

where

ϵ_B = porosity of the bed;

C_o = concentration in gas phase;

U_o = filtration velocity;

D = dispersion coefficient;

r_p = reaction rate per unit volume.

This is followed by diffusion in the pores inside the particle to the grains, solid diffusion through the product layer of each of the grain and finally the chemical reaction occurring on the surface of the grain. The important step controlling this process is solid diffusion to the surface (Figure 32), where C_i (mol/m^3) is the concentration of the ith species inside the pore and C_s (mol/m^3) is the surface concentration.

Figure 32: Solid Diffusion through the Product Layer

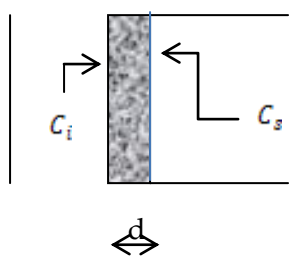

Source: North Carolina State University

Now let us consider in detail the grain present inside the pore. As the reaction starts at the surface of the grain, the products begin to form a layer of thickness, denoted in the above figure by d (in). Further, gases have to diffuse through to this layer to reach the reaction site where the reaction will take place.

The reaction rate at the surface is given by the relation

$$R_s = K_s C_s, \tag{3}$$

where K_s (ft/s) is the rate constant of surface reaction.

The total, reaction rate occurring within a single pore is

$$R_{ip} = 4\pi r^2 n_p \, K_s \frac{D_s C_i}{D_s + K_s(r_o - r)} \tag{4}$$

where n_p is the number of grains per unit volume.

The reaction is considered to be irreversible and first order with respect to concentration of the gas at the reaction surface. This assumption is valid in the range of temperatures under consideration (200 – 600°C [392-1,112 °F]), the equilibrium constant varies from $1.7 \cdot 10^{18}$ to $2.5 \cdot 10^{20}$.

The species transport model has been incorporated within the combined heat transfer and fluid flow model developed. Cycling have been done to observe the variation of the concentration and also to determine the capacity of the sorbent material. Shown below are Figure 33 and Figure 34 related to the concentration variation across the system and the thickness of the product layer formed on the sorbent material for the 20th cycle.

Figure 33: Concentration Profile at the End of 20th Cycle Across the Bed for 50 Ppm Inlet Concentration.

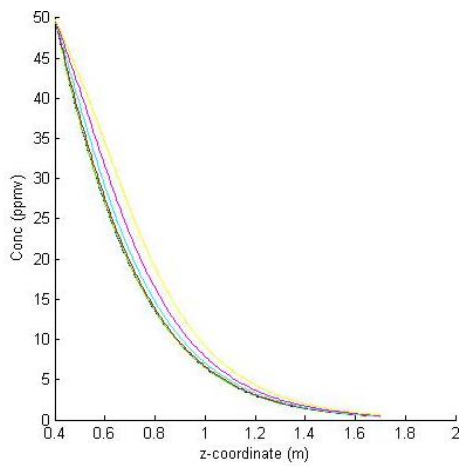

Source: North Carolina State University

Figure 34: Thickness Variation of the Product Layer on the Sorbent Material during 20th Cycle

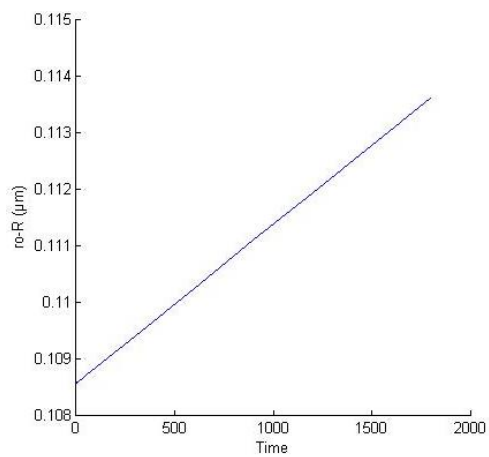

Source: North Carolina State University

Figure 35 and Figure 36 indicate the concentration variation and thickness formation at the end of 50 cycles. The concentration profile in the system has not changed significantly, however the rate of formation of the thickness decreases as the HCl gas needs diffuses through the product layer.

Figure 35: Concentration Profile at the End of 50th Cycle across the Bed for 50 ppm Inlet Concentration

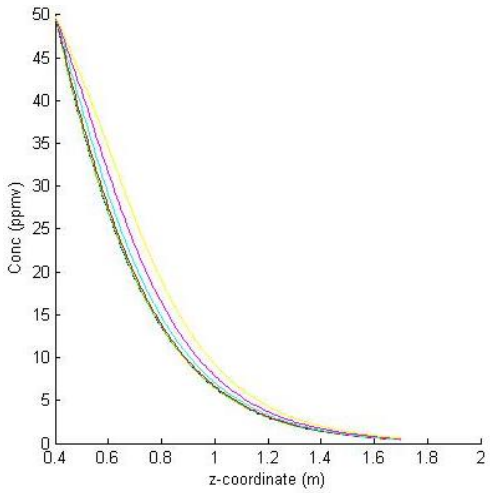

Source: North Carolina State University

Figure 36: Thickness Variation of the Product Layer on the Sorbent Material during 50th Cycle.

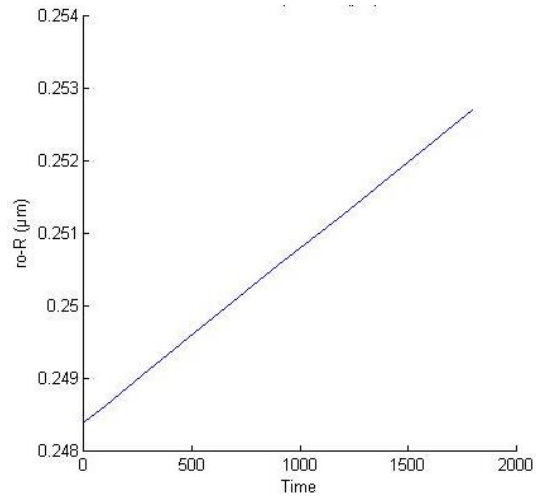

Source: North Carolina State University

Figure 37 shows the thickness variation for the entire 50 cycles under consideration.

Figure 37: Product Layer Thickness Increase on the Sorbent Surface

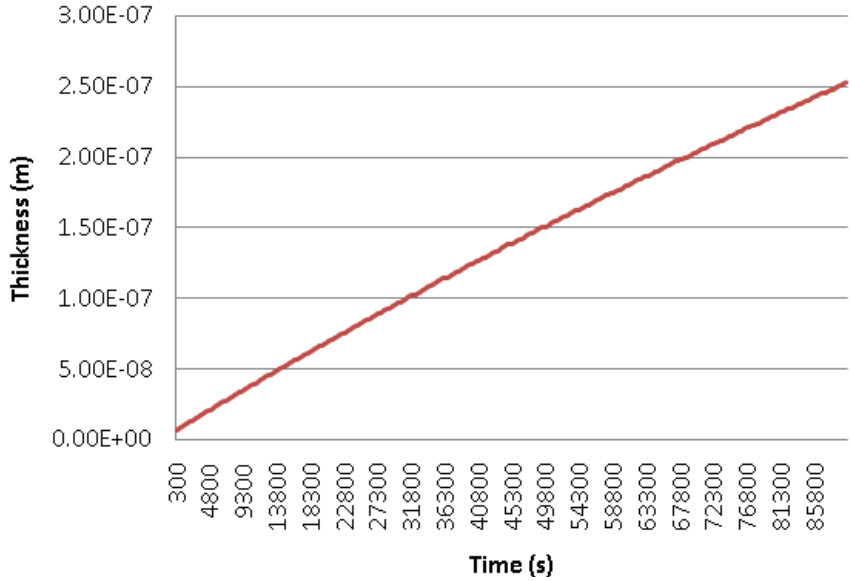

Source: North Carolina State University

What we can observe from the above graph is that there is still much more capacity available for the sorbent material to hold HCl. Once the threshold is reached the curve will flatten out, thereafter the material ceases to retain Cl from HCl.

Figure 38 and Figure 39 show the concentration profile for 900 ppm inlet concentration and thickness of sorbent material at the end of 50th cycle. We consider 900 ppm to be able to compare our results with published data. The break through concentration occurs at around 1/10th of the inlet concentration and 50 cycles of 1 hour each represents a week of simulation. Considering the ratio of our inlet concentration of 50 ppm to that of 900 ppm, we can expect a preliminary capacity of the sorbent material to be around 180 days.

Figure 38: Concentration Profile at the End of 50th Cycle across the Bed for 900 ppm Inlet Concentration.

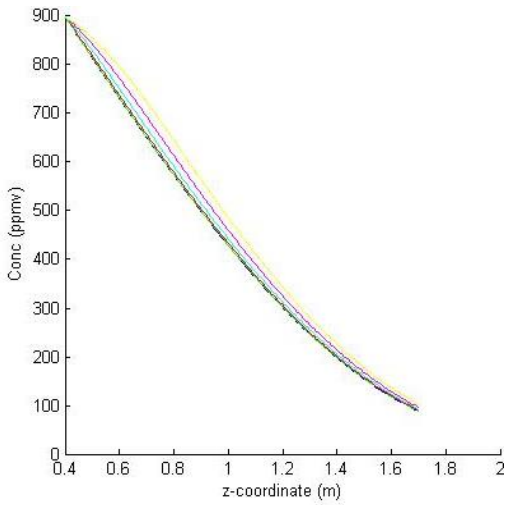

Source: North Carolina State University

Figure 39: Thickness Variation of the Product Layer on the Sorbent Material during 50th Cycle.

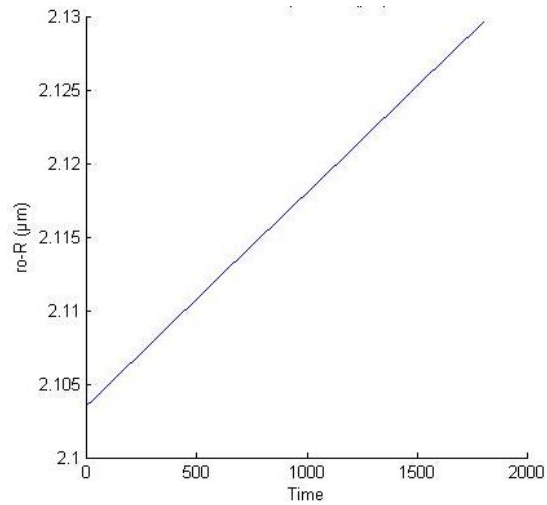

Source: North Carolina State University

Parametric Modeling of the GGR to Achieve Optimal Performance Characteristics

The original model developed in axisymmetric form has been used to perform the parametric analysis. The different parameters evaluated for study include inflow flue gas temperature, inflow velocity and concentration of the HCl flue gas. First parameter to be varied was temperature. The temperature of flue gas entering the system has been varied from 850 K (1070.3 °F) to 1,000 K (1,340.33 °F) in increments of 50 K (°F) to study the effect of temperature distribution across the bed.

Figure 40 shows the specific location selected to study the effect of temperature variation. The velocity of inflow gas has been maintained at 1 m/s (3.28 ft/sec).

Figure 40: Location of Parameter Study

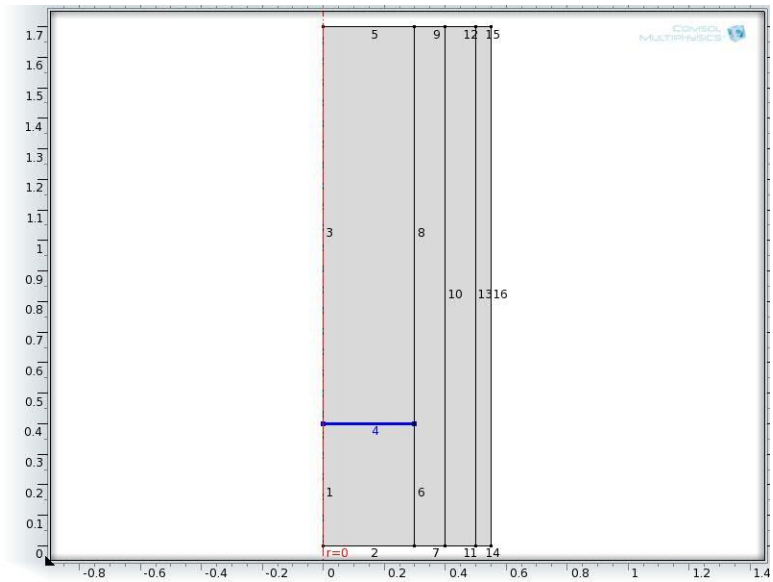

Source: North Carolina State University

This location was chosen to study the temperature at which the flue gases will enter the sorbent medium with a specific range for optimal performance.

Shown in Figure 41 is the temperature at the location under consideration for different inflow level temperatures through the bed.

Figure 41: Temperature Curves at Interface for Varying Inlet Temperature

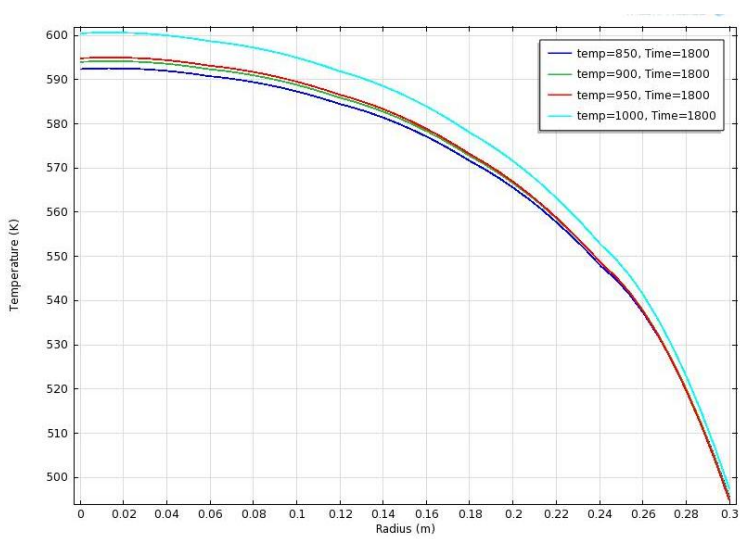

Source: North Carolina State University

It can be seen from Figure 41 that temperature increases at the inert-sorbent interface as the inflow temperature rises. This is in line with our expectations that a higher inlet temperature would result in more heat energy being carried to the sorbent medium.

Figure 42 shows the effect of fluid at the same location for different inflow temperatures.

Figure 42: Velocity Curves at Interface for Varying Inlet Temperature

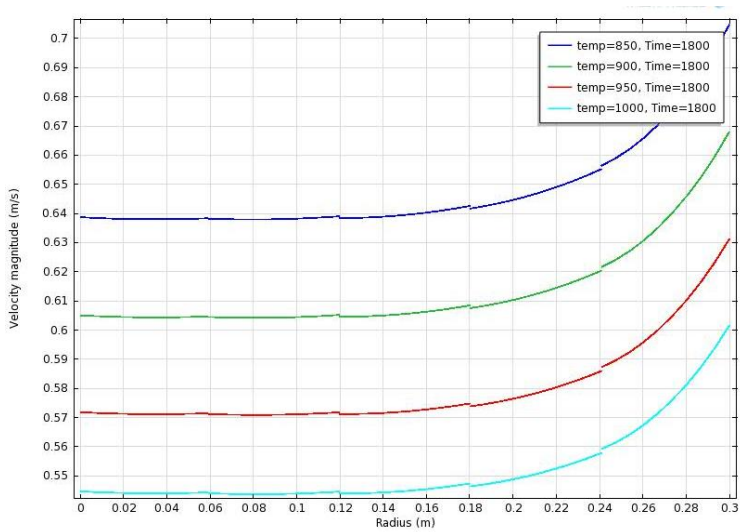

Source: North Carolina State University

The second parameter under study was inflow velocity through the bed. It was varied from 0.7 m/s (2.3 ft/sec) to 1 m/s (3.28 ft/sec) in increments of 0.1 m/s (0.33 ft/sec). The effect of temperature at the same location was studied for a constant inflow temperature of 1,000 K (1,340.3 °F).

Figure 43 shows the temperature for different velocities at the interface between the two porous layers. According to Figure 43 as the inflow velocity increases, the temperature at the interface also increases. This is because the momentum of the fluid is greater and effect of temperature can be felt further down the bed. Figure 44 shows the velocity at the interface as the inflow velocity is varied.

Figure 43: Temperature Curves at Interface for Varying Inlet Velocity

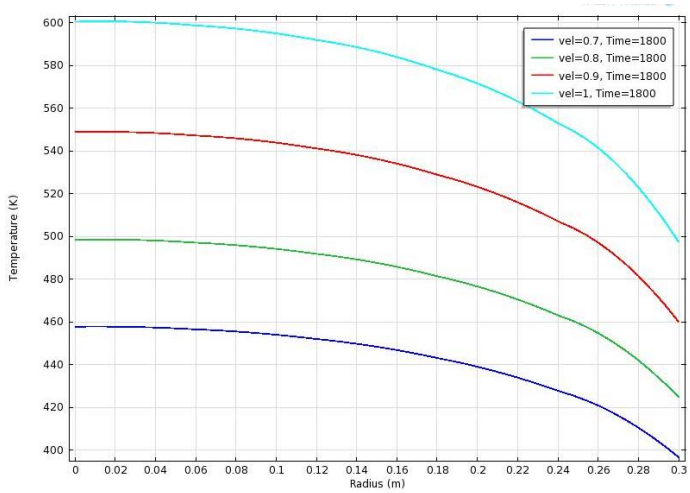

Source: North Carolina State University

Figure 44: Velocity Curves at Interface for Varying Inlet Velocity

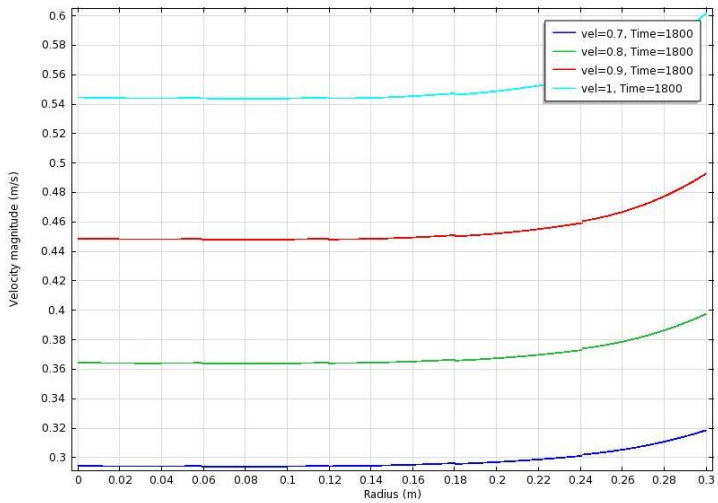

Source: North Carolina State University

The general trend can be seen, as the inflow velocity increases, the velocity at the interface is also greater. This can be confirmed from Figure 43, the temperature at the interface also being greater.

The last parameter under consideration is concentration profile. The concentration at inlet was varied and studied at 50 ppm, 100 ppm, 200 ppm and 500 ppm having the inlet velocity at 1 m/s. Figure 45 shows the concentration profile in the bed at end of one cycle. This shows that the capacity of the bed seems to be sufficient even for higher inlet concentration of 500 ppm. This would suggest the bed is capable of holding much more HCl for 50 ppm inlet concentration through many cycles before a replacement is required.

Figure 45: Concentration Curves across the Sorbent Media for Varying Inlet Concentration

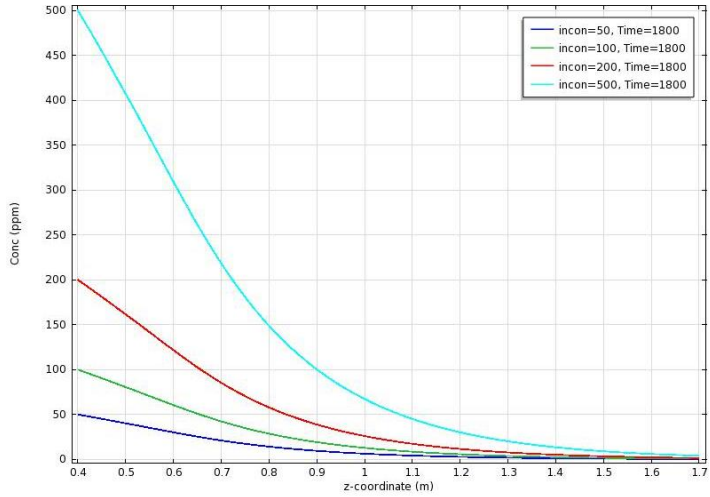

Source: North Carolina State University

A parametric study was conducted on the particle size used in the regenerator. The diameters of the particles were 6 mm, 5 mm and 4 mm. The property change which occurs due to a change in particle size is the permeability of the medium.

Shown in Figure 46 is the pressure drop across the bed for different size of the particles. The effect of change in the diameter of the particles seems significant due to the change in permeability which is proportional to the cube of the diameter of the particles.

Figure 46: Pressure Drop for Various Particle Sizes under Consideration

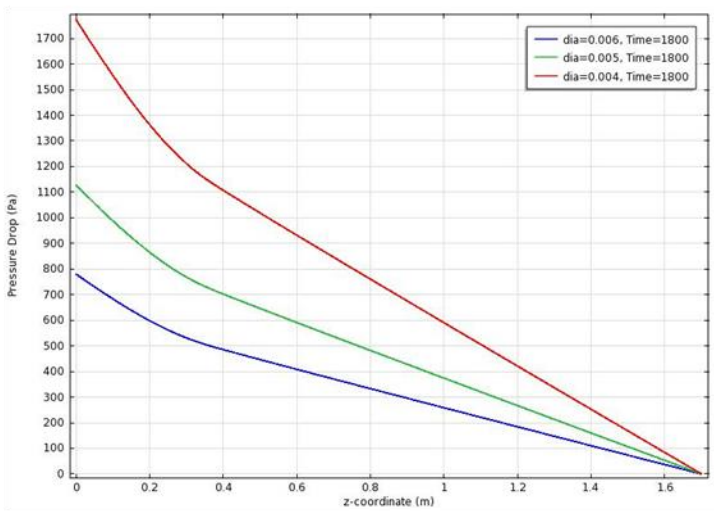

Source: North Carolina State University

Figure 47 shows the fluid velocity across the bed at the alumina-sorbent interface due to a change in the temperature of the fluid. It is also interesting to note the change in fluid velocity

near the edge of the regenerator seems to be peculiar, as one would expect uniform velocity profile across the bed.

Figure 47: Velocity Curves at the Interface for Temperature Dependent Viscosity Value

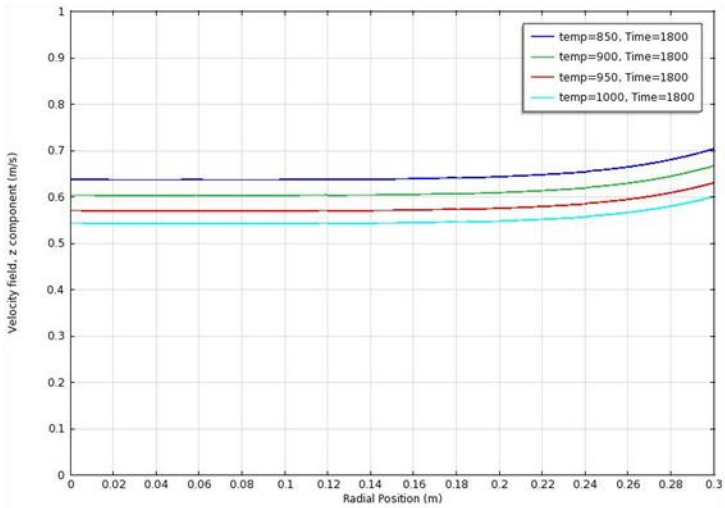

Source: North Carolina State University

Shown below in Figure 48 is the contour plot of velocity curves near the edge of the regenerator.

Figure 48: Velocity Contour Curves

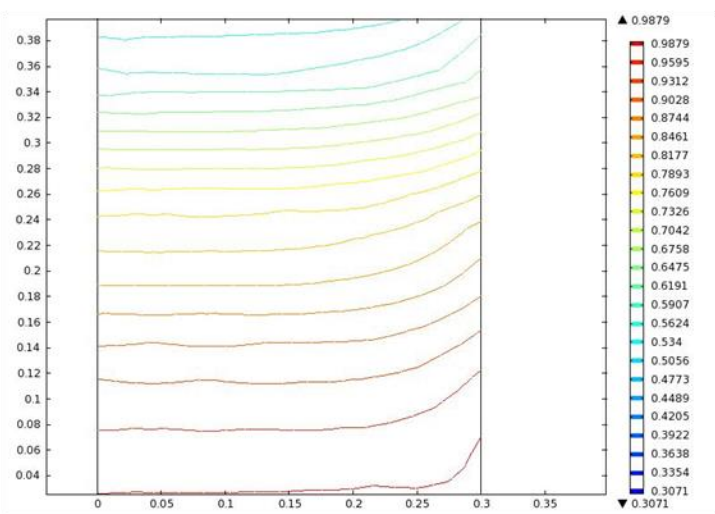

Source: North Carolina State University

It can be seen from Figure 48 that the velocity near the edge seems to be greater than at the center. The fluid is accelerating near the edge, which may be due to the drop in viscosity of the air near the edge.

As shown in Figure 49, there is heat loss from the inert alumina to the surrounding layers of insulation and refractory bricks. This causes a significant temperature gradient across the interface and viscosity is strongly dependent on temperature. As the temperature drops, the viscosity also reduces enabling the fluid to accelerate along those regions.

Figure 49: Temperature Contour Curves

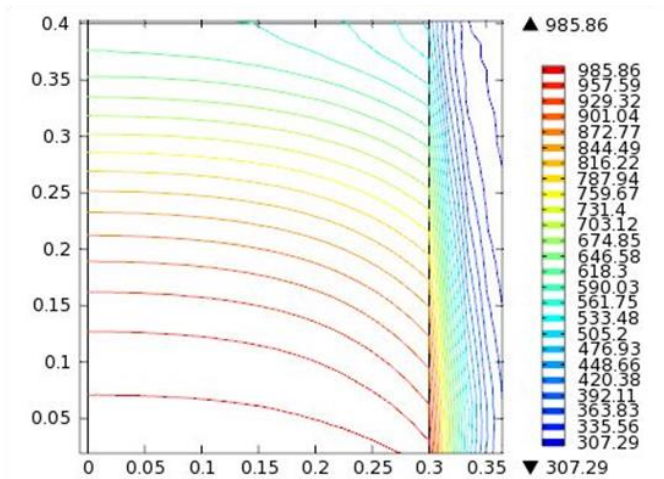

Source: North Carolina State University

Figure 50 shows the fluid velocity curve for an analysis in which viscosity is temperature independent. As we expected the velocity curve is constant at the interface of the sorbent-alumina.

Figure 50: Velocity Profile at the Interface for Temperature Independent Viscosity Value

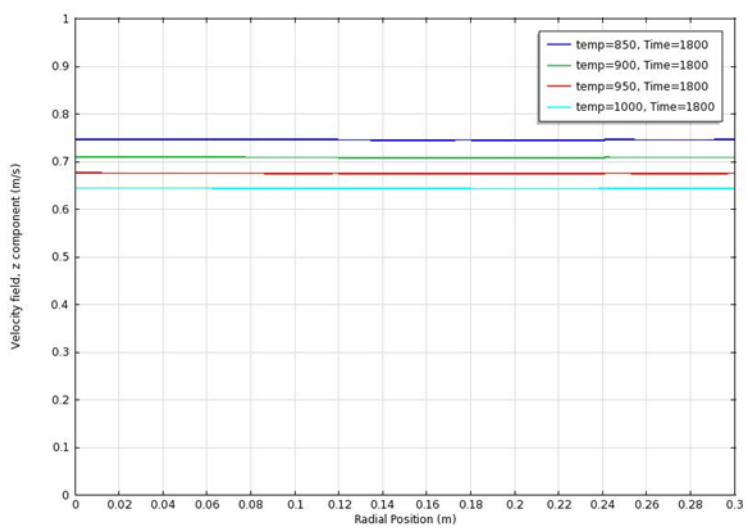

Source: North Carolina State University

Development of Preliminary Design Specifications

The purpose of the regenerator is to recover heat energy and to reduce effluent flue gas concentrations. It consists of an inlet, outlet and three way valves as shown in the schematic diagram. The flue gas enters from the inert ceramic end and exits out through the sorbent, while in the reverse cycle the cold air enters through the sorbent and exits from the inert ceramic as hot air.

As the flow enters the inert ceramic medium, it transfers a significant amount of heat energy to the porous bed before entering the sorbent medium, where surface adsorption takes place, reducing the concentration of the effluent to minimal levels as it exits. At the end of one cycle, cold air is sent through in the opposite direction to recover the heat energy stored in the inert bed while the other regenerator continues to function in the forward cycle. This alternating arrangement enables continues treatment of flue gas without any gap while switching between the cycles.

Shown below in Table 9 are the design parameters for the regenerator.

The performance parameters were matched against simulation data to arrive at the dimensions for the regenerator. The inert bed consists of spherical Alumina particles having high heat capacity. They are capable of retaining the heat energy from the incoming high temperature flue gas. Then the gas flows into the sorbent bed where the chemical reaction occurs, reducing the effluent concentration as it exits the regenerator. The numerical model coupled porous flow, heat transfer and chemical reactions.

Table 9: Design Parameters for the Regenerator

Max flue gas inlet temperature, °F	1,000
Max flue gas outlet temperature, °F	300
Max flue gas flow, SCFH	10,000
Air inlet temperature, °F	60
Air outlet temperature, °F	700 - 800
Max air flow, SCFH	9,000
Max sorbent and inert ceramic temperature prior to switching, °F	1,000
Specific heat of sorbent material, J/(kg·K)	1,000
Specific heat of inert ceramic material, J/(kg·K)	880

Source: North Carolina State University

Figure 51 displays the dimensions for the regenerator. The regenerator will consist of 2 sections as shown by the shading. The lower section of the regenerator shaded in by the diagonal lines,

will house the inert Alumina, where most of the heat energy will be stored from the incoming high temperature flue gas. The upper section of the regenerator shown by the shaded triangles, will house the sorbent material where the chemical reaction between the particles and flue gas will take place. The regenerator will also be surrounded by several layers of material that may include a Refractory Layer, Steel Lining and Insulation as shown in the sketch. These layers will be required to reduce heat losses and to provide structural stability. The dimensions of the thickness *d* of the layers surrounding the regenerator are to be decided.

Figure 51: Preliminary Dimensions of the Recuperator

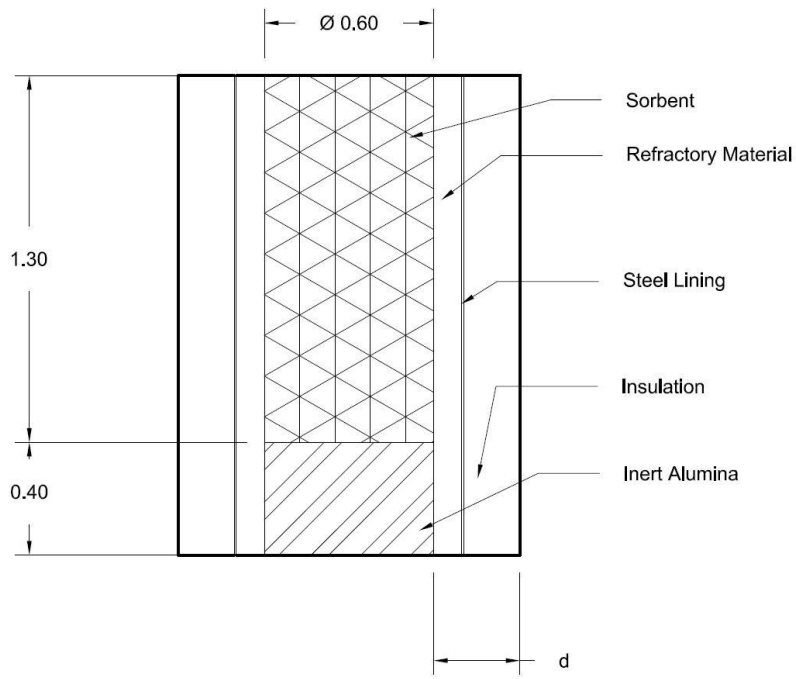

All dimensions in meters

Source: North Carolina State University

Table 10 shows the design specifications of the regenerator.

Table 10: Preliminary Design Specifications of the Regenerator

Design Specifications		SI Units	En Units
Sorbent Bed (upper section)			
Diameter of particle	d_s	4 mm	.157 in
Porosity	ε	0.4	0.4
Velocity in Bed	V_s	0.3 m/s	1 ft/s
Temperature at Exit	T_s	300 K	80°F
Diameter of Bed	D_s	0.6 m	2 ft
Height of Bed	H_s	1.3 m	4.26 ft
Density of Sorbent	ρ_s	2.5 g/cc	156 lb/cu ft
Weight of Sorbent	W_s	367 kg	809 lb
Inert Bed - Alumina (lower section)			
Particle Diameter	d_i	5 mm	0.2 in
Porosity	ε	0.4	0.4
Velocity in Bed	V_i	1 m/s	3.28 ft/s
Temperature at Entry	T_i	1,000 K	1,340°F
Diameter of Bed	D_i	0.6 m	2 ft
Height of Bed	H_i	0.4 m	1.31 ft
Density of Ceramic	ρ_i	3.7 g/cc	230 lb/cu ft
Weight of Ceramic	W_i	167 kg	368 lb

Source: North Carolina State University

The objective of the regenerator is to store heat energy and to recover some portion of this energy. During this process, there is a heat loss from the material to the surroundings. The regenerator will be covered by three layers of insulation including a refractory brick, insulation material and also structural steel for structural stability and integrity. The values of thermal conductivity, heat capacity and density are available for each of the materials. Heat losses from the sides include natural convection and also radiation to the ambient temperature. The inner layer will consist of refractory brick, followed by Insblok-19 insulation layer bounded by steel which is the outer material.

The analysis was carried out in COMSOL and the cycling was conducted with the help of MATLAB interface. Figure 52 shows the region where the temperature distribution was studied.

Figure 52: Location of Study Where Temperature is Monitored

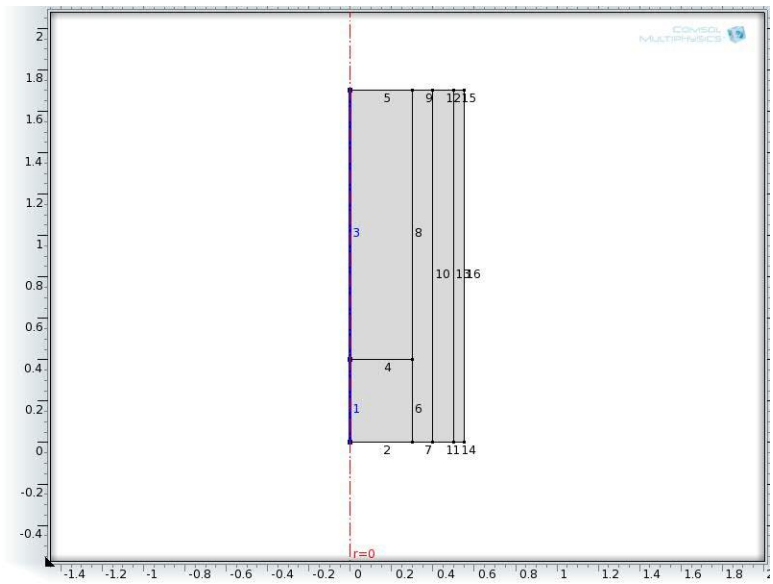

Source: North Carolina State University

Table 11 lists temperatures at the sorbent/inert interface. This temperature is crucial and is tabulated for every 5th cycle. The change in temperature for every 5th cycle reduces and we can assume that at the end of the 25th cycle that the system has reached a quasi steady equilibrium condition. The average temperature at any location in the regenerator would not change significantly for further cycles.

Table 11: Temperatures at the Sorbent/Inert Interface

#	Inlet velocity (m/s)	Insulation thickness (cm)			Temperature at the sorbent/inert interface (°F)				
					# of cycles				
		Brick	Insblok	Steel	5	10	15	20	25
1	0.6	6.35	1.5	0.635	505	544	558	562	563
2	0.6	6.35	1.5	0.635	511	537	542	544	545
3	0.7	6.35	1.5	0.635	626	667	675	678	679
4	0.7	6.35	2.5	0.635	617	666	684	691	695
5	0.7	6.35	5	0.635	620	673	694	704	709
6	0.7	6.35	10	0.635	621	677	701	713	718

Source: North Carolina State University

Shown in Table 12 are the corresponding values for pressure drop, and exit temperature and velocity of air as it leaves the regenerator.

Table 12: Pressure Drops and Exit Temperatures of Air Leaving the Regenerator

#	Exit temperature (°F)	Pressure drop (Pa)
1	600	400
2	612	400
3	700	500
4	710	500
5	715	500
6	725	520

Source: North Carolina State University

From the above simulation data it is possible to determine the optimal level of insulation thickness that would be required for our purpose. Adding too much insulation would not be cost effective and may cause excessive temperature build up within the regenerator. Table 1 shows that it would be the most effective to select the insulation from the 5th row. It also

indicates a higher temperature during the return cycle than expected, but would be ideal for the sorbent reaction to take place.

Shown in the following page are the temperature distribution graphs for different cycles under the study region indicated in Figure 53. Shown in Figure 54 and Figure 55 are the surface temperature plots for the forward and backward runs during 26th cycle. It can be seen that due to heat losses, as the temperature profile is being pushed towards the inlet, there is significant rise in the temperature of the refractory brick layer (Figure 54).

Figure 53: Axial Temperature Profiles for Different Cycles

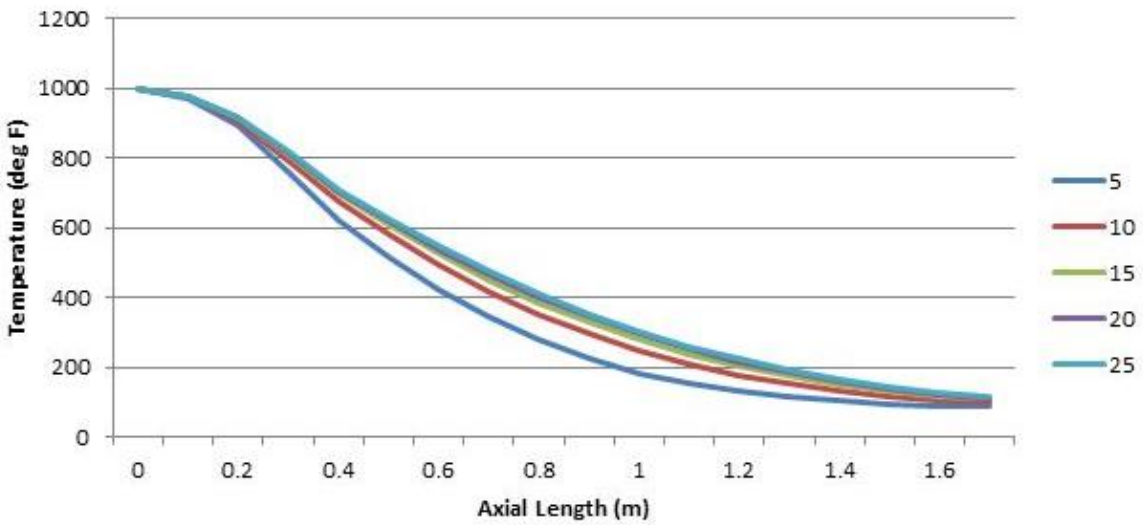

Source: North Carolina State University

Figure 54: 2-D Temperature Distribution at the End of the Forward Run during the 26th Cycle

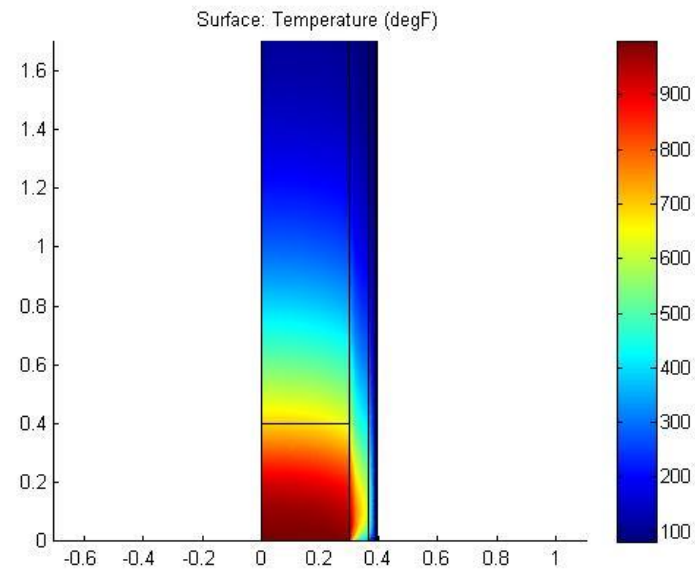

Source: North Carolina State University

Figure 55: 2-D Temperature Distribution at the End of the Backward Run during the 26th Cycle

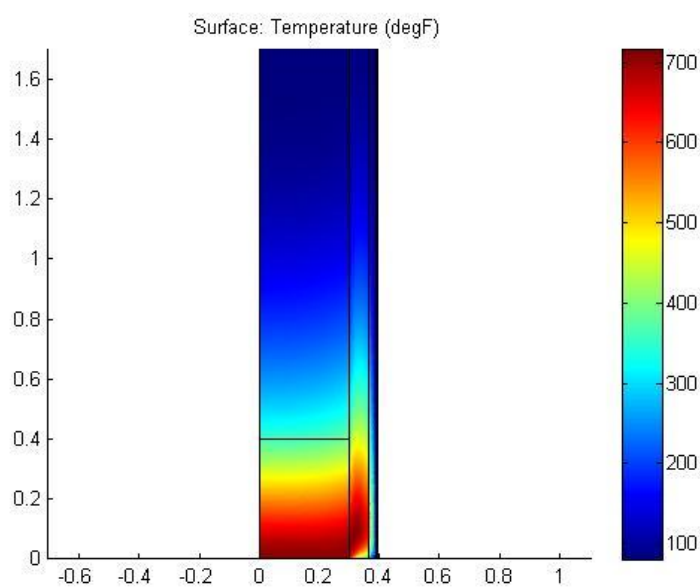

Source: North Carolina State University

Conclusions and Recommendations

The numerical model of the GGR was developed. The parametric study was conducted to analyze the effect of different parameters such as inflow velocity, inflow temperature and

inflow concentration levels of flue gas and its effect on the inert-sorbent bed. The results indicate that the regenerator is capable of holding a wide range of temperatures. The sorbent capacity is sufficient to handle higher concentration levels through the bed. The parametric study was also conducted to analyze the effects of particle size and viscosity on fluid temperature and pressure drop. The study reveals that changing the particle size affects the pressure drop. Strong temperature dependence of viscosity results in velocity changes near the edge of the regenerator.

The simulations of the regenerator with the insulation layers applied to prevent heat losses were been conducted. An optimal thickness of insulation was specified for the present regenerator design. The thermal insulation and other design parameters of the regenerator are met by the current design.

2.3.3.2 Finalization of the Design of Gas Guard Recuperator

The concept design for a GGR demonstration unit is shown in Figure 56. Its major features are:

- Each GGR reactor has a layer of inert ceramic material (heat transfer media) topped by a layer of sorbent material (HCl removal)
- The sorbent and ceramic beds are supported by a perforated plate and screens
- The reactors are lined on the inside with hard refractory backed by insulating boards.
- The top and bottom lids of each reactor are removable for filling the bed and for inspection.

Figure 56: Concept Design of a GGR Demonstration Unit

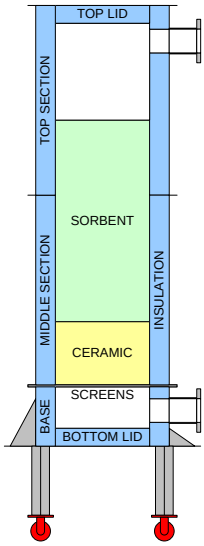

Source: Gas Technology Institute

The operating concept for a GGR demonstration unit is shown in Figure 57. Note that the orientation of the inlet and outlet flow streams and the switching valves depend on the specifics of the application. The major features of the operating concept are:

- The furnace delivers hot exhaust gas at the bottom while cold combustion air is supplied at the top
- In one reactor inert ceramic recovers heat while the sorbent removes corrosive gases from the exhaust gas
- In the other reactor inert ceramic heats combustion air but corrosive gases stay in the sorbent
- Cooled exhaust gas exits from the top while heated combustion air exits from the bottom
- Switching valves divert the flow streams to opposite reactors
- The flow direction through the GGR reactors reverses automatically after a fixed time interval or after a maximum temperature is reached at the ceramic-sorbent boundary

Figure 57: Concept Operation of a GGR Demonstration Unit

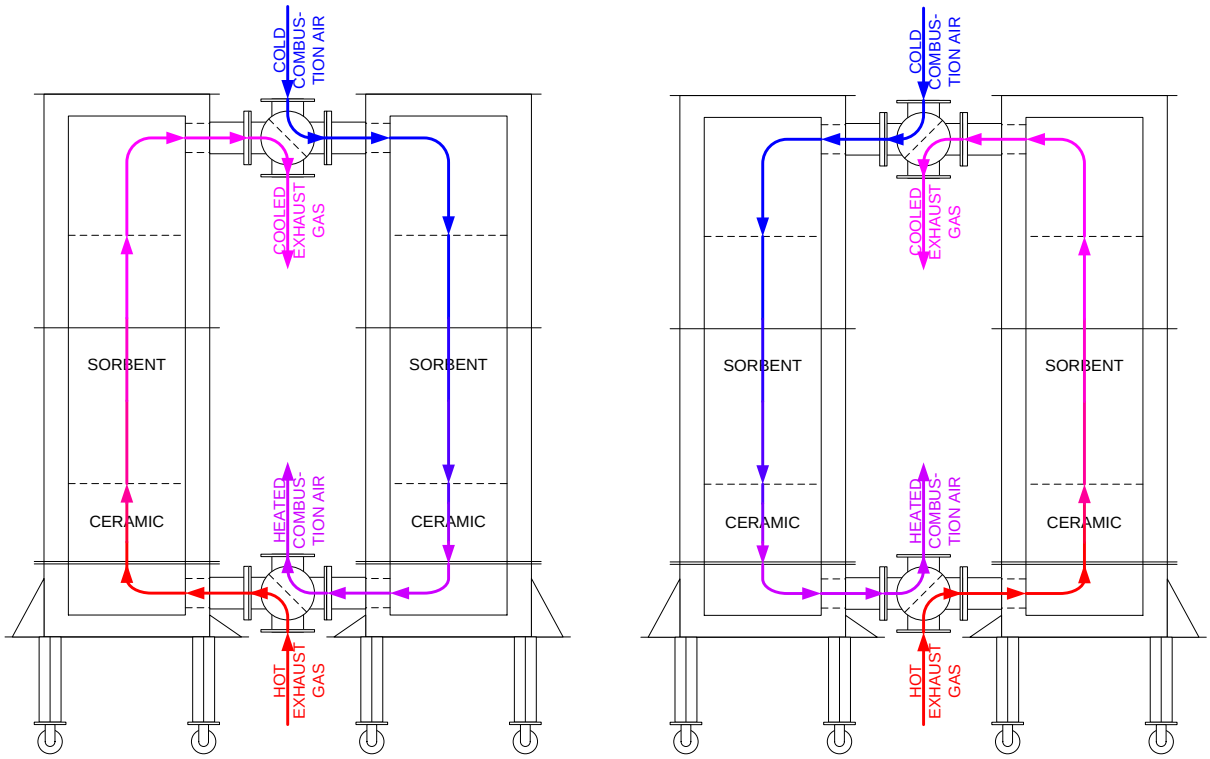

First Half of CycleSecond Half of Cycle

Source: Gas Technology Institute

A design of the GGR reactors was completed by Thermal Transfer Corporation based on the modeling results, with input from GTI regarding the height of the legs, locations for measurement ports, locations for the inlets and outlets, and the type of valves between the two reactors. The general arrangement of the GGR reactor is shown in Figure 58. The reactors' internal dimensions are approximately 2 feet in diameter and 8 feet in height. There are 13

cubic feet of sorbent and 4 cubic feet of ceramic in each reactor. The sorbent and ceramic bed in each reactor is supported by a perforated plate with screening over the holes in the plate. The reactors are lined on the inside with approximately 4 inches of refractory and insulation. Ports for thermocouples line the side of each reactor at 6" intervals. Three ports are included in the inlet and outlet ports from each reactor for temperature, pressure, and sampling measurements. The reactors sit on casters for ease of movement. The top of each reactor is removable for filling the bed. The bottom of each reactor is removable for inspection.

The layout between the two reactors is shown in Figure 59. A pair of 4-way valves will be used to switch the flow of flue gas and cold air between the reactors. During the first half of each regenerative cycle, the flue gas entering the bottom of the lower 4-way valve will be diverted by this valve to the lower port of the right-side reactor. Upon exiting the upper port of the right-side reactor, the upper 4-way valve will divert the cooled and cleaned flue gas downward to the induced draft (ID) fan. At the same time, the cold air entering the top of the upper 4-way valve will be diverted to the upper port of the left-side reactor. Upon exiting the lower port of the left-side reactor, the lower 4-way valve will divert the heated air upward. In a production scenario, the heated air would be used for combustion, but for testing purposed, the heated air will be sent to the ID fan.

Figure 58: General Arrangement View of a Gas Guard Recuperator

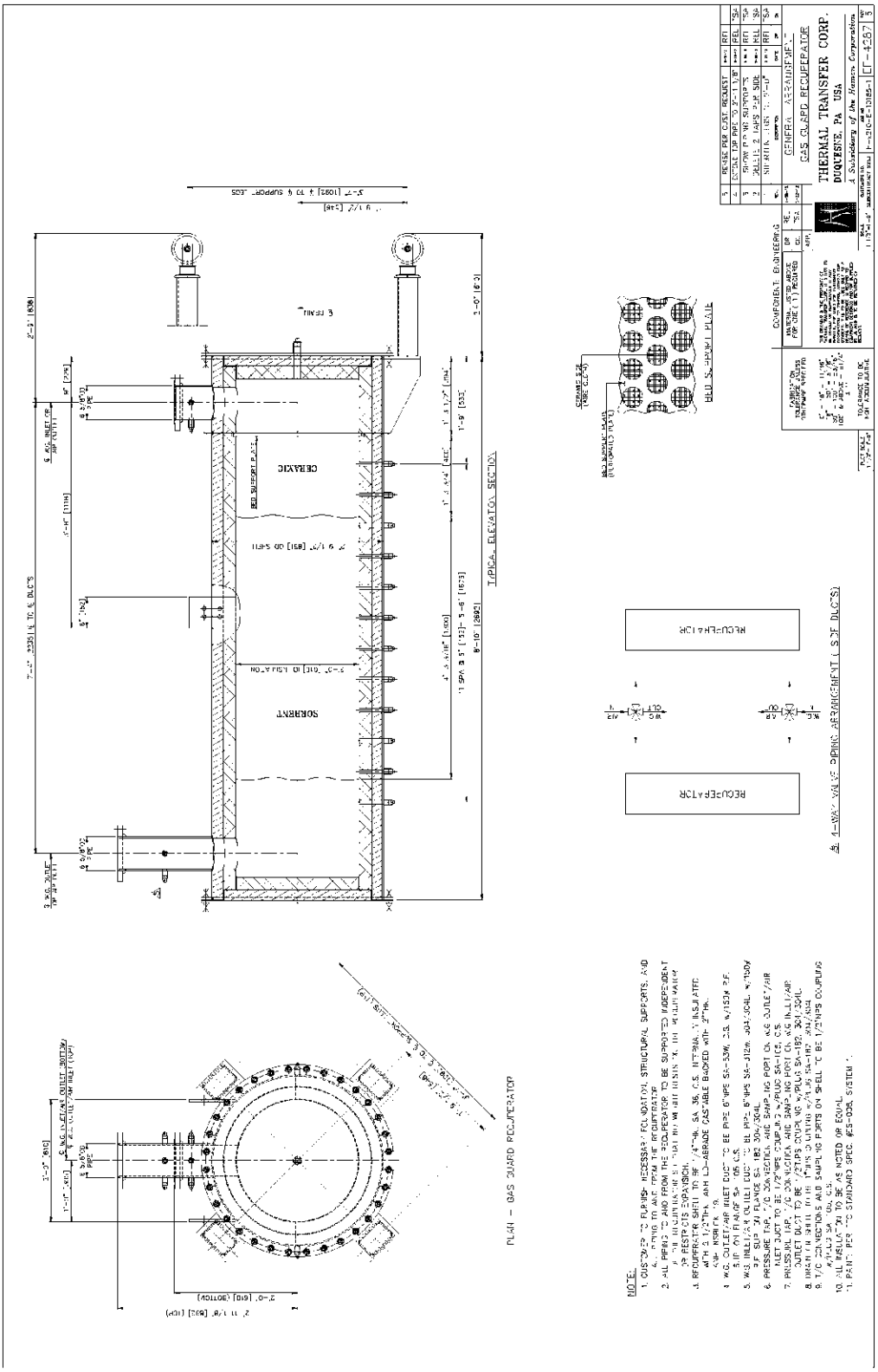

Source: Thermal Transfer Corp.

Figure 59: Elevation Views of a Gas Guard Recuperator

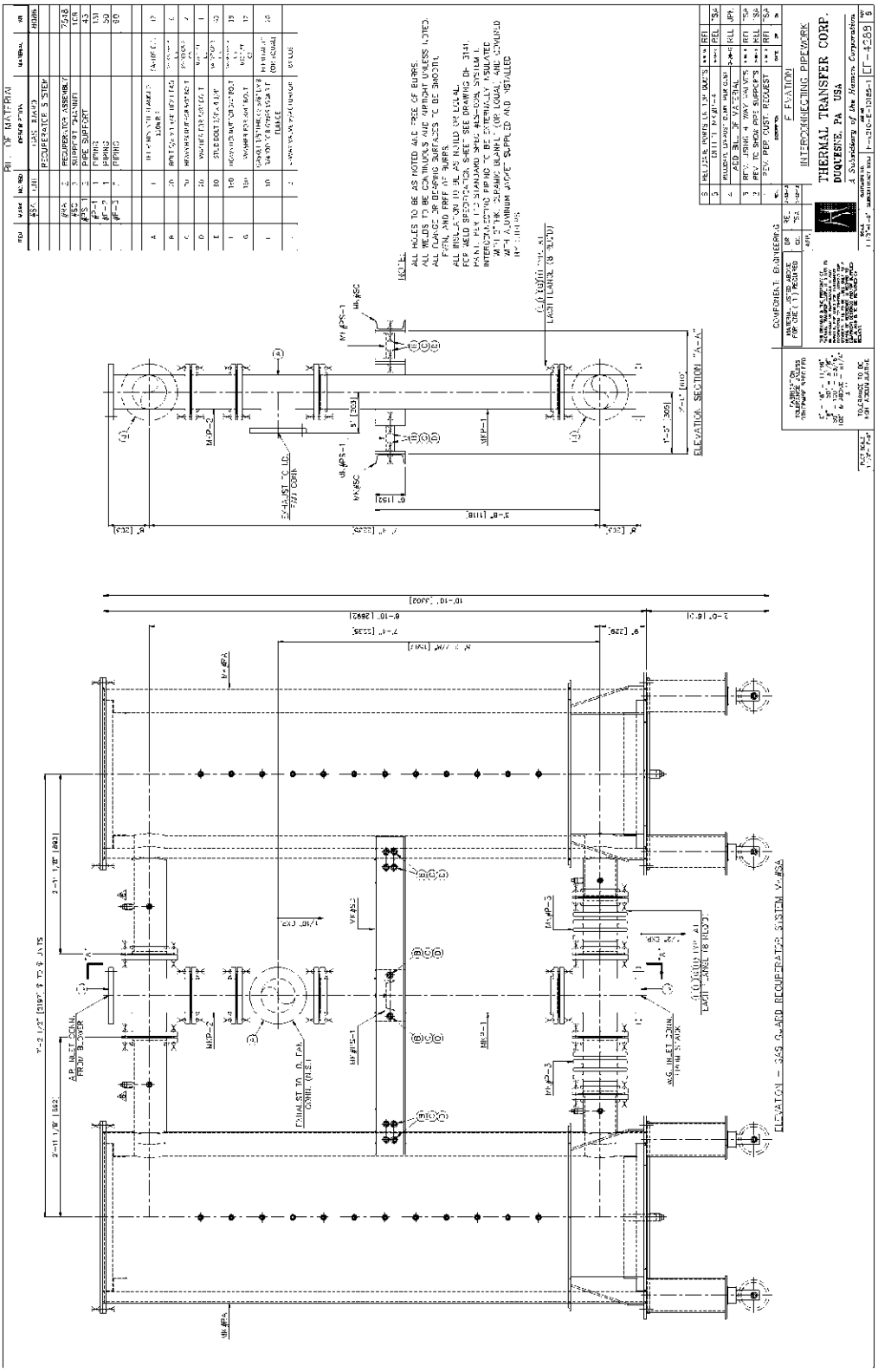

Source: Thermal Transfer Corp.

At the end of each half-cycle, both valves will be switched simultaneously. During the second half of each regenerative cycle, the flue gas entering the bottom of the lower 4-way valve will be diverted through the left-side reactor and then diverted out the bottom of the upper 4-way valve to the ID fan. At the same time, the cold air entering the top of the upper 4-way valve will be diverted through the right-side reactor and then diverted out the top of the lower 4-way valve to the ID fan.

The use of 4-way valves was selected after analyzing the requirements and availability of different types of valves for switching the flows between the two GGR reactors. Originally, four 3-way valves were specified by Thermal Transfer Corporation (see Figure 60). Finding a commercially available 3-way valve in the 6" size that could operate at 1,000°F took much effort, and those found required high differential pressures to properly seal or cost upwards of $18,000 each. Simpler 2-way high-temperature butterfly valves were more readily found, but 8 would be required (see Figure 60), along with 8 valve actuators, or 4 actuators on 4 pairs of mechanically linked valves, and additional piping between the 2 GGR reactors. Only a single actuator would be needed to operate a 4-way valve, which would take the place of two 3-way or four 2-way valves, and greatly simplify the interconnecting piping.

Figure 60: Valve Arrangements

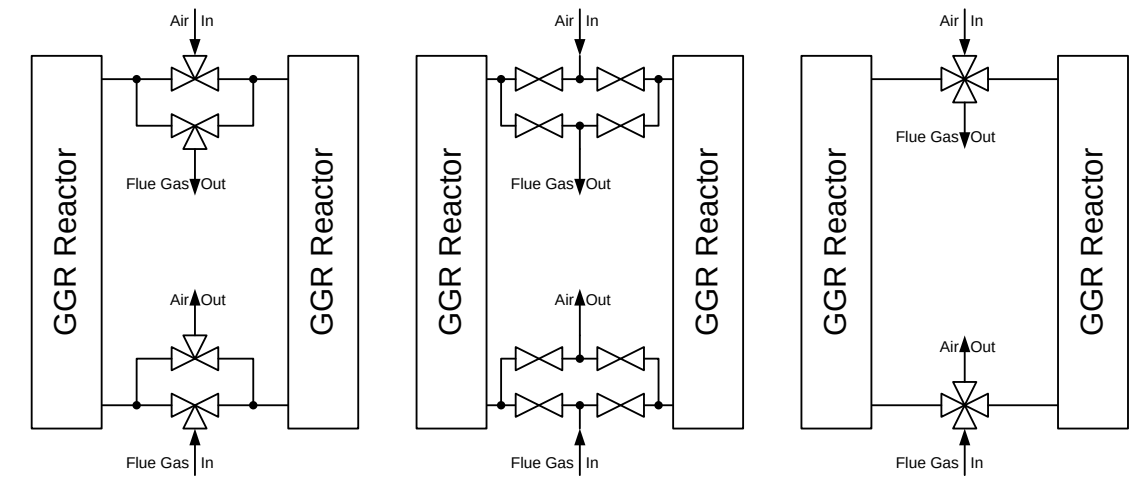

Source: Gas Technology Institute

A rough design of a 4-way valve had already been developed by GTI for low-pressure applications. The design was modified for high-temperature operation, to be fabricated from commonly available materials, of the same external dimensions a flanged 6" cross pipe fitting, to be operated by a standard pneumatic actuator. Cross sectional views of the final design are shown in Figure 61. Detailed drawings of the individual parts of the valve were prepared for water jet cutting, machining, welding, and assembly.

Figure 61: 4-Way Switching Valve Design

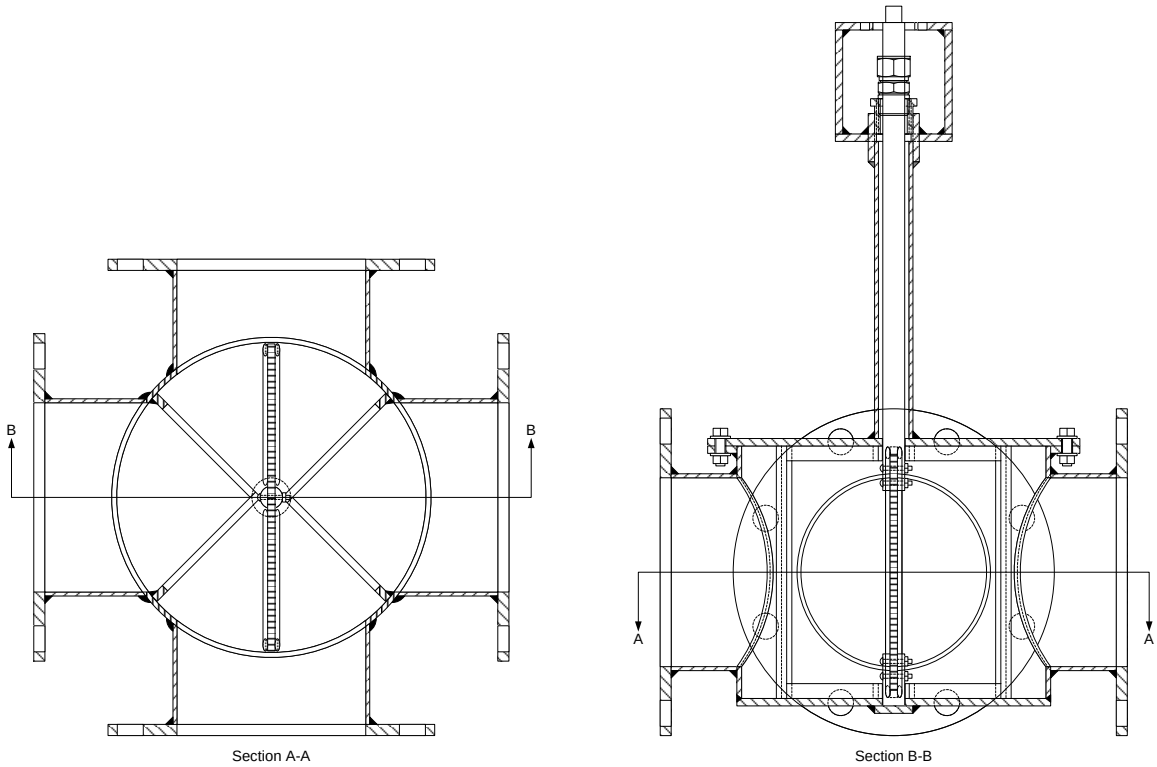

Front Cross-Sectional View

Top Cross-Sectional View

Source: Gas Technology Institute

With the GGR reactor design completed and the valve design complete, layout drawings were prepared for the installation of the GGR reactors in GTI's Combustion Laboratory. The chosen furnace is GTI's large box furnace. It was chosen because is it well sealed, so it can hold 5"water column (wc) of negative pressure, it has a large load, so the flue gas can exit at 1000°F, it has flue gas piping amenable to be redirected to the GGR reactors, and it has enough space around the furnace for the GGR reactors and the ancillary equipment (blowers for combustion air and process air, induced draft (ID) fan for flue gas). Three views of the layout of equipment around the furnace are shown in Figure 62 to Figure 64. The burner installed on the furnace is an existing Eclipse Thermjet of 1,000,000 Btu/h capacity. This model of burner is known to be used on aluminum melting furnaces.

Detailed drawings of each component of the GGR were prepared based on the design provided by Thermal Transfer Corporation. Four small changes were made by GTI to the design. The first change was to increase the outer diameter of the reactors from 33.5" to 34" based on standard sizes of rolled angle flanges. The second change was to split the reactors into three sections each for ease of handling and for ease of manufacturer so that the outer wall of each section could be rolled from a single sheet of steel. The third change was to make the reactors about 0.5' taller so that the outer wall of the upper sections could each be rolled from a full 48"

sheet of steel. The fourth change was to make the bed support plate as a separate piece from the reactor sections and not welded permanently to the lower section. The design feature of a removable top lid and removable bottom lid were kept.

Figure 62: Proposed General Layout View of the GGR Laboratory Test Setup

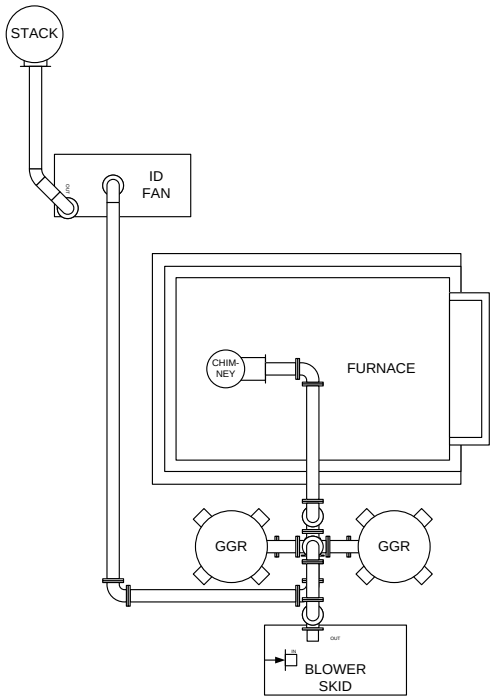

Source: Gas Technology Institute

Figure 63: Proposed Front Elevation View of the GGR Laboratory Test Setup

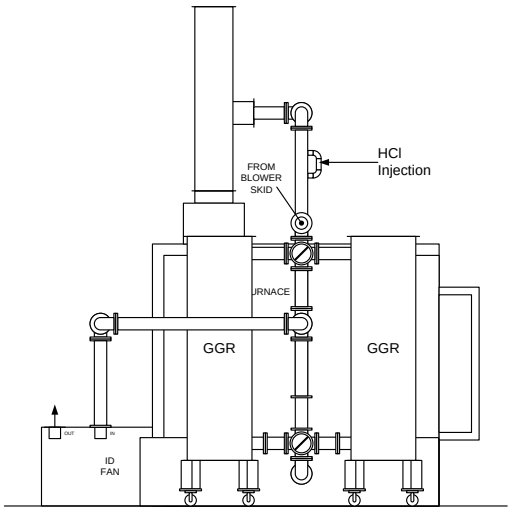

Source: Gas Technology Institute

Figure 64: Proposed Side Elevation View of the GGR Laboratory Test Setup

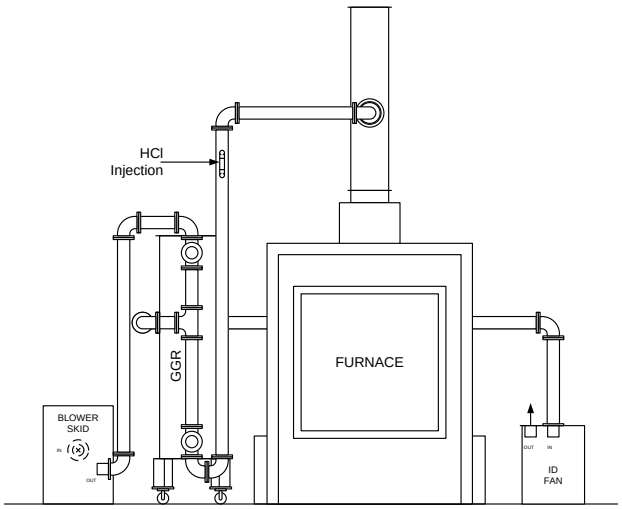

Source: Gas Technology Institute

2.3.3.3 Fabrication of the GGR Demonstration Unit

The metalwork for the GGR reactors was fabricated by American Metals Installer and Fabricators (AMIF), which completed the effort in August 2012. AMIF committed in-kind to the project at $10,000 level as

- Conversion of the GTI supply design documents to the shop fabrication drawings
- Delivery of fabricated components, supervision labor, and
- Consultation and meeting with GTI during fabrication.

The interconnecting piping between the two reactors was fabricated. The switching valves were fabricated and test fitted to the GGR reactors with the interconnecting piping at AMIF's shop. The GGR reactors were broken down into three sections each and transported to a local refractory installation shop directly from the welding shop. The switching valves and interconnecting piping were delivered to GTI.

At the refractory installation shop, the lids were removed from the GGR reactor sections. These cylindrical sections were lined on the inside with refractory insulation. The insulation consists of two layers. There is an outer layer of fiberboard material and an inner layer of hard refractory. Anchors were placed on the inner walls of the sections to hold the refractory layer, and a cardboard tube was placed inside the cylindrical sections before the refractory layer was poured. The cardboard tubes were removed and the lids were then placed back on the top and bottom sections before the refractory insulation was added to the inner sides of the lids. The refractory layer in the cylindrical sections acted as a form for the pouring of the refractory on the lids.

The completed sections were transported to GTI (see Figure 65). Some trace patches of the cardboard tube that formed the core around which the refractory was poured had to be scraped off the refractory to yield a clean surface. Some of the edges of the refractory had to be patched and leveled for proper fit of the sections. Personnel from the refractory installation shop performed these tasks.

A bed support plate (see lower right section in Figure 65) and triple screens were placed on top of the lower two sections (see Figure 66). The GGR reactors were reassembled from their three sections (see Figure 67). Ceramic paper gaskets were put between the sections with high temperature silicone added between the flanges and gaskets and between the gaskets and the bed support plate.

The 4-way switching valves (see Figure 68) and interconnecting piping was installed between the GGR reactors (see Figure 67). Graphite gaskets were put between the flanges of the interconnecting piping.

An HCl injection subsystem was assembled with welded stainless steel piping (see Figure 69). This subsystem was designed for a staged mixing of a metered, concentrated HCl source from a compressed gas cylinder into the flue gas between the furnace and the GGR reactors.

Compressed gas cylinders and regulators were ordered for the HCl injection subsystem. The cylinders ordered included a high concentration of HCl in nitrogen, with a concentration level high enough that each cylinder will last an entire eight hour test campaign, and a low concentration of HCl in nitrogen, at nearly the same concentration level expected in the flue gas, for calibration purposes.

Figure 65: GGR Reactor Sections with Refractory Insulation

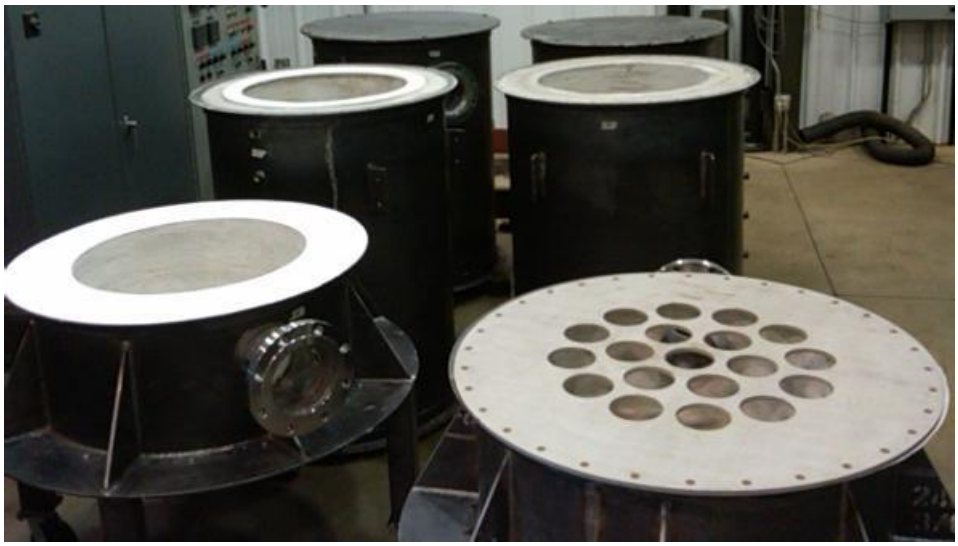

Photo Credit: Gas Technology Institute

Figure 66: Bed Support Plate with Screens and Gasket

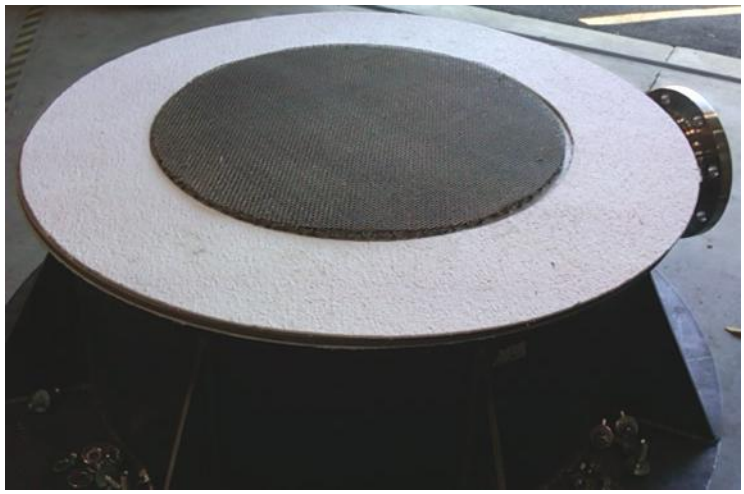

Photo Credit: Gas Technology Institute

The design of the external piping to and from the GGR reactors was finalized, which determined the ultimate position of the GGR reactors with respect to the furnace (see Figure 70 to Figure 72). The upward turn in the piping from the chimney to the GGR reactors was necessary to clear the framework that sits on top of the furnace.

Figure 67: GGR Reactors Assembled with Interconnecting Piping

Photo Credit: Gas Technology Institute

Figure 68: 4-Way Switching Valve with Actuator

Photo Credit: Gas Technology Institute

Figure 69: HCl Injector Subsystem for Flue Gas

Photo Credit: Gas Technology Institute

Figure 70: General Layout View of the External Piping

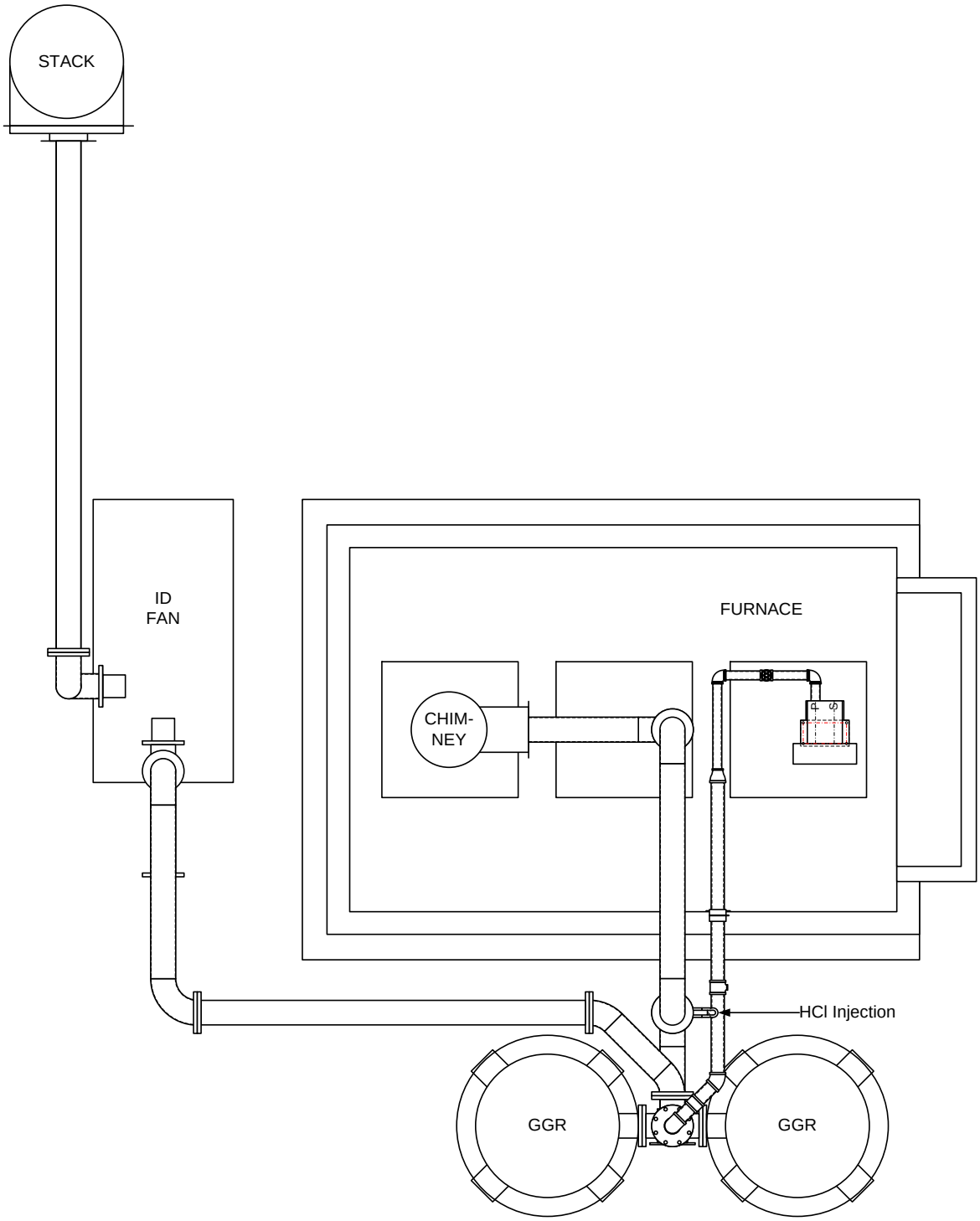

Source: Gas Technology Institute

Figure 71: Front Elevation View of the External Piping

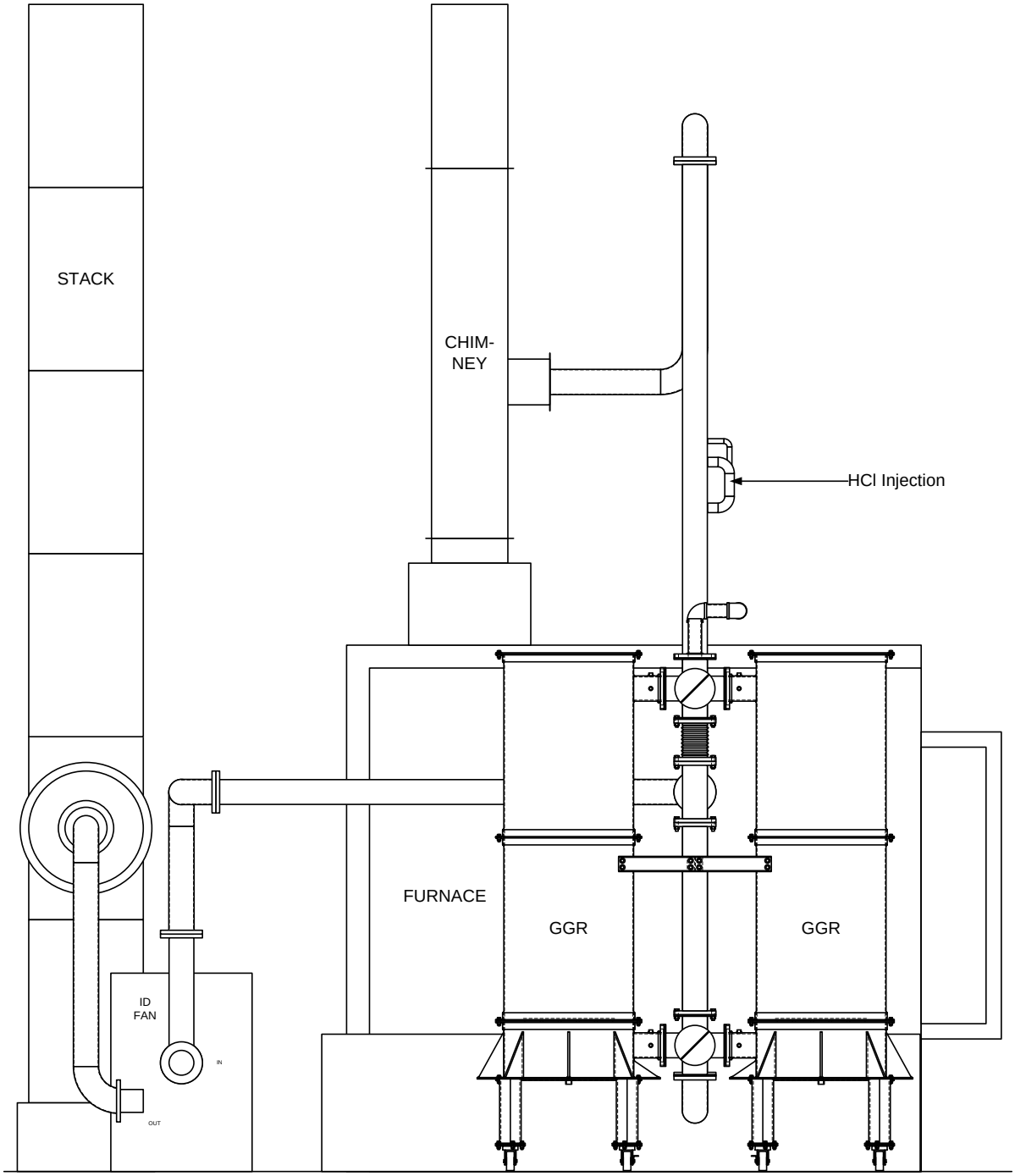

Source: Gas Technology Institute

Figure 72: Side Elevation View of the External Piping

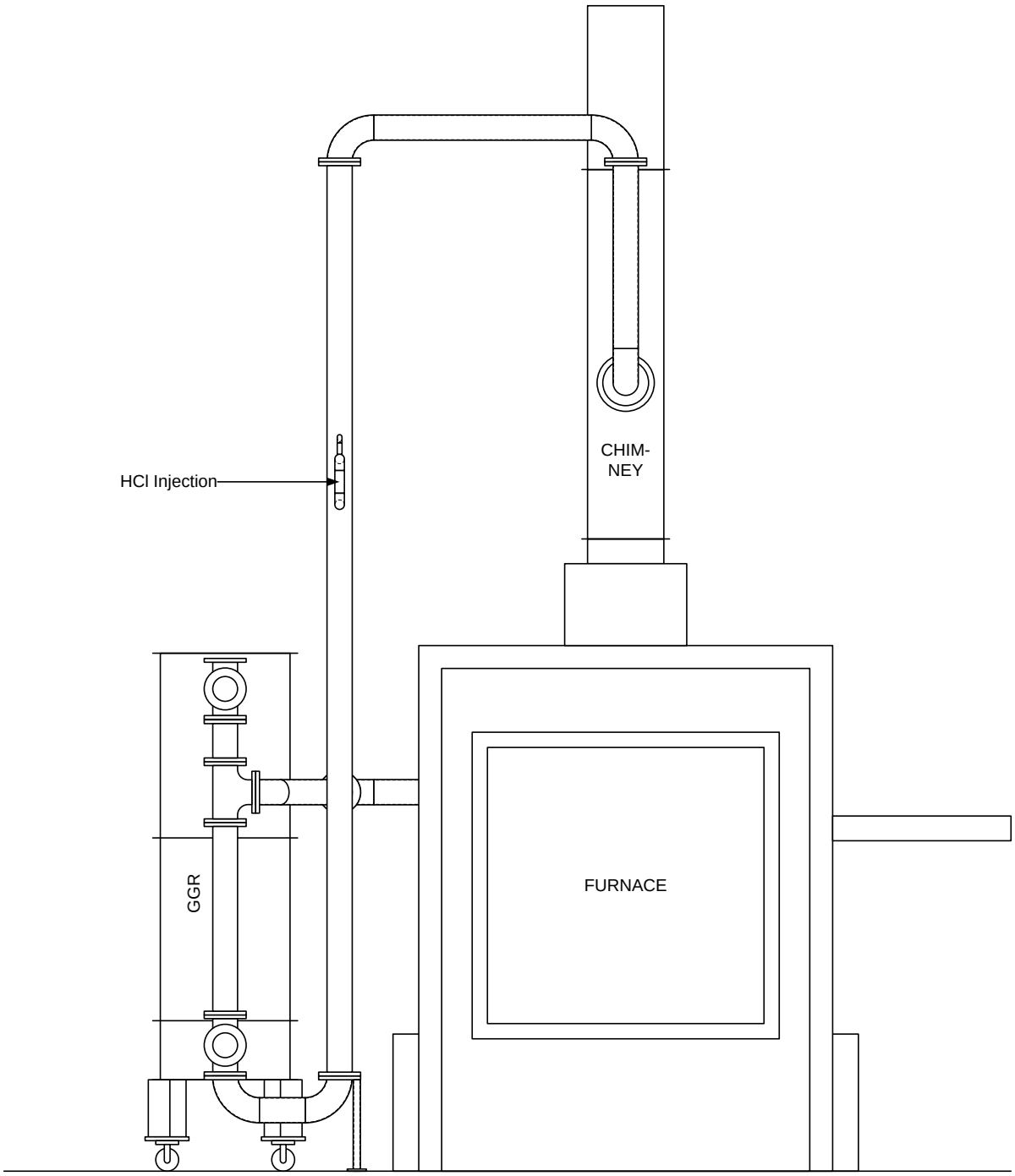

Source: Gas Technology Institute

During the fourth quarter of 2012, 6" stainless steel piping segments were fabricated and installed between the furnace chimney and the bottom inlet of the lower 4-way valve between the GGR reactors (see Figure 73). The HCl injection subsystem was welded to the side of the piping between the furnace chimney and the bottom inlet of the lower 4-way wave between the GGR reactors (see Figure 74).

Figure 73: Piping to/from GGR Reactors

Photo Credit: Gas Technology Institute

Figure 74: HCl Injector on the Side of Insulated Pipe

Photo Credit: Gas Technology Institute

The 6" stainless steel piping between the furnace's chimney and the GGR reactors was insulated (see Figure 74 and Figure 75). The insulation is 2" of mineral wool rated for 1200°F. Custom insulating jackets were fabricated for the pipe flanges and the lower 4-way valve. The actuators were installed on the 4-way valves (see Figure 75) and the valves were tested. The shafts were found to be binding in the packing fittings and had to be turned down on a lathe to provide the necessary clearance.

Figure 75: Insulated Piping to GGR Reactor

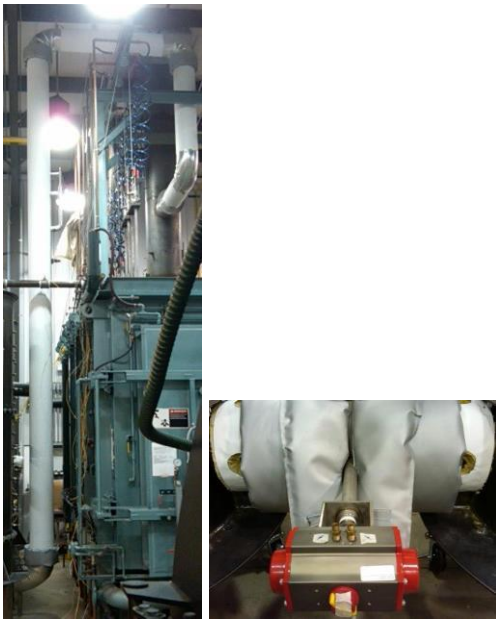

Photo Credit: Gas Technology Institute

Figure 76: Cold Air Line from Blower

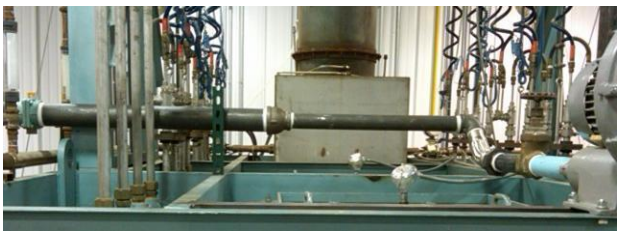

Photo Credit: Gas Technology Institute

The cold air blower was installed on the roof of the furnace. A power cord with an inline switch was connected to the cold air blower and run to a nearby 480 volts alternating current (VAC) 3-phase outlet. A steel pipeline was installed between the cold air blower on the furnace's roof and the GGR reactors (see Figure 76). The pipeline includes a 2" gate valve to throttle the flow from the blower and a 3" orifice meter for measuring the flow rate.

The ID fan was positioned behind the furnace. Carbon steel piping segments were fabricated and installed between the tee located between the GGR reactors and the ID fan, and between the ID fan and the stack.

The burner was installed on the furnace. A flame safeguard and ignition transformer was connected to the burner (see Figure 77. A solenoid valve and rotameter were installed between the natural gas supply and the burner.

Figure 77: Burner Connections

Photo Credit: Gas Technology Institute

Figure 78: Data Acquisition System

Photo Credit: Gas Technology Institute

The data acquisition system for the furnace (see Figure 78) was restored, and two additional modules were added to accommodate the thermocouples to be installed in the GGR reactors. Seventeen thermocouple wire cables were run from the enclosure which houses the data acquisition system to the GGR reactors (see Figure 79). Thermocouple wells were designed, fabricated, and installed in the GGR reactors (see Figure 80). Six wells were located in each reactor.

Figure 79: Thermocouple Wiring

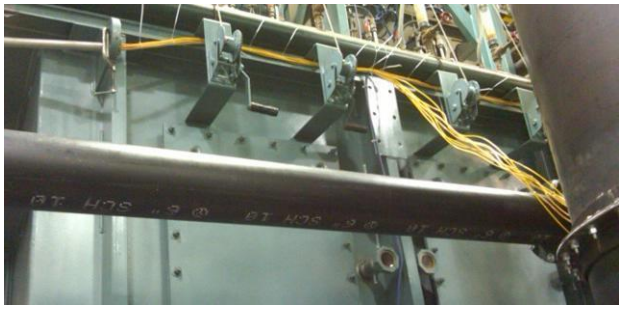

Photo Credit: Gas Technology Institute

Figure 80: Thermocouple Wells

Photo Credit: Gas Technology Institute

Ceramic beads and sorbent beads were ordered and received for the GGR reactors. The lids were removed from each GGR reactor. Both GGR reactors were loaded with an equal amount (200 lb each) of the original procurement of ceramic beads. An additional 2,500 lb of ceramic beads was procured from another vendor. The GGR reactors were then loaded with enough of these beads (400 lb each) to achieve the designed 16" column height. The GGR reactors were finally loaded with 810 lb of sorbent beads and additional 1,550 lb ceramic beads to achieve the

total column height of 67" for both reactor columns (see Figure 81 and Figure 82). The lids were placed back on the tops of each GGR reactor.

Figure 81: Beads in Left GGR Reactor

57/10 split

Photo Credit: Gas Technology Institute

Figure 82: Beads in Right GGR Reactor

16/51 split

Photo Credit: Gas Technology Institute

A thermocouple was installed in each of the 6 thermocouple wells in each GGR reactor (see Figure 83 and Figure 84). Thermocouples were also installed in the inlets and outlets of each GGR reactor and in the pipe from the cold air blower, for a total of 17 thermocouples.

Figure 83: Thermocouples in Left GGR Reactor

Photo Credit: Gas Technology Institute

Figure 84: Thermocouples in Right GGR Reactor

Photo Credit: Gas Technology Institute

The thermocouple cables were connected to the thermocouples in the GGR reactors (see Figure 85 and Figure 86) and to the modules in the data acquisition system. Brackets (see Figure 86) were attached to the GGR reactors to support the cables. The exhaust pipe leaving the GGR reactors was insulated in the vicinity of the thermocouples in the GGR reactors (see Figure 85). Additional insulation was added to the piping above the lower 4-way switching valve between the GGR reactors.

Figure 85: Thermocouples Wired to Left GGR Reactor

Photo Credit: Gas Technology Institute

Figure 86: Thermocouples Wired to Right GGR Reactor

Photo Credit: Gas Technology Institute

The combustion air blower was positioned near the GGR reactors. A hose was run from the burner to this blower. A 480 VAC 3-phase power distribution box for this blower and the ID fan was situated nearby.

Figure 87: Combustion Air Blower and Power Box

Photo Credit: Gas Technology Institute

Figure 88: Pressure Gauges and Sampling Ports with Switching Solenoid in Background

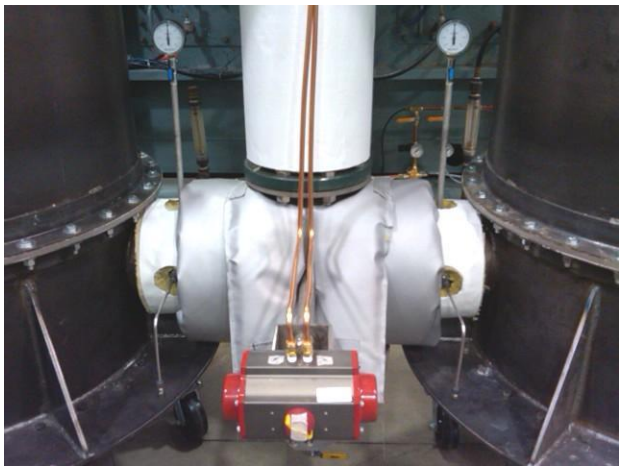

Photo Credit: Gas Technology Institute

A switching solenoid valve (see Figure 88) was installed at the nitrogen (serving as instrumentation air) supply manifold on the furnace. The solenoid valve was connected to the actuators on the 4-way valves with copper tubing. A repeat cycle timer relay was installed and wired to the solenoid valve so that automated timed switching of the 4-way valves can be set when desired.

Sampling ports were installed and pressure gauges with a ±30"water column (wc) range were installed at the inlet and outlet of each GGR reactor (see Figure 88). A pressure gauge with a ±10"wc range was installed on the furnace chamber. A U-tube manometer was installed on the orifice to measure the cold air flow rate to the GGR reactors.

A piping train for metering a concentrated (2 percent) HCl gaseous mixture into the injector on exhaust gas between the furnace and the GGR reactors was assembled and installed. The 2 percent HCl concentration in one supply cylinder allows for a 50 ppm HCl concentration in the exhaust gas over an eight hour period. A stainless steel tubing line was connected between the piping train and the HCl injector on the exhaust gas piping. The HCl injector was insulated to minimize heat loss. A solenoid valve in the piping train was interlocked with the flame safeguard on the burner so that in event of flame loss in the furnace, the HCl injection is shut off. A manual valve allows the nitrogen to purge the interconnecting tubing line.

Figure 89: HCl Piping Train and Manometer for Cold Air Orifice

Photo Credit: Gas Technology Institute

Figure 90: Heat Shielding

Photo Credit: Gas Technology Institute

Various preparations were made to ready the furnace for operation:

- Drain hoses were attached to the furnace's water cooled-loads.
- Heat shielding (see Figure 90) was redeployed between the furnace's chimney and the supply hoses for the water cooled-loads.
- Missing thermocouples for these loads were replaced.
- A thermocouple was installed in the furnace's chimney.
- Drain valves were installed on the GGR reactors.
- A thermocouple was added at the ceramic-sorbent interface in the right GGR reactor
- The data acquisition system was updated to include the new thermocouples.

2.3.3.4 Testing of the GGR Demonstration Unit

The GGR demonstration unit was subjected to a cold dry (no HCl) test to set flow rates, and a hot dry test to set furnace conditions and switching frequency. A series of hot wet (with HCl) tests were then conducted.

Dry Tests

Cold Dry Test

A cold dry test of the GGR reactors and the furnace was conducted. This test was conducted without heat in the furnace and without HCl in the exhaust gas from the furnace. The purpose of this test was to:

- Validate all the readings in the data acquisition system
- Flow test and leak test the water lines

- Pressure test the furnace and exhaust line
- Check operation of the 4-way switching valves
- Test flow the HCl injection subsystem with nitrogen
- Set the flow rates for the combustion air and the cold air
- Preliminarily set the ID fan speed to balance the pressure (zero draft) in the furnace
- Test fire the burner

Hot Dry Test

A hot dry test of the GGR reactors and the furnace was conducted. This test was conducted with heat in the furnace but without HCl in the exhaust gas from the furnace. The purpose of this test was to:

- Set the flow rates for the combustion air and the cold air for 900,000 Btu/h
- Set the ID fan speed to balance the pressure (zero draft) in the furnace
- Fire the burner and bring the furnace to operating temperature
- Adjust the furnace loading to try to reach 1000°F in the exhaust gas at the GGR reactor inlets. All of the variable load elements were withdrawn from the furnace chamber, and the firing rate was increased to 1,000,000 Btu/h, with a corresponding increase in the combustion air and cold air flow rates. The exhaust gas was over 900°F and climbing at the conclusion of the test period.
- Check the operation of the 4-way switching valves with hot exhaust gas. The switching of the valve was done manually based on the ceramic-sorbent interface temperature. As the towers increased in temperature, the switching time interval was reduced until a consistent interval (about 30 minutes per reactor) was achieved.

Wet Tests

An HCl analyzer system was rented from a local stack testing and continuous emissions monitoring rental firm. The system included a non-dispersive infrared (NDIR) analyzer, a heated sampling line with filter, and a drying train with sampling pump. GTI added another heated sampling line connecting the port at the GGR reactor outlet to the filter. The port at the GGR reactor inlet when used was connected directly to the filter.

Figure 91: Heated Sampling Line on Right GGR Reactor Outlet and Heated Filter Box

Photo Credit: Gas Technology Institute

Figure 92: Partially Obscured Load in Furnace

Photo Credit: Gas Technology Institute

Testing of the GGR reactors with hot exhaust gas with HCl injection was conducted over a four day period.

Hot Wet Test #1

During the first day of testing, the furnace was operated with the parameters determined during the dry hot test. The GGR reactor inlet temperature was maintained above 900°F for five hours, peaking at 930°F, which was below the 1,000°F desired. There were problems with getting the HCl analyzer to respond, which were eventually traced to having a bad calibration gas cylinder and having an improper filter on the sampling pump. This was resolved by renting another calibration gas cylinder and removing the filter. Another problem arose when the HCl was injected into the hot exhaust gas from the furnace and was barely detectable at the inlets of the GGR reactors. The cause of this problem may be that the HCl is converted to some other chemical by the heat and chemical components in the exhaust gas, further analysis may be necessary. The other chemical may revert back into HCl once the exhaust gas is cooled in the ceramic bed in the GGR reactor for capture by the sorbent bed. Once the fuel was shut off to the furnace, HCl was detectable in the heated air exhaust gas.

Hot Wet Test #2

During the second day of testing, about half of the fixed load elements in the furnace were insulated from the flame heat radiation (see Figure 92). The furnace was again operated with the parameters determined during the dry hot test. The GGR reactor inlet temperature was

maintained above 950°F for five hours, with the last two hours over 1000°F. The HCl injection point was moved from about 20' before the GGR reactors to about 3' before to reduce the residence time of HCl in the hot exhaust gas. The concentrated HCl mixture was diluted 7:1 with nitrogen prior to injection to improve the mixing into the exhaust gas since this injection point does not have a staged mixing-injection apparatus like the upstream injection port. With this arrangement, HCl was partially detectable in the hot exhaust gas.

Hot Wet Test #3

During the third day of testing, the furnace was brought up to operating temperature and then the fuel was shut off so that exhaust gas consisted of hot air. When HCl was injected into the closer injection port, it was reasonably measured in the hot air at the inlet of the GGR reactors and mostly absent from the cooled hot air at the outlet of the GGR reactors.

Hot Wet Test #4

The fourth day of testing was a repeat of the third day, with a longer period of operation with the furnace running for more heat recovery data measurement. The period of HCl injection into the closer injection port was followed by a period of HCl injection into the original 20' upstream injection port for comparison.

2.3.3.5 GGR Demonstration Unit Test Results and Analysis

A graph of the temperatures at the lower inlet (hot exhaust gas for first half of cycle, heated combustion air for second half of cycle) and at the upper outlet (cooled exhaust gas for first half of cycle, cold combustion air for second half of cycle) of the right GGR reactor is shown in Figure 93 for the second day of testing. The 30 minutes time for each half cycle is clearly shown on the graph. Toward the end of the testing, the exhaust gas was cooled from an average of 1006°F to an average of 176°F during the first half of the cycle, while the combustion air was heated from an average of 124°F to an average of 810°F during the second half of the cycle (see Figure 94). The change in temperature of the exhaust gas is equal to an extraction of 63 percent of the energy (sensible and latent) contained in the exhaust gas at 1,006°F.

Data collected from the HCl analyzer during the third and fourth day of testing is shown in Figure 95. The "Before" data was measured at the lower inlet of the right GGR reactor during one half cycle with the exhaust gas flowing into the reactor at that point, while the "After" data was measured at the upper outlet of the right GGR reactor during the next half cycle in the same flow direction (i.e., one hour later) with the exhaust gas flowing out of the reactor at that point. The average inlet concentration of HCl was 46.2 ppm, while the average outlet concentration of HCl was 1.9 ppm. The average removal was 96 percent.

Figure 93: Inlet and Outlet Temperatures at the Right GGR Reactor Showing Cycling

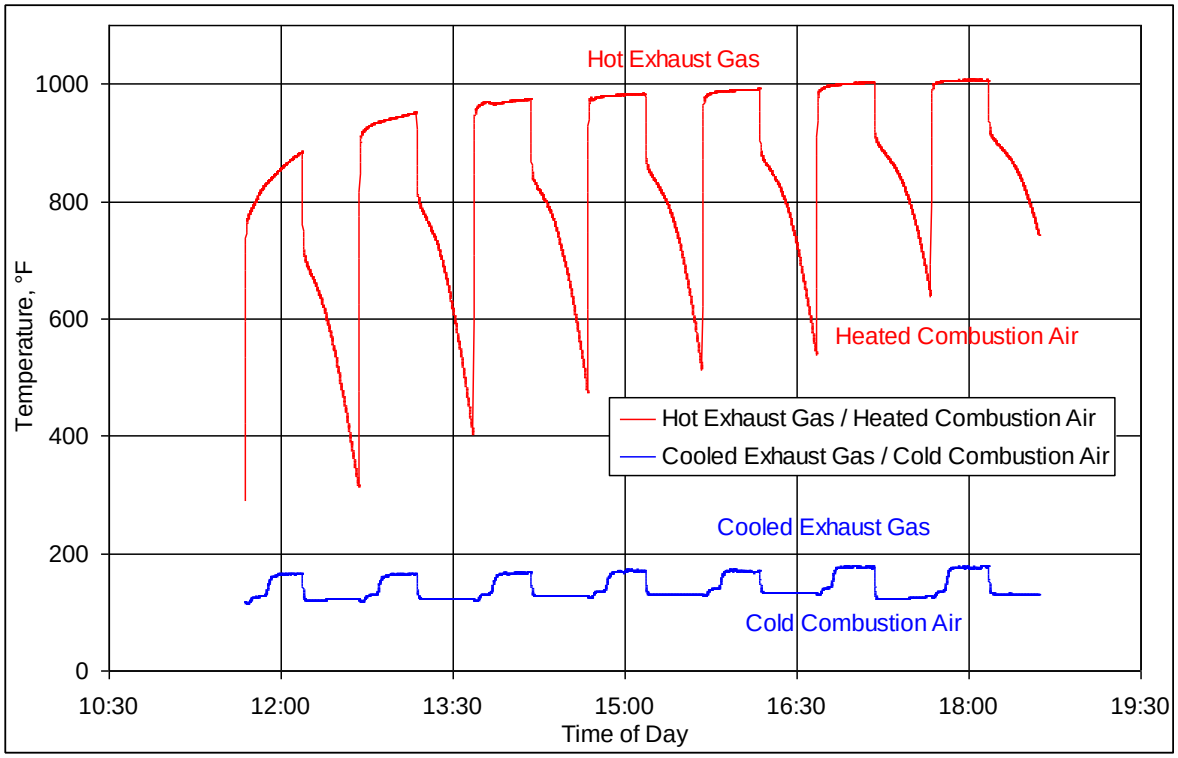

Source: Gas Technology Institute

Figure 94: Heat Recovery Results

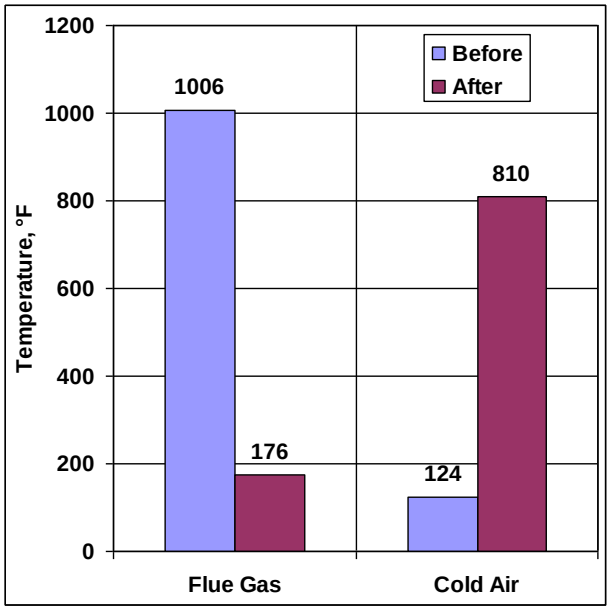

Source: Gas Technology Institute

Figure 95: Acid Gas Removal Results

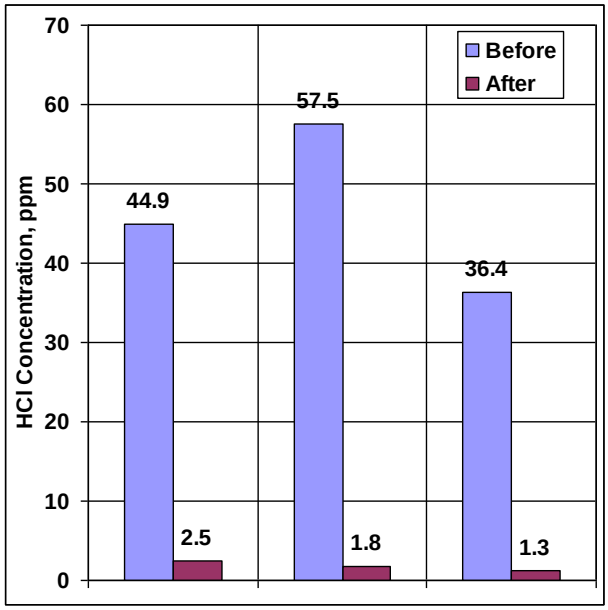

Source: Gas Technology Institute

Due the temperature gradient within the GGR reactor, the sorbent temperature always stayed below 700°F despite the higher hot exhaust gas and higher heated combustion air temperatures. Only the ceramic in the GGR reactor exceeded this temperature.

The pressure drop through the GGR reactor at the highest flow rate at the hottest temperature was measured at 6.5"wc. This measurement was higher than the modeling indicated (~600 Pa or 2.4"wc). The achieved half cycle time of 30 minutes (1800 seconds), was precisely what the modeling indicated. The outlet temperature of 810°F was better than the modeling indicated (700 to 800°F).

Conventional recuperators can be damaged when used to recover heat from corrosive flue gas. For non-corrosive applications, they typically provide 450°F to 750°F combustion air using 1,300°F to 1,600°F exhaust as the waste heat source. For higher exhaust temperatures, the exhaust gas is often diluted with ambient air to be compatible with the materials of the recuperator.

For a furnace with 1,800°F of corrosive exhaust gas, the ability to preheat the combustion air to 800°F would increase the furnace thermal efficiency from 35 percent to 45 percent and yield a fuel savings of 23 percent. The ability to preheat the combustion air to 1,000°F, which is within the capability of the GGR reactors with higher hot exhaust gas temperature, would result in an increase of furnace thermal efficiency from 35 percent to 49 percent and yield a fuel savings of 28 percent.

2.4 Task 4: Technology Transfer Plan

Results and knowledge gained from this project will be summarized in a "White Paper" that is in preparation and will be sent to end user companies in California that could potentially retrofit GGR for waste heat recovery or incorporate the waste heat recovery system into the design of a new aluminum melting furnace.

- A critical component of the White Paper is articulating what makes this technology valuable to the end user and the Value Propositions (Technical, Economic and Other Performance Improvements).

As indicated, the first step in the Technology Transfer Plan (TTP) plan is to send White Papers to all qualified and pre-identified companies operating in California. The White Paper includes language soliciting responses from the potential end users to guide further development and introduce the technology into their industry.

The second step is to identify a list of potential commercialization partner(s) for GGR technology and forward the White Papers seeking to gain their interest in partnering with GTI to develop the GGR technology from a prototype to a commercial state. GTI has developed

collaborative relationships with potential waste heat recovery technology commercialization partners on numerous projects who would be amenable to partnering with GTI.

- Once a qualified commercialization partner, or partners, joins with GTI, a pre-commercial design of a scaled-up GGR system to match that of a typical existing aluminum melting furnace will be developed. Per joint follow ups by GTI and the commercialization partner, an end user willing to act as a host site will be selected. The pre-commercial design of a GGR system will be engineered and further tailored for the specific site.
- A GGR system will be fabricated and assembled by the commercialization partner and installed by the host site to the aluminum melting furnace.

The third step in the TTP will be to retrofit the GGR system to the host site aluminum melting furnace and carry out a field test to confirm the Value Propositions under actual industrial operating conditions.

- An agreement will be negotiated with the host site. Upon completion of the field test, the host site will be showcased by virtue of publicizing the results to the previously identified end users in California and to the entities identified in the table below (see Table 13). GTI has found the technique of showcasing successful field tests of developed technology to be extremely beneficial to the roll out of newly developed and successfully tested technology.

GTI will develop a licensing arrangement (Memorandum of Understanding and licensing terms) with a commercialization partner(s). Shortly after completion of the full scale field test, it is expected that a successful demonstration of the concept will lead to signing a licensing agreement with first commercial units ready for deployment and installation in 2015 in California and to other markets within the United States.

GTI's Technology Transfer Plan to licensees and end users, is shown below in Table 13. It involves four fundamental components that GTI has used successfully in over 400 programs, to create visibility and accelerate technology adoption for over 70 years.

Table 13: GTI Technology Transfer Plan Fundamentals

TECHNOLOGY TRANSFER COMPONENT	METHOD HIGHLIGHTS	FREQUENCY
1. Trade Journal Publications	GTI develops a plan and creates, at least one article for publication in GasTIPS and at least one article suitable for publication in Gas Technology or Industrial Heating.	At least two articles
2. Technical Presentations at Industry Meetings	GTI works with the North American Die Casting Association (NADCA), California Metals Coalition (CMC), Cast Metal Association (CMA), and the Energy Solutions Center to identify five targeted industry meetings, where GTI can present the results of the GGR field test.	Five industry meeting presentations
3. Website Posting	GTI dedicates a section on their website for the combustion community. GTI's website averages 1,600 users each workday, and about 20 percent of visitors return within 30-days. GTI provides links to CEC website for additional project information. GTI can provide HTML (or similar web-related) files to CEC for their website.	Create GGR section on GTI website; Prepare FAQ sheet, update as required; Provide links to CEC website
4. Exposure at Industry Trade Shows	GTI provides exhibit booth, showcasing combustion technology developments at key industry trade shows; GTI showcases the GGR technology in at least two industry trade shows/conferences per year.	Two trade show booths per year

Source: Gas Technology Institute

Deployment of this new technology will generate benefits, both private and public in California. The range of specific energy consumption for aluminum melting furnaces is 2.6 to 7.7 MMBtu (million Btu) per ton of melt [Worrel, E. 2008 p. 21]. Domestically, aluminum melting furnaces consume an estimated 9.1 trillion Btu of natural gas[1] with fuel costs representing a significant percentage (up to 15 percent) of total operating costs. When GGR for exhaust heat recovery is commercially developed and adopted, operators of aluminum melt furnaces will have the potential for realizing a significant reduction in their operating costs.

More than 1.7 million tons [U.S. Geological Survey. 2013 p. 16] of aluminum is re-melted annually in the United States and more than 10 percent of that total is estimated as re-melted in

[1] Using an average of 5.2 MMBtu per ton of melt.

California. California aluminum re-melters typically operate at 35 percent thermal efficiency with 60 percent of input energy lost to the exhaust gas without recovery. GGR has the potential to recover 63 percent of the energy in the exhaust gas heat that would increase furnace thermal efficiency aby over 40 percent and save 2.37 trillion Btu of natural gas annually in the United States and nominally 0.24 trillion in California including annual emissions reductions in carbon dioxide of 14,000 tons and reductions in oxides of nitrogen of 56,000 pounds.

Typically, the aluminum melting furnace population is expected to either retrofit or include GGR systems into new melting furnaces over a 5 to 10 year period when the benefits will be the fully accrued rates.

REFERENCES

Binlin, D. et. al., "Single and Combined Removal of HCl and Alkali Metal Vapor from High-temperature Gas by Solid Sorbents", Energy & Fuels, 21 (2), 1019-1023, 2007

Brockhoff, R. et. al., "Process for reducing the dioxin and furan content in waste gases from furnaces, and use of the filter dusts produced thereby", U.S. patent number: 6077328, June, 2000.

Cook, C. et. al., "Method for removing HCl and HF from coal derived fuel gas", U.S. patent number: 5118480, June, 1992.

Duo, W, Kirkby, N.F., Seville, J.P.K, Kiel, J.H.A, Bos, A. and Denuil, H., Kinetics of HCl reaction with Calcium and Sodium sorbents for IGCC fuel gas cleaning, Chem. Eng. Sci., Vol. 51, 2541-2546, 1996.

Garea et. al., "Sorbent behavior in urban waste incineration: acid gas removal and thermogravimetric characterization", Thermochimica Acta, 397 (1-2), 227-236, 2003

Hisashi, K. et. al., "Characteristics on HCl absorption on and release from limestone", Kagaku Kogaku Ronbunshu, 27 (5), 624-628, 2001

Hsu, J. et. al., "Cleaning composition for treating acid waste gas", U.S. Pat. Appl. Publ. US 2007006730 A1, Jan 2007

Jatta, P. et. al., "Absorption of HCl by limestone in hot flue gases. Part I: the effects of temperature, gas atmosphere and absorbent quality", Fuel, 84 (12-13), 1664-1673, 2005

Jatta, P. et. al., "Absorption of HCl by limestone in hot flue gases. Part II: importance of calcium hydroxychloride", Fuel, 84 (12-13), 1674-1684, 2005

Mura, G. and Lallai, A., Reaction Kinetics of Gas Hydrogen Chloride and Limestone, 1994.

Pigford, R.L. and Sliger, G., Rate of diffusion controlled reaction between a gas and a porous solid sphere, Ind. Eng. Chem. Pro. Des. Dev., 12, 85-91, 1973.

Roine, A., HSC Chemistry® Software Package Ver. 4.0, www.outotec.com, Outokumpu Research Oy, Pori, Finland, 2000.

Slimane, R., Choi, C., Masyukov, A., "Sorbent-based HCl Removal from High-temperature Flue Gas," Final Report for GTI IR&D Project No. 20612 (Period of Performance: Sept. 24 – Dec. 31, 2007), January 2008.

Slimane, R.B., Akpolat, O.M., Lau, F.S., Newby, R.A., Jain, S.C., "Experimental Studies In Support of the Ultra-Clean Gas Cleanup Process Development," 18th Annual International Pittsburgh Coal Conference, Dec. 4-7, 2001, Newcastle, New South Wales, Australia.

U.S. Geological Survey, Mineral Commodity Summaries, January 2013, p. 16.

Verdone, N. and De Filippis, P., Reaction kinetics of Hydrogen chloride with sodium carbonate, Chem. Eng. Sci, 61, 7487-7496, 2006.

Weinell, E.C., Jensen, I.P., Dam-Johansen, K. and Livebjerg, H., Hydrogen Chloride Reaction with lime and limestone: Kinetics and Sorption Capacity, Ind. Eng. Chem. Res., 31, 164-171, 1992.

Wen, C.Y., Non Catalytic heterogeneous solid fluid reaction models, Ind. Eng. Chem, 60, 34-35, 1968.

Worrell, E., Neelis, M., Price, L., Galitsky, C., and Zhou, N. World Best Practice Energy Intensity Values for Selected Industrial Sectors, LBNL-62806, Rev. 2, Environmental Energy Technologies Division, February 2008, p. 21.

GLOSSARY

Term	Definition
°F	Degrees Fahrenheit
µGC	Micro-gas Chromatograph
Al	Aluminum
Al_2O_3	Aluminum oxide
AMIF	American Metals Installer and Fabricators
atm	atmosphere
Btu/h	British Thermal units per hour
C	Carbon
c	heat capacity
°C	Degrees Celsius
Ca	compounds of calcium
CAM	Commission Agreement Manager
Cl	Chlorine
CMA	Cast Metal Association
CO_2	Carbon Dioxide
CPR	Critical Project Review
DVBE	Disabled Veteran Business Enterprise
ECRS-	Environmental and Chemical Research Services
F	Fluorine
Fe	iron
FTIR	Fourier Transform Infrared
g	grams
GGR	Gas Guard Recuperator
GTI	Gas Technology Institute
H	Hydrogen
h	enthalpy
H_2O	Water
HCl	hydrogen chloride
HF	hydrogen fluoride
ID	Induced Draft
K	potassium
K	Degrees Kelvin
KCO_3	Potassium chloride

L/D	length/diameter
lb/ft^3	Pounds per cubic foot
m/s	meters per second
Mg	Magnesium
micro-GC	micro-gas chromatograph
mm	millimeter
MMBtu	Million BTu
Mn	Manganese
Mo	Molybdenum
N_2	Nitrogen
Na	Sodium
Na_2CO_3	Sodium Carbonate
$Na_2CO_3 \cdot NaHCO_3 \cdot 2H_2O$	Trona
Na_2O	Sodium Oxide
NaCl	Sodium Chloride
$NaClO_2$	Sodium Chlorite
$NaClO_3$	Sodium Chlorate
$NaClO_4$	sodium perchlorate
NADC	North American Die Casting Association
$NaHCO_3$	Nahcolite (Sodium Bicarbonate)
NaO_2	Sodium Superoxide
NCSU	North Carolina State University
NDIR	Non-Dispersive Infrared
NOx	Oxides of nitrogen
O_2	Oxygen
Pa	Pascal
ppm	Parts-per-million
ppmv	Parts-per-million by volume
psi	Per square inch
S	entropy
s	seconds
SO_2	sulfur dioxide
SS	Stainless Steel
SV	Space velocity
TTP	Technology Transfer Plan
VAC	Volts Alternating Current
wc	Water column